Modeling the Spatial and Temporal Distribution of Planktonic Foraminifera

Dissertation zur Erlangung des
Doktorgrades der Naturwissenschaften
am Fachbereich Geowissenschaften
der Universität Bremen

vorgelegt von

Igaratza Fraile Ugalde

September 2008

The question is not what you look at, but what you see
- Henry David Thoreau -

Contents

Acknowledgements **vii**

Abstract **viii**

1 Introduction **1**
1.1 Planktonic foraminifera 1
1.2 Planktonic foraminifera as paleoproxy 6
1.2.1 Foraminiferal abundance as a paleotemperature proxy 7
1.2.2 Foraminiferal shell chemistry as a paleotemperature proxy . . 9
1.2.3 Difficulties associated with foraminifera-based proxies 10
1.3 Seasonality of planktonic foraminifera 11
1.4 Scientific objectives 13

2 A dynamic global model for planktonic foraminifera **25**
2.1 Introduction 25
2.2 Model setup 27
2.2.1 Ecosystem model 27
2.2.2 PLAFOM 27
2.2.3 Standard model experiment: grid, forcing and boundary conditions 33
2.2.4 Comparison to core-top data 35
2.2.5 Comparison to sediment-trap data 35
2.2.6 Sensitivity analysis of the parameters 36
2.3 Results 38
2.3.1 Spatial distribution patterns 38
2.3.2 Temporal distribution patterns 41

2.3.3 Spatio-temporal distribution pattern . . . 45
2.3.4 Sensitivity experiment: spatio-temporal distribution patterns with constant temperature . . . 45
2.4 Discussion . . . 47
2.4.1 Comparison with core-top data . . . 47
2.4.2 Comparison with sediment-trap data . . . 50
2.4.3 Sensitivity analysis . . . 51
2.4.4 Model experiment with constant mixed-layer temperature . . . 51
2.5 Summary and conclusions . . . 53

3 Seasonal bias in Foraminifera-based Proxy records 67
3.1 Introduction . . . 67
3.2 Data and Methods . . . 69
3.2.1 Description of the model . . . 69
3.2.2 Sediment-trap data . . . 69
3.2.3 Experimental design . . . 71
3.3 Results . . . 71
3.3.1 Influence of seasonality and temperature sensitivity on temperature estimates . . . 71
3.3.2 Sensitivity analysis . . . 73
3.4 Discussion . . . 77
3.4.1 Latitudinal species distribution . . . 77
3.4.2 Sensitivity of species to changes in SST . . . 79
3.5 Conclusions . . . 80

4 Seasonality of planktonic foraminifera during the Last Glacial Maximum 91
4.1 Introduction . . . 91
4.2 Methods . . . 92
4.2.1 Foraminifera model and experiment setup . . . 92
4.2.2 CCSM3 Climate Model simulations . . . 93
4.2.3 UVic Earth System - Climate Model simulations . . . 95
4.2.4 Sedimentary faunal assemblages . . . 97
4.2.5 Flux-weighted temperature signal . . . 98
4.3 Results . . . 100
4.3.1 Relative abundances of the species during the LGM . . . 100
4.3.2 Foraminiferal seasonality during the LGM . . . 102
4.4 Discussion . . . 104
4.4.1 Comparison between model output and sediment samples . . . 104
4.4.2 Influence of seasonality on proxy records . . . 105

4.5 Conclusions 109

5 Vertical distribution of living planktonic foraminifera in the Azores Front 119
5.1 Introduction 119
5.2 Material and methods 120
5.2.1 Sampling and processing 120
5.2.2 Oceanographic setting 122
5.3 Results 126
5.3.1 Total foraminiferal fauna 126
5.3.2 Foraminiferal assemblage composition 126
5.3.3 Model prediction 127
5.4 Discussion 131
5.4.1 Depth habitat of the species 131
5.4.2 Comparison between samples and model prediction 132
5.5 Conclusions 134

6 Summary 139

7 Conclusions 141
7.1 Outlook 142

A Model notation and equations 145
A.1 Coupling between ecosystem and foraminifera models 145
A.2 Parameters for the foraminifera model 146
A.2.1 Variables and initial values 146
A.2.2 Biological parameters common to all species 146
A.2.3 Species specific biological parameters 147
A.3 Model equations 149

Acknowledgments

This work was carried out at the Geosciences Department of Bremen University, and was funded by Deutsche Forschungsgemeinschaft (DFG) within the European Graduate Collegue "Proxies in Earth History" (EUROPROX). They supported me during three years giving the opportunity to participate in several international conferences and exchange programs.

I would like to thank to my supervisors, Prof. Michael Schulz and Dr. Stephan Mulitza, whose thoughtful advise often served to give me a sense of direction during my PhD studies. I would have been lost without them. Thank you for believing in me, and for always encouraging me to go beyond my past achievements. I also like to express my gratitude to Prof. Michal Kucera who, during my stay in the University of Tübingen, shared with me a lot of his expertise and research insight.

I am indebted to my many colleagues and PhD students at Bremen University for providing a stimulating and fun environment in which to learn and grow. I am especially grateful to the 'palmod' group, who created a friendly working environment. Andreas Manschke was particularly helpful in computer support, patiently teaching me to work with Linux. Mathias Prange has been always interested in my research and I would like to thank him for all his contributions. Jörg Franke, who spent plenty of time fighting with my computer problems and provided me several useful pieces of his code, turned out a great office mate.

I wish to thank everybody with whom I have shared experiences in life. From the people who first persuaded and got me interested in science to those that have joined me in the discovery of life. I would specially like to thank Catalina González and Ilham Boumetarham who, with the gift of their company and unconditional friendship, made my days in Bremen more enjoyable and worth living.

Finally, I would like to thank my family for the understanding. They have always supported and encouraged me to do my best in all matters of life. To them I dedicate this thesis.

Igaratza Fraile Ugalde
Bremen
October 17, 2008

Abstract

Planktonic foraminifera contribute substantially to the fossil record of marine sediments, and due to their excellent preservation in sediments, the fossil shells are of great paleoceanographic significance. Temporal variations in sedimentary faunal assemblages and geochemical composition of the individual fossil shells have become important proxies for past oceanic conditions. Different ecological preferences between species cause distinct seasonal patterns, and the imprint of differing seasonal production is preserved in the sedimentary record. Accurate knowledge of foraminiferal ecology and seasonal succession is indeed crucial to correctly interpret corresponding proxy-based reconstructions. Planktonic foraminifera are known to be sensitive to temperature, and therefore climate changes may alter the seasonal pattern of species. Any change in the timing of the largest flux to the seafloor that may have occurred in the past will lead to a bias in estimated paleotemperature. Therefore, this dissertation focuses on the variability of planktonic foraminiferal seasonality through time, and discusses its implications for paleotemperature reconstructions.

A numerical model simulating the population dynamics of planktonic foraminifera was developed and coupled to an existing marine ecosystem model. This model is forced with a global hydrographic dataset (e.g., temperature, mixed layer depth) and with biological information taken from the ecosystem model to predict monthly concentration of the following foraminifera species: *Neogloboquadrina pachyderma* (dextral and sinistral varieties), *Globigerina bulloides*, *Globigerinoides ruber* (white variety) and *Globigerinoides sacculifer*. These species are sensitive to sea-surface temperature, and due to their high spatial coverage and abundance are the most common planktonic foraminifera species used in paleoceanography. The model results for the global distribution of planktonic foraminifera for modern conditions are compared to available core-top and sediment-trap data. In the North Atlantic, model prediction is compared to the living population collected by plankton-nets.

The modeled spatial distribution of most of the species compares favorably with core-top data. The model prediction indicates that polar regions are dominated by *N. pachyderma* (sin.); *N. pachyderma* (dex.) and *G. bulloides* are the most common species in high productivity zones; and tropical-subtropical species like *G. ruber* and *G. sacculifer* are more abundant in oligotrophic waters. The predicted seasonal flux patterns coincided with sediment-trap records in most of the locations, although the comparison was hampered by interannual variability not captured by the model.

Using the foraminifera model, we carried out sensitivity experiments to study the response of foraminifera to different boundary conditions. A sensitivity experiment using a constant temperature of 12°C indicated that food availability is an important factor controlling foraminiferal distribution.

Another sensitivity experiment consisted of decreasing the temperature globally by 2°C and 6°C, and assessing the influence of this temperature variation on the recorded signal. In most of the regions at mid and high latitudes, due to the cooling and temperature sensitivity of the species, maximum production shifted to a warmer season. Thus, the foraminiferal population as a whole recorded little change in the temperature. By contrast, in tropical waters, where temperature cycle has relatively low amplitude, the recorded signal is close to annual mean SST regardless of the timing of maximum production. Therefore, at low latitudes foraminifera recorded the entire temperature change. These experiments emphasize the importance of considering changes in seasonality through time, as they can mask the total temperature variation.

Finally, we studied the response of foraminifera to the boundary conditions of the Last Glacial Maximum. We forced the foraminifera model using the physical and chemical parameters predicted by coupled climate models. In tropical waters variations in foraminiferal seasonality did not cause significant change in the recorded temperature. By contrast, at high latitudes the foraminiferal flux to the sea floor has a pronounced seasonal cycle, and the amplitude of temperature seasonality is also high. Therefore, changes in the seasonality of foraminifera had large influence on the seasonal imprint of the fossil record. The assessment and quantification of seasonal bias on a global scale allows the improvement of foraminifera-based proxy calibrations.

Kurzfassung

Planktische Foraminiferen tragen wesentlich zum Fossilieninhalt in marinen Sedimenten bei und sind daher von grosser Bedeutung für die Paläozeanografie. Zeitliche Veränderungen in der faunalen Zusammensetzung oder die geochemische Beschaffenheit ihrer fossilen Schalen sind zu einem wichtigen Proxy bei der Rekonstruktion mariner Paläoumweltbedingungen geworden. Unterschiede in der Ökologie verschiedener Foraminiferenarten erzeugen unterschiedliche jahreszeitliche Muster, die im Sediment aufgezeichnet werden. Ein genaues Wissen über die Ökologie der Foraminiferen und ihrer saisonalen Sukzession ist von entscheidender Bedeutung für die korrekte Interpretation von proxy-basierten Rekonstruktionen. Planktische Foraminiferen reagieren sensitiv auf Temperaturschwankungen, so dass Klimaänderungen jahreszeitliche Muster der Foraminiferenarten verändern können. Jede Veränderung des Zeitpunktes des maximalen Foraminiferen-Flusses zum Meeresboden kann zu Fehlern bei der Abschätzung von Paläotemperaturen führen. Aus diesem Grund behandelt die vorliegende Dissertation die Veränderung der Saisonalität planktischer Foraminiferen im Laufe der Zeit sowie die daraus resultierenden Implikationen für Paläotemperatur-Rekonstruktionen.

Ein numerisches Modell zur Simulation der Populationsdynamik planktischer Foraminiferen wurde entwickelt und an ein bereits existierendes marines Ökosystemmodell gekoppelt. Angetrieben wird das Modell mit einem globalen hydrografischen Datensatz (z.B., für Temperatur, Deckschichmächtigkeit) sowie mit biologischen Informationen, die dem Ökosystemmodell entnommen werden, um die monatliche Konzentration folgender Arten zu berechnen: *Neogloboquadrina pachyderma* (dextral und sinistral), *Globigerina bulloides*, *Globigerinoides ruber* (weiš) and *Globigerinoides sacculifer*. Diese Arten reagieren sensitiv auf Meeresoberflächentemperaturen und zählen aufgrund ihrer grossen räumlichen Abdeckung und Häufigkeit zu den

wichtigsten planktischen Foraminiferen für die Paläozeanografie. Die Modellergebnisse hinsichtlich der globalen heutigen Verteilung der Foraminiferen werden mit verfügbaren Oberflächen und Sedimentfallendaten verglichen.

Die modellierten räumlichen Verteilungsmuster der meisten Arten stimmen gut mit den Daten überein. Die Modellrechnungen ergeben, dass die polaren Regionen von *N. pachyderma* (sin.) dominiert werden, dass *N. pachyderma* (dex.) und *G. bulloides* die häufigsten Arten in Hochproduktivitätszonen sind und dass tropisch-subtropische Arten wie *G. ruber* und *G. sacculifer* am häufigsten in oligotrophen Gebieten auftreten. Die simulierten saisonalen Flussmuster stimmen weitgehend mit Sedimentfallendaten überein, wenngleich der Modell-Daten-Vergleich durch interannuelle Variabilität, die das Modell nicht simuliert, erschwert wird.

Mit Hilfe des Foraminiferen-Modells werden Sensitivitätsexperimente durchgeführt, um den Einfluss unterschiedlicher Randbedingungen auf die Artenverteilung zu untersuchen. Ein Experiment bei einer konstante Temperatur von 12°C , zeigt, dass die Nahrungsverfügbarkeit ein wichtiger Kontrollfaktor ist.

Ein weiteres Sensitivitätsexperiment besteht darin, die Temperatur global um 2°C und 6°C zu reduzieren und den Einfluss dieser Temperaturvariation auf das aufgezeichnete Signal zu berechnen. In den meisten Regionen mittlerer und hoher Breiten verschiebt sich die Maximalproduktion hin zu einer wärmeren Jahreszeit. Infolgedessen zeichnet die Population von *N. pachyderma* als Ganzes nur eine geringe Temperaturveränderung auf. In tropischen Gebieten hingegen, wo jahreszeitliche Temperaturschwankungen nur eine kleine Amplitude haben, liegt das aufgezeichnete Signal nahe am Wert der Jahresmitte.

Darüberhinaus wurde die Reaktion des Foraminiferensignals auf die Randbedingungen des Letzten Glazialen Maximums untersucht. Das Modell wurde von chemischen und physikalischen Randbedingungen angetrieben, die gekoppelten Klimamodellen entnommen wurden. In den Tropen änderte eine Änderung der Saisonalität der Foraminiferen das Temperatursignal im Sediment nur wenig. In den hohen Breiten zeigt der Foraminiferenflux zum Meeresboden dagegen deutliche saisonale Zyklen und die Amplitude der Temperatur-Saisonalität ist hoch. Änderungen in der Saisonalität der Foraminiferen haben daher einen deutlichen Einfluss auf den saisonalen Charakter der Sedimentabfolge. Die Bewertung und Quantifizierung des Einflusses dieses saisonalen Signals auf das globale Signal erlaubt die Verbesserung der Kalibration von Foraminiferen-Proxies.

Chapter 1

Introduction

1.1 Planktonic foraminifera

Planktonic foraminifera are single-cell marine zooplankton which live everywhere in the open ocean. They can survive in extreme conditions like within sea-ice (Dieckman et al., 1991), but are normally absent from coastal waters. Most of the species live in the upper water column, where the food availability is high (Murray, 1991). During their life cycle they produce a a multi-chambered calcareous shell. The life of foraminifera ends after reproduction, and its calcareous shell sinks to the seafloor. This shell is normally well preserved in sediments, and therefore the fossils of planktonic foraminifera are extensively used for paleostudies. Due to the global spatial coverage and good preservation, planktonic foraminifera are the most important fossil used in paleoceanography. Foraminifera represent a minor component of the total zooplankton biomass (between 2-10%, Arnold and Parker, 1999) but their calcareous shells accumulated on the sea floor account for about 20% of the total carbonate sequestrated in the deep sea (Langer et al., 1997). Because the oceanic carbonate system is closely linked to both atmospheric CO_2 and the global carbon cycle, carbonate production of foraminifera holds great interest for paleoclimatologists.

Depending on their specific ecological needs, different foraminifera species are distributed latitudinally and vertically in the water column. Murray (1897) was the first to note that the dead shells of foraminifera species were distributed globally in horizontal belts, and concluded that temperature must be the most important controlling factor in such distribution. Later, plankton-tows (e.g., Bé, 1960) and laboratory culture studies confirmed the importance of temperature in the physiology of foraminifera (e.g., Bijma et al., 1990). As a result, planktonic foraminiferal assemblages occur in five major faunal provinces: tropical, subtropical, transitional (or temperate), subpolar and polar (Bé, 1977) (Fig. 1.1, lower panel). Although the temperature limits of foraminifera are not sharply defined, each foraminiferal species has an optimum temperature and a range of temperature tolerance (Fig. 1.1, upper

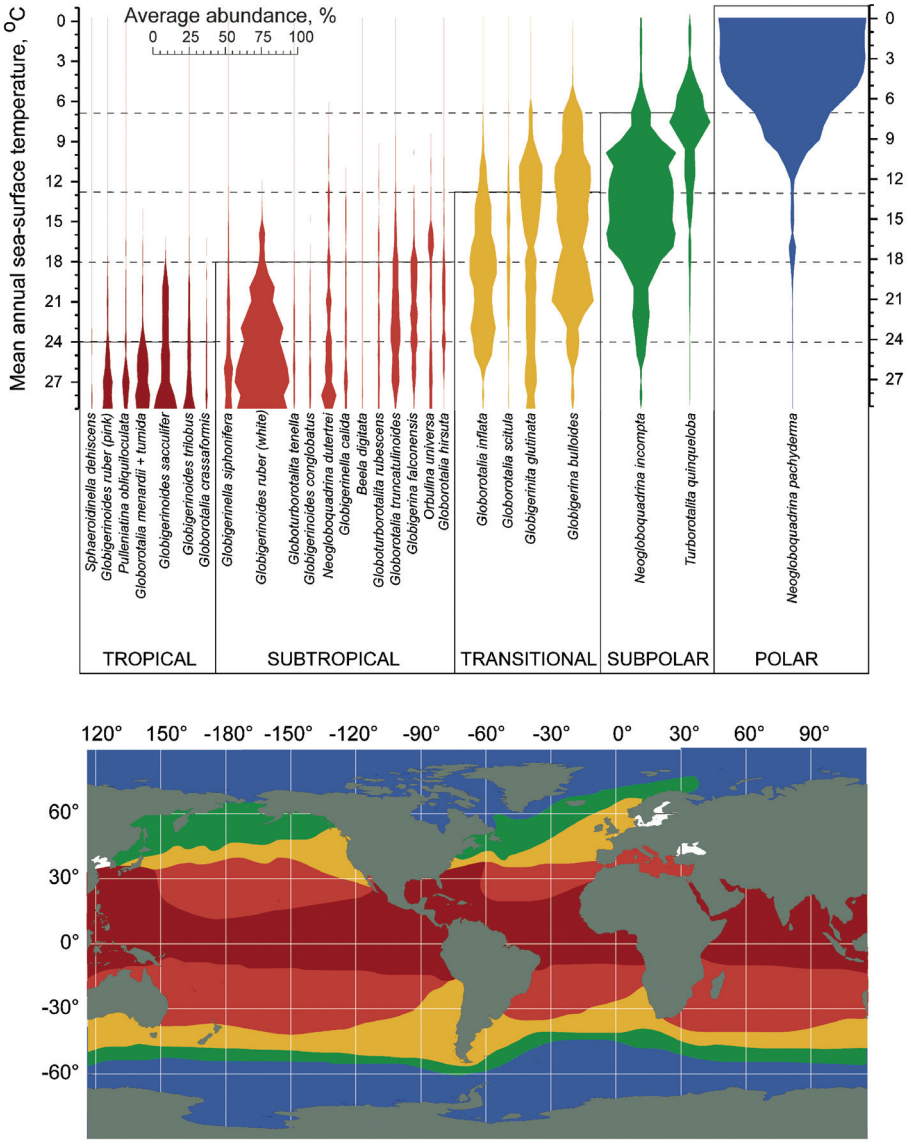

Figure 1.1: *The five major faunal provinces of modern planktonic foraminifera (lower panel). The distribution reflects the strong relationship between species occurrence and SST. in the upper panel, relative abundance of planktonic foraminifera species in surface sediment-samples of the Atlantic Ocean is shown (Kucera, 2007).*

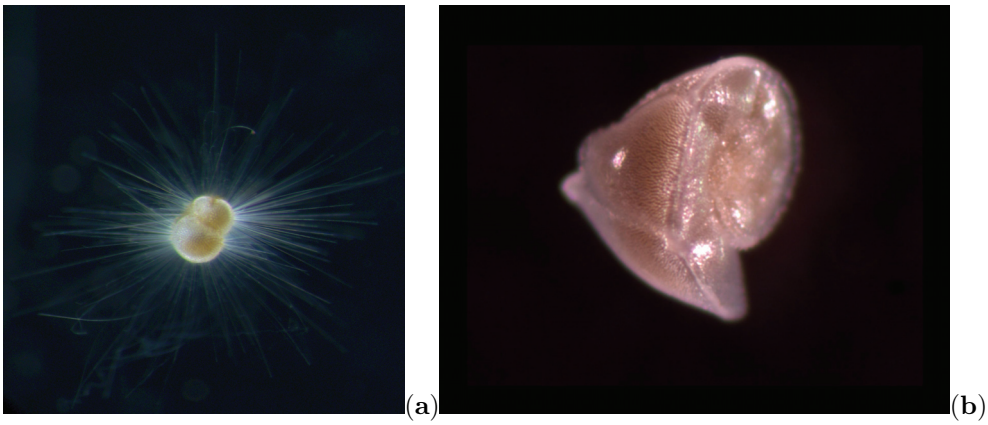

(a) **(b)**

Figure 1.2: *A living planktonic foraminifera,* **(a)** *G. sacculifer (approx. 300μm), one of the two most important spinose species in warm tropical surface waters.* **(b)** *G. truncatulinoides (approx. 500μm), a non-spinose species, living preferentially at the base of the thermocline. Photo: C. de Vargas, University of Alaska.*

panel). However, temperature seems to be critical only when it is at the limits of the tolerance range (Ortiz et al., 1995; Žarić et al., 2005). At a regional scale, food availability is an important factor controlling the abundance of foraminifera. The diet of foraminifera varies between species, but most species can consume a wide variety of preys. Some foraminifera species posses spines (Fig. 1.2), which seems to be a device for capturing preys (Bé, 1977; Sexton et al., 2006), although this is still not clear. Most foraminiferal species are opportunistic to some extent, but in general, spinose species depend on animal prey, including metazoans such as copepods or pteropods (Anderson, 1983; Caron and Bé, 1984; Spindler et al., 1984). Non-spinose species have more herbivorous behavior, and feed mainly on diatoms and dinoflagellates (Anderson et al., 1979; Spindler et al., 1984; Hemleben et al., 1985). Spinose species usually bear symbionts, commonly dinoflagellates or chrysophycophytes (e.g., Bé, 1977). The presence of symbionts enables foraminifera to survive in areas where nutrients and food are scarce but light is abundant, in particular subtropical and tropical oceanic environments (Hemleben et al., 1989; Murray, 1991; Hallock et al., 1991; Norris, 1996). Algal symbionts are also important for the calcification process, as they can modulate the chemical microenvironment around the shell (Kucera, 2007). Species-specific ecological needs are summarized in Table 1.1.

There are around 40-50 planktonic foraminifera species. However, genetic studies during the last years have shown that many of these species are comprised by dif-

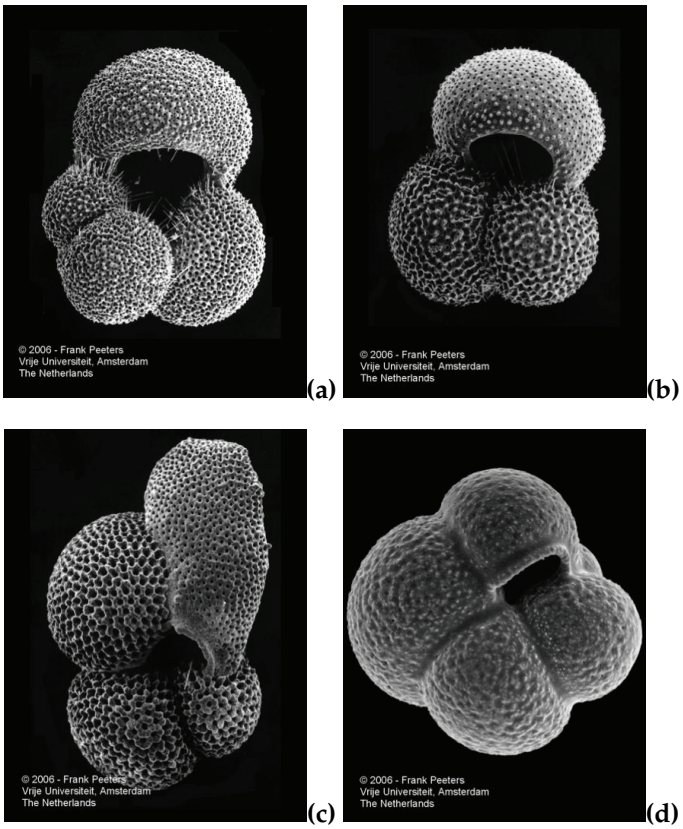

Figure 1.3: *Planktonic foraminifera fossil specimens:* **(a)** *G. bulloides (approx. 200μm),* **(b)** *G. ruber (approx. 200μm),* **(c)** *G. sacculifer (approx. 300μm) and* **(d)** *N. pachyderma (sin.) (approx. 150μm). Photo: F. Peeters, Free University of Amsterdam.*

ferent genotypes which are morphologically indistinguishable (Darling et al., 1999; Kucera and Darling, 2002; Darling et al., 2004, 2006). The main part of this dissertation focuses on the following foraminiferal species: *N. pachyderma* (sinistral and dextral varieties), *G. bulloides*, *G. ruber* (white variety) and *G. sacculifer* (Fig. 1.3). These five species, which have different geographical and ecological characteristics, are distributed worldwide and are well studied. Therefore, they represent the best subset of foraminifera used in paleoceanography.

***N. pachyderma* (sinistral variety)** *N. pachyderma* (sin) is a typical cold-water species and is the dominant species in polar water masses where it can survive even

within sea ice (Dieckman et al., 1991). It is a non-spinose species, and has an herbivorous diet, feeding mainly on diatoms (Hemleben et al., 1989; Murray, 1991). Therefore, maximum fluxes primarily occur when primary productivity is high (Žarić et al., 2005). *N. pachyderma* (sin.) is normally associated with weakly stratified waters and with deep mixed-layer depth. In polar waters it is found to live in the upper 100 m (Volkmann, 2000), whereas at temperate regions it seems to prefer deeper waters (Murray, 1991).

***N. pachyderma* (dextral variety)** *N. pachyderma* (dex.) is a subpolar species, typically occurring at high latitudes and upwelling regions. It has a preference for warmer temperatures than the sinistral variety, between $\sim$ 8-22°C (Žarić et al., 2005). The food is the same as the sinistral variety, which consists of phytoplankton (Hemleben et al., 1989). *N. pachyderma* (dex.) lives at the thermocline, and is often associated with maximum chlorophyll levels (Ortiz et al., 1995).

G. bulloides Temperature does not seem to strongly affect the abundance of *G. bulloides*. It can be found from polar to subtropical waters and is related to high productivity areas (Schiebel et al., 1997). Therefore, it is often used as an indicator of upwelling intensity. *G. bulloides* is a spinose species, but does not bear algal symbionts (e.g., Murray, 1991; Hemleben et al., 1989). It is considered an intermediate-dwelling species, and has a preference for weakly-stratified waters as characteristic of upwelling regions (Hemleben et al., 1989; Murray, 1991; Pujol and Grazzini, 1995).

***G. ruber* (white variety)** *G. ruber* (white) is in surface-dwelling species typically living in tropical-subtropical waters (Murray, 1991). It is a spinose species feeding mainly on zooplankton (copepods and tintinids), although it has less zooplankton dependence than other spinose species (Hemleben et al., 1989). It has a preference for stratified waters (Pujol and Grazzini, 1995), and is especially tolerant to varying sanities (Watkins et al., 1996).

G. sacculifer *G. sacculifer* is a typical tropical species. It possesses spines and bears dinoflagellate symbionts (Hemleben et al., 1989; Murray, 1991; Watkins et al., 1996). Its diet consists mainly of copepods, pteropods, tunicates and other zooplankton. It prefers shallow, stratified waters and is absent at low temperatures (optimum temperature range is $\geq$ 23°C) (Žarić et al., 2005).

Table 1.1: *Diet preferences of different foraminiferal species.*

Species	Diet	Spines	Symbiont	Source
N. pachyderma (sin.)	herbivore	no	barren	Hemleben et al. (1989)
N. pachyderma (dex.)	herbivore	no	barren	Hemleben et al. (1989)
G. bulloides	herbivore (more opportunistic)	yes	barren	Hemleben et al. (1989) Watkins and Mix (1998) Murray (1991) Lee and Anderson (1991)
G. ruber (white)	mostly carnivore	yes	bearing	Spindler et al. (1984) Hemleben et al. (1989) Watkins and Mix (1998)
G. sacculifer	mostly carnivore	yes	bearing	Spindler et al. (1984) Hemleben et al. (1989) Watkins and Mix (1998)

1.2 Planktonic foraminifera as paleoproxy

Reconstruction of past environmental conditions is possible by the use of proxies. These proxies allow the comparison and validation of climate-model simulations, thereby improving our ability to predict future climate change. Most evidence for paleoclimate is based on information derived from biological sources preserved in the fossil record. The mineralized shells of planktonic foraminifera preserve physico-chemical information of the water in which they grew. Thus, the shells of foraminifera deposited on the sea-floor are one of the most important fossils used in paleoceanography studies. Different oceanic properties such as paleoproductivity (e.g., Mulitza et al., 1999), paleotemperature (e.g., Malmgren et al., 2001) or surface-water stratification (e.g., Mulitza et al., 1997) can be derived from fossil shells.

Planktonic foraminifera can be used to reconstruct past oceanic temperatures by different methods: (1) Species abundances can be directly related to sea-surface temperature (SST), as most of the species are sensitive to temperature; (2) the chemical composition of calcitic shells is extensively used to derive the physico-chemical conditions of the environment where foraminifera grew; (3) morphological features of the shell can also be related to SST. Some examples of proxies based on morphology include shell size (Malmgren and Kennet, 1978; Hecht, 1976; Schmidt et al., 2003, 2004), shape (Kennett, 1968a,b; Spencer–Cervato and Thierstein, 1997), porosity (Berger, 1968; Frerichs et al., 1972; de Vargas et al., 1999; Itou et al., 2001) and coiling direction (Ericson, 1959; Kucera and Kennett, 2002) in particular species

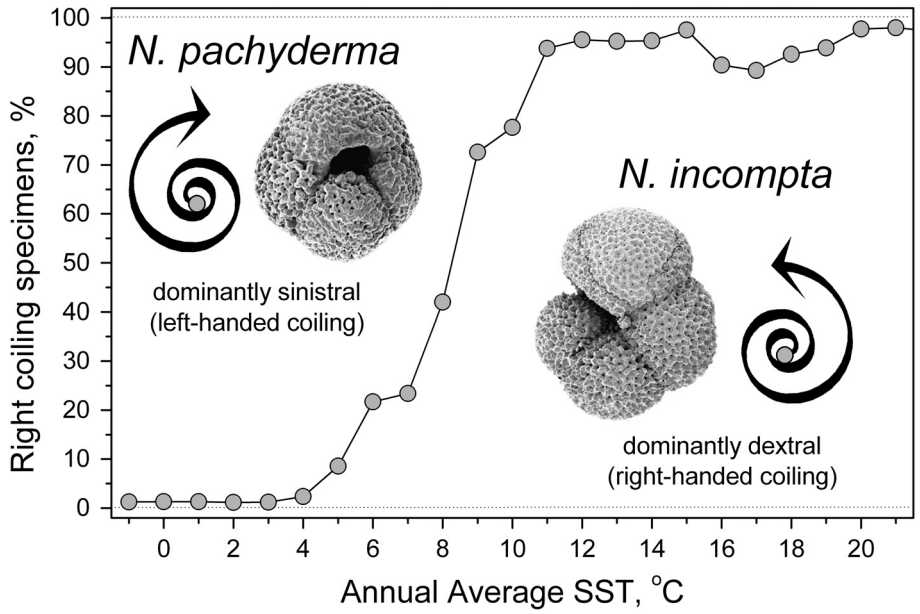

Figure 1.4: *Changes in coiling direction of Neogloboquadrina with temperature. At low temperatures the left-coiling specimens are dominant (N. pachyderma), and between 6-10°C the left coiling shells are replaced by the right-coiling shells (N. incompta) (Kucera, 2007).*

(Fig. 1.4). However, shell formation is a complex process which depends on many more factors than temperature. Therefore, the use of morphology as a paleotemperature proxy is considered less reliable. A detailed description of morphology-based proxies is described in the review paper by Kucera (2007). The following section is focused on species abundance and chemical composition as paleotemperature proxies, as these are the methods most widely used by paleoceanographers.

1.2.1 Foraminiferal abundance as a paleotemperature proxy

Most foraminifera species are sensitive to temperature. Murray (1897) was the first to infer that the foraminiferal distribution pattern was influenced by the climate. Since then, many investigations have demonstrated the potential use of foraminifera to study climate change. As foraminifera collection and species identification are relatively easy and economic techniques, these methods have been extensively used in paleoceanography. Using species composition for paleotemperature reconstructions can be done by two different approaches, using indicator species or assemblage composition.

Indicator species

This is the simplest technique for using planktonic foraminifera to trace environmental changes. It is based on variations in the abundance of individual species which are adapted to specific environmental conditions. For example, *G. bulloides* is species which is adapted to high productivity regions. Therefore, the presence of *G. bulloides* in sediments is an indicator of upwelling conditions (e.g., Thiede, 1975). Another example is the abundance of *N. pachyderma* (sin.), a typical polar species, which in temperate waters as a cooling indicator. However, ecological knowledge of individual species is often limited, and grouping similar species into assemblages may provide a more robust proxy.

Assemblage composition

The composition of planktonic foraminifera assemblages can be used to estimate past SSTs via transfer functions. Transfer functions provide a mathematical relationship relating species abundance to their life habitats, which is applied to the fossil fauna. The most simple equation to predict paleotemperature was introduced by Berger (1969). This equation relates the optimal temperature of each species to its relative abundance to yield an average estimate of SST. However, this approach does not account for the complex interactions between temperature and other parameters that influence distribution. A well known improvement in the precision of transfer function reconstructions was introduced by Imbrie and Kipp (1971). They applied multiple regression statistical techniques and Q-mode factor analysis to relate environmental parameters with species abundances in core-top samples. This method was the basis of the CLIMAP project to reconstruct the SST fields of the last glacial period (e.g., CLIMAP, 1976).

In more recent times, new statistical methods have been developed to improve the accuracy of paleotemperature reconstructions. For example, the modern analog technique (MAT) (Hutson, 1980) searches the entire calibration data set to find the most similar assemblages, and uses average SST of these locations. The modern analog technique with similarity index (SIMMAX) (Pflaumann et al., 1996) is also based on the degree of similarity between fossil and modern assemblages. This method uses a new similarity index and incorporates geographic information giving higher weight to samples that are closer to the fossil sample. The revised analog method (RAM) (Waelbroeck et al., 1998) increases the number and range of calibration samples and introduces more rigorous criteria for the selection of the best analog samples. Artificial neural network (ANN) is a computer-based method which, using artificial intelligence techniques, has the capability to autonomously "learn" the re-

lationship between assemblages of planktonic foraminifera and SST (Malmgren and Nordlund, 1997).

The transfer functions have yielded very good temperature reconstructions, with a prediction error of about 1°C (Malmgren et al., 2001). The simultaneous application of different transfer function techniques provides an objective tool for assessing the reliability of the proxies, and contributes to minimize bias associated with the technique (Kucera et al., 2005).

1.2.2 Foraminiferal shell chemistry as a paleotemperature proxy

Shells of foraminifera are built with calcite, but the exact composition of the calcite depends on the surrounding environmental conditions. During their life cycle, foraminifera record a chemical signature in their shell, that reflects the physico-chemical conditions of the surrounding water. The chemical composition of the shell is, thus, used to reconstruct paleoceanographic conditions (e.g., Rohling and Cooke, 1999). The most important proxies for SST are based on the oxygen isotope composition and Mg/Ca ratio of the calcite.

Stable isotopes in foraminiferal shells

Oxygen has three naturally occurring stable isotopes: ^{16}O ($\geq$99%), ^{17}O and ^{18}O. The absolute abundances of the isotopes are difficult to determine, and therefore the ratios between isotopes are often used to assess the isotopic composition. The term $\delta^{18}O$ is used to describe the oxygen isotope composition of the calcite, corresponding to the parts per thousand difference between the $^{18}O/^{16}O$ ratio of the sample and a known external standard (PDB standard). The $^{18}O/^{16}O$ in the shell depends mainly on two factors: on one hand, it depends on the isotopic composition of the sea-water, which at the same time depends on global ice volume. On the other hand, the oxygen isotope fractionation in carbonate is also a function of temperature. Therefore, by using an independent method to calculate ice volume, the temperature effect in the isotopic composition can be isolated and used to reconstruct paleotemperatures. The early work by Emiliani (1955) has been a basis for later studies. Although he initially overestimated the glacial-interglacial temperature changes by not removing the ice volume effect, this pioneering work has played an important role in paleoceanography and become one of the most important techniques in the reconstruction of past climates (Rohling and Cooke, 1999). Although $\delta^{18}O$ of the calcite is directly related to temperature, due to this double signal, it is most commonly used to reconstruct global ice volume by removing the temperature effect derived from an independent proxy (Shackleton, 1967; Shackleton and Opdyke, 1973).

Trace element composition in foraminiferal shell

The foraminiferal calcite is 99% $CaCO_3$, with the remaining 1% corresponding to trace elements such as Mg, Sr, Ba or Na (Lea, 1999). The ratios between trace elements can also be used to reconstruct past oceanic conditions, as some of the elemental substitution depends on environmental factors (Bender et al., 1975). The review paper by Rosenthal (2007) presents detailed description of proxies based on trace-elements. The most commonly used paleotemperature proxy is the ratio between Mg and Ca. The substitution of Ca by Mg is a temperature-dependent process: at higher temperatures more Mg is incorporated into the calcite (Mucci and Morse, 1990). Various approaches have been made to calibrate Mg/Ca ratios and temperature for several species of planktonic foraminifera. These include multi-species core-top calibration (e.g., Elderfield and Ganssen, 2000), culture calibrations for a limited number of species (e.g., Nürnberg et al., 1996) and sediment-trap based multi-species calibration (e.g., Anand et al., 2003). In general, there is good agreement between all these approaches. In recent years, foraminiferal Mg/Ca ratio has become one of the most important proxies for SST reconstructions (e.g., Cronblad and Malmgren, 1981).

1.2.3 Difficulties associated with foraminifera-based proxies

Although the precision of foraminifera-based proxies has increased in recent years, all these approaches bear problems associated with both pre-depositional and post-depositional alteration. Post-depositional alteration includes processes such as bioturbation, which mixes different age layers (e.g., Bé, 1977; Bé and Hutson, 1977; Boltovskoy, 1994) or advection of the shells during and after sinking (e.g., Bé, 1977). When using assemblage composition for reconstructions, selective dissolution may also lead to a bias in estimated temperature by removing the more fragile foraminiferal species preferentially (e.g., Berger, 1968; Thunell and Honjo, 1981; Le and Thunell, 1996; Dittert and Henrich, 1999).

There are other problems associated with environmental uncertainties during shell formation, often making the interpretation of proxy records difficult. One issue is related to the depth habitat of the species: some foraminiferal species migrate in the water column in order to satisfy their ecological needs (Bé, 1977). Therefore, the chemical signature recorded in the shell corresponds to an integrated signal over the life of the foraminifera at different depths. Differences in migration patterns between species and regions causes difficulties in the interpretation of the proxy records.

Another difficulty is related to differential foraminiferal production over the year: planktonic foraminifera have a relatively short life span, typically on the order of one month (Sautter and Thunell, 1991), and the signal recorded in a shell corresponds to the environmental conditions during this month. The proxy record in sediments is therefore dominated by the conditions during the season of maximum production. Depending on the species and ecological circumstances, the recorded signal may either represent the annual average or a single season of the year (Mix, 1987). As seasonal distribution plays an important role in the interpretation of proxy records, the main part of this dissertation will be focused on it.

1.3 Seasonality of planktonic foraminifera

One of the most important aspects of foraminiferal ecology is their annual distribution pattern, which has major implications for paleoceanography. Planktonic foraminifera have large seasonal variations in abundance tied closely to surface water hydrography (Bé, 1960; Deuser et al., 1981; Thunell and Reynolds, 1987; Sautter and Thunell, 1991). Such seasonality is an important issue when reconstructing past oceanic conditions, as the signal recorded in the shell corresponds to the time of the year during which the calcitic shell was deposited. Mix (1987) showed in a very simplified model that the temperature recorded by a temperature-sensitive foraminiferal population depends on the annual temperature cycle and the temperature sensitivity of the species. The overall flux (SF(T)) depends on the annual SST distribution at the site (W(T)) and the preferred temperature of the species (F(T)). Thus, theoretically, the temperature sensed by the mean population of a species (T_r) is the flux-weighted mean of all temperatures at the site:

$$T_r = \frac{\sum SF(T) \cdot W(T)}{\sum SF(T)} \tag{1.1}$$

This relation shows how temperature distribution and species-specific ecological preferences can influence the recorded signal. The ecology of planktonic foraminifera is therefore an important issue in paleoceanography, as the flux pattern influences the paleotemperature interpretation. One of the assumptions in paleoceanography is that the seasonality of foraminifera has remained unchanged through time,

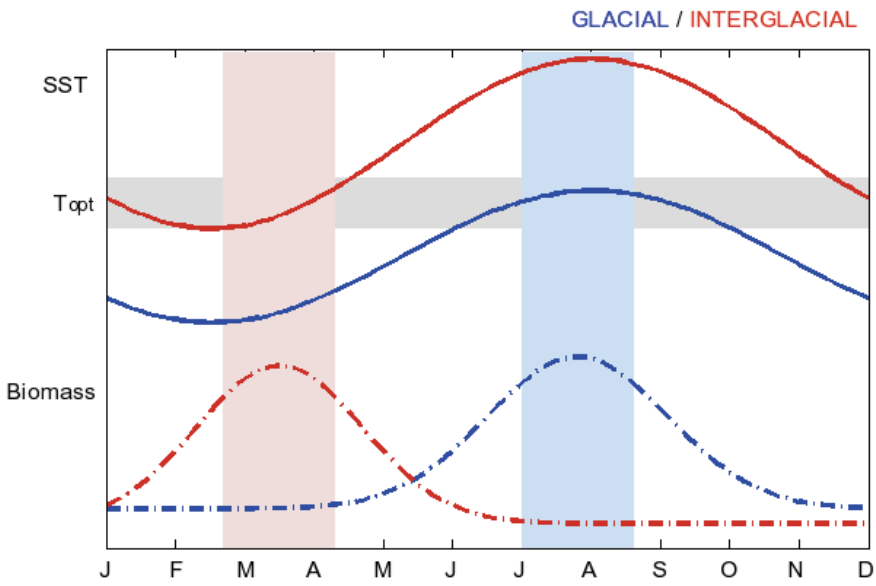

Figure 1.5: *Theoretical annual variation of SST in the northern hemisphere (solid line) and seasonal variation of a foraminiferal species at the same site (dashed line) for glacial (blue) and interglacials (red). During the interglacial, the optimal temperature range of the species (gray bar) occurs during spring, thus the species mainly records a spring signal. During glacials, the optimal temperature occurs during summer and the species will then record a summer signal.*

and therefore the sedimentary records reflect the same season as at present day. However, no researcher has shown this assumption to be true. If environmental conditions change (e.g., by climate change), foraminifera may respond by varying their seasonal distribution. Any shift in foraminiferal seasonality that may have occurred in the past will then lead to a bias in the estimated paleotemperature (Fig. 1.5). A growing number of proxies are derived from trace-element composition of foraminiferal shells, and are all affected by the differential seasonal production of foraminifera. The aim of our work is to assess this bias by studying variations in foraminiferal seasonality through time.

1.4 Scientific objectives

The goal of this study is to contribute to a better knowledge of foraminiferal seasonality. A modeling approach is used for a global assessment of the potential bias of foraminifera-based proxy records resulting from changes in seasonality at glacial-interglacial timescales. The main questions that arise from this study are:

- Is it possible to model planktonic foraminiferal distribution at a global scale?
- Can we predict the seasonal pattern of each foraminiferal species, and quantify the imprint of the distinct seasonal patterns preserved in the sedimentary record?
- Can we assess the response of planktonic foraminifera to different boundary conditions?
- Did the seasonal distribution of planktonic foraminifera vary from glacial times to present day?
- What are the implications of shifts in seasonal fluxes for the interpretation of down-core proxy records?

This work attempts to answer the mentioned questions by using a modeling approach. For that purpose, a numerical foraminiferal distribution model has been developed and implemented within an existing ecosystem model (Moore et al., 2002). The planktonic foraminifera model predicts the abundance of five frequently used foraminiferal species: *N. pachyderma* (sinistral and dextral varieties), *G. bulloides*, *G. ruber* (white variety) and *G. sacculifer* (Fig. 1.6). A fundamental issue in setting up the foraminiferal model is the food requirement for the different species. In addition, it is also important to know if a species has algal symbionts. Physico-chemical properties of the water are also important in influencing foraminiferal distribution, in particular SST. Based on climatological data and the specific ecological preferences of the different species, the model predicts monthly concentrations for each species. Both the ecosystem and foraminifera model are forced with physical and chemical boundary conditions. The forcing includes SST, solar radiation, mixed-layer depth, vertical velocity and the turbulent exchange rate at the base of the mixed-layer, sea-ice coverage and atmospheric iron flux. At each time step, the phytoplankton and zooplankton concentration predicted by the ecosystem model are used by the foraminifera model as food availability. Information on temperature sensitivity (optimum temperature and tolerance range) of planktonic foraminifera is available from a global set of moored sediment traps from the main oceanic provinces (Žarić et al.,

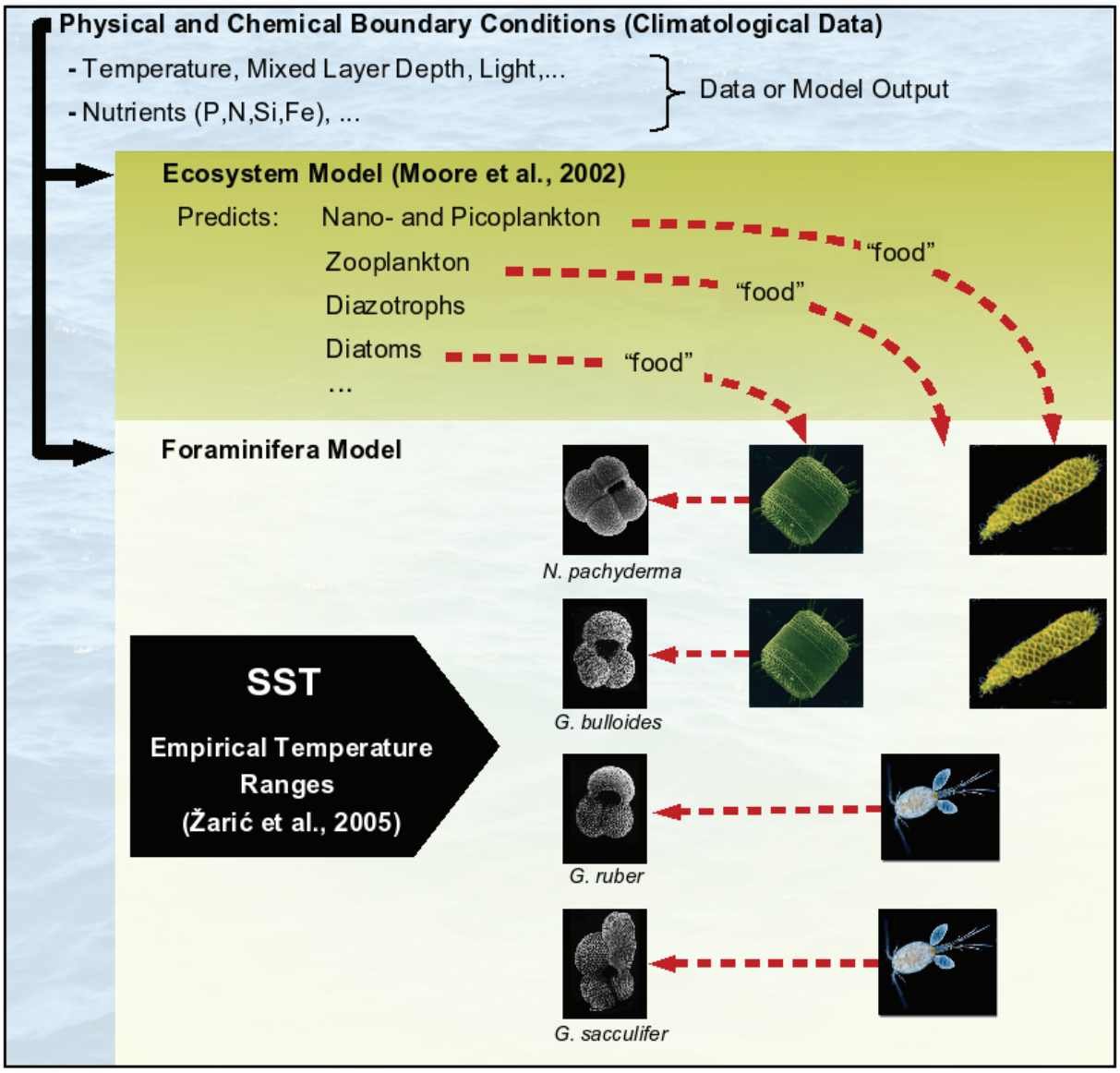

Figure 1.6: *Global Model Structure*

2005). Using this nonlinear dynamic model, monthly concentrations of the previously mentioned species have been predicted on a global scale. Sediment-trap data has been used to calibrate the model with respect to temperature, and to validate the predicted distribution with observational data. The spatial distribution of the species has been compared to core-top data (Pflaumann et al., 1996; Martinez et al., 1998; Prell et al., 1999). The model setup, equations and predicted distributions are described in detail in the first paper (chapter 1). Additionally, plankton-net samples from the North Atlantic have been analyzed to compare the model output with the living population in the upper water column (chapter 5).

Several sensitivity experiments have been carried out to study the response of planktonic foraminifera to changing environments (chapter 3). In these experiments, we varied the boundary conditions of temperature (decreasing SST globally or increasing the amplitude of temperature seasonality) and looked at the response of foraminifera to different environmental conditions. Temperature estimates derived using a species-specific methodology are strongly influenced by the seasonality of temperature-sensitive species. We assessed the implications that changes in foraminiferal seasonality may have in the recorded temperature signal under varying boundary conditions.

Chapter 4 presents model results for the distribution of planktonic foraminifera during the LGM. The modeled spatial distribution patterns of the species have been compared to GLAMAP and MARGO datasets (Pflaumann et al., 2003; Barrows and Juggins, 2004; Kucera et al., 2004a,b; Niebler et al., 2004; Kucera et al., 2005). The seasonal distribution of the species during the LGM has been compared to present day conditions. This study aims to detect shifts in foraminiferal seasonality between glacial-interglacial periods, and to quantify this seasonal bias due to interspecies differences in seasonality. The presented study suggests that foraminiferal seasonality has varied from LGM to present day conditions. These variations have to be taken into account in order to improve the accuracy of glacial SST reconstructions. A global assessment of the potential bias of foraminifera-based temperature estimates due to changes in seasonality at glacial-interglacial timescales is now possible.

Bibliography

Anand, P., Elderfield, H. and Conte, M. H.: Calibration of Mg/Ca thermometry in planktonic foraminifera from a sediment trap time-series, Paleoceanography, 18, 15, doi:10.1029/2002PA000846, 2003.

Anderson, O. R., Spindler, M., Be, A. W. H., and Hemleben, C.: Trophic activity of planktonic foraminifera, J. Mar. Biol. Assoc. U.K., 59, 791–799, 1979.

Anderson, O. R.: Radiolaria, Springer-Verlag, New York, pp. 355, 1983.

Arnold, A. J. and Parker, W. C.: Biogeography of planktonic Foraminifera, in: Modern Foraminifera, edited by: Gupta, B. S. K., Dortrecht, Boston, London, 103–122, 1999.

Barrows, T and Juggins, S., Compilation of planktic foraminifera LGM assembages from the Indo-Pacific Ocean, doi:10.1594/PANGAEA.227319, 2002.

Bé, A. W. H.: Ecology of recent planktonic foraminifera. Part 2. Bathymetric and seasonal distributions in the Sargasso Sea off Bermuda, Micropaleontology, 6, 373–392, 1960.

Bé, A. W. H.: Shell Porosity of Recent Planktonic Foraminifera as a Climatic Index, Science, 161, 881–884, 1968.

Bé, A. W. H.: An ecological, zoogeographic and taxonomic review of recent planktonic foraminifera, in: Oceanic Micropalaeontology, edited by: Ramsay, A. T. S., 1–100, Academic Press Inc., London, 1977.

Bé, A. W. H. and Hutson, W. H.: Ecology of planktonic foraminifera and biogeographic patterns of life and fossil assemblages in the Indian Ocean, Micropal., 23, 369–414, 1977.

Bender, M. L., Lorens, R. B. and Williams, D. F.: Sodium, magnesium and strontium in the test of planktonic foraminifera, Micropaleontology, 21, 448–459, 1975.

Berger, W. H.:Planktonic foraminifera: Selective solution and paleoclimatic interpretation, Deep–Sea Res., 15, 31–43, 1968.

Berger, W. H.: Ecologic patterns of living planktonic foraminifera, Deep–Sea Res., 16, 1–24, 1969.

Bijma, J., Faber, W. W. J., and Hemleben, C.: Temperature and salinity limits for growth and survival of some planktonic foraminifers in laboratory cultures, J. Foramin. Res., 20, 95–116, 1990.

Boltovskoy, D.: The sedimentary record of pelagic biogeography, Prog. Oceanogr., 34, 135–160, 1994.

Boyle, E. A.: Cadmium, zinc, copper, and barium in foraminifera tests, Earth Planet Sc. Lett., 53, 11–35, 1981.

Caron, D. A. and Bé, A. W. H.: Predicted and observed feeding rates of the spinose planktonic foraminifer *Globigerinoides sacculifer*, B. Mar. Sci., 35, 1–10, 1984.

CLIMAP Project Members: The surface of the ice–age earth, Science, 191, 1131–1137, 1976.

Cronblad, H. G. and Malmgren, B. A.: Climatically controlled variation of Sr and Mg in Quaternary planktonic foraminifera, Nature 291, 61–64, 1981.

Darling, K. F., Wade, C. M., Kroon, D., Leigh Brown, A. J., and Bijma, J.: The diversity and distribution of modern planktonic foraminiferal small subunit ribosomal RNA genotypes and their potential as tracers of present and past ocean circulations, Paleoceanography, 14, 3–12, 1999.

Darling, K. F., Kucera, M., Pudsey, C. J. and Wade, C. M.: Molecular evidence links cryptic diversification in polar plankton to Quaternary climate dynamics, Proc. Natl. Acad. Sci., U. S. A., 101, 7657-7662, 2004.

Darling, K. F., Kucera, M., Kroon, D., and Wade, C. M.: A resolution for the coiling direction paradox in *Neogloboquadrina pachyderma*, Paleoceanography, 21, 2011, doi:10.1029/2005PA001189, 2006.

de Vargas, C., Norris, R., Zaninetti, L., Gibb, S. W. and Pawlowski, J.: Molecular evidence of cryptic speciation in planktonic foraminifera and their relation to oceanic provinces, Proc. Natl. Acad. Sci. USA, 96, 2864–2868, 1999.

Deuser, W. G., Ross, E. H., Hemleben, C., and Spindler, M., Seasonal changes in species composition, numbers, mass, size, and isotopic composition of planktonic foraminifera settling into the deep Sargasso Sea, Palaeogeogr. Palaeocl., 33, 103–127, 1981.

Dieckmann, G. S., Spindler, M., Lange, M. A., Ackley, S. F., and Eicken, H.: Antarctic sea ice: a habitat for the foraminifer *Neogloboquadrina pachyderma*, J. Foramin. Res., 21, 182–189, 1991.

Dittert, N. and Henrich, R.: Carbonate dissolution in the South Atlantic Ocean: evidence from ultrastructure breakdown in *Globigerina bulloides*, Deep-Sea Res. I, 47, 603–620, 1999.

Duplessy, J. C., Delibrias, G., Turon, J. L., Pujol, C., and Duprat, J.: Deglacial warming of the Northeastern Atlantic Ocean: correlation with the paleoclimatic evolution of the European continent, Palaeogeogr. Palaeocl., 35, 121–144, 1981.

Elderfield, H. and Ganssen, G.: Past temperatures and $\delta^{18}O$ of surface ocean waters inferred from foraminiferal Mg/Ca ratios, Nature, 405, 442–445, 2000.

Emiliani, C.: Pleistocene temperatures, J. Geology, 63, 538–578, 1955.

Ericson, D. B.: Coiling Direction of Globigerina pachyderma as a Climatic Index, Science, 130, 219–220, 1959.

Frerichs, W. E., Heiman, M. E., Borgman, L. E. and Bé, A. W. H.: Latitudinal variations in planktonic foraminiferal test porosity; Part 1, Optical studies, J. Foramin. Res., 2, 6–13, 1972.

Hallock, P., Premoli Silva, I. and Boersma, A.: Similarities between planktonic and larger foraminiferal evolutionary trends through Paleogene paleoceanographic changes, Paleogeogr. Palaeocl, 83, 49–64, 1991.

Hecht, A. D.: An ecologic model for test size variation recent planktonic foraminifera: Application to the fossil record, J. Foramin. Res., 6, 295–311, 1976.

Hemleben, C., Spindler, M., Breitinger, J., and Deuser, W. G.: Field and laboratory studies of the ontogeny and ecology of *Globorotalia truncatulinoides* and *G. hirsuta* in the Sargasso Sea, J. Foramin. Res., 15, 254–272, 1985.

Hemleben, C., Spindler, M., and Anderson, O. R.: Modern Planktonic Foraminifera, Springer–Verlag, New York, 1989.

Hutson, W. H.: The Agulhas Current during the Late Pleistocene: Analysis of modern faunal analogs, Science, 207, 64–66, 1980.

Imbrie, J. and Kipp, N. G.: A new micropaleontological method for quantitative paleoclimatology: application to a late Pleistocene Caribbean core, in: The Late Cenozoic Glacial Ages, edited by K. K. Turekian, Yale University Press, New Haven, 71–181, 1971.

Itou, M., Ono, T., Oba, T. and Noriki S.: Isotopic composition and morphology of living *Globorotalia scitula*: a new proxy of sub–intermediate ocean carbonate chemistry?, Mar. Micropal., 42, 189–210, 2001.

Kennett, J. P.: *Globorotalia truncatulinoides* as a paleo–oceanographic index, Science, 159, 1461–1463, 1968.

Kennett, J. P.: Latitudinal Variation in *Globigerina pachyderma* (Ehrenberg) in surface sediments of the southwest Pacific Ocean, Micropaleontology, 14, 305–318, 1968.

Kucera, M. and Darling, K. F.: Cryptic species of planktonic foraminifera: their effect on paleoceanographic reconstructions, Philos. Tr. Roy. Soc. A, 360, 695–718, 2002.

Kucera, M. and Kennett, J. P.: Causes and consequences of a middle Pleistocene origin of the modern planktonic foraminifer *Neogloboquadrina pachyderma* sinistral, Geology, 30, 539–542, 2002.

Kucera, M., Weinelt, M., Kiefer, T., Pflaumann, U., Hayes, A., Weinelt, M., Chen, M. T., Mix, A. C, Barrows, T., Cortijo, E., Duprat, J., Juggins, S., Waelbroeck, C.: Compilation of planktic Foraminifera census data, LGM and SSTs from the Pacific Ocean, doi:10.1594/PANGAEA.227329, 2004.

Kucera, M., Weinelt, M., Kiefer, T., Pflaumann, U., Hayes, A., Weinelt, M., Chen, M. T., Mix, A. C, Barrows, T., Cortijo, E., Duprat, J., Juggins, S., Waelbroeck, C.: Compilation of planktic Foraminifera census data, LGM and SSTs from the Pacific Ocean, doi:10.1594/PANGAEA.227325, 2004.

Kucera, M., Rosell–Mele, A., Schneider, R., Waelbroeck, C., and Weinelt, M.: Reconstruction of sea–surface temperatures from assemblages of planktonic foraminifera: multi–technique approach based on geographically constrained calibration data sets and its application to glacial Atlantic and Pacific Oceans, Quat. Sci. Rev., 24, 951-998, 2005.

Kucera, M.,: Planktonic Foraminifera as Tracers of Past Oceanic Environments, in: Proxies in late Cenozoic paleoceanography, Developments in Marine Geology, Vol. 1, edited by: Hillaire–Marcel, C. and de Vernal, A. , Elsevier, Amsterdam, 213–262, 2007.

Langer, M. R., Silk, M. T. and Lipps, J. H.: Global ocean carbonate and carbon dioxide production: The role of reef foraminifera, J. Foramin. Res., 27, 271–277, 1997.

Lea, D. W.: Trace elements in foraminiferal calcite, in: Modern foraminifera, edited by: Gupta, B. S. K., Dortrecht, Boston, London, 259–277, 1999.

Le, J. and Thunell, R. C.: Modelling planktic foraminiferal assemblage changes and application to sea surface temperature estimation in the western equatorial Pacific Ocean, Mar. Micropal., 28, 211–229, 1996.

Lee, J. J., and Anderson, O. R.: Biology of Foraminifera, Academic Press, London, 1991.

Malmgren B. A. and Kennet, J. P.: Test size variation in *Globigerina bulloides* in response to Quaternary paleoceanographic changes, Nature, 275, 123–124, 1978.

Malmgren B. A. and Nordlund, U.: Application of artificial neural networks to paleoceanographic data, Paleogeogr. Palaeocl., 136, 359-373, 1997.

Malmgren, B. A., Kucera, M., Nyberg, J., and Waelbroeck, C.: Comparison of statistical and artificial neural network techniques for estimating past sea surface temperature from planktonic foraminifer census data, Paleoceanography, 16, 520–530, 2001.

Martinez, J. I., Taylor, L., Deckker, P., and Barrows, T.: Planktonic foraminifera from the eastern Indian Ocean: distribution and ecology in relation to the Western Pacific Warm Pool (WPWP), Mar. Micropal., 34, 121–151, 1998.

Mix, A., 1987. The oxygen–isotope record of glaciation, in: North America and adjacent oceans during the last deglaciation, The Geology of North America, Vol. K–3., edited by: Ruddiman, W. F. and Wright, H. E., Geol. Soc. Am., Boulder CO, 111–135, 1987.

Moore, J. K., Doney, S. C., Kleypas, J. A., Glover, D. M., and Fung, I. Y.: An intermediate complexity marine ecosystem model for the global domain, Deep-Sea Res. II, 49, 403–462, 2002a.

Moore, J. K., Doney, S. C., Glover, D. M., and Fung, I. Y.: Iron cycling and nutrient-limitation patterns in surface waters ofthe World Ocean, Deep-Sea Res. II, 49, 463–507, 2002b.

Mucci, A. and Morse, J. W.: Chemistry of low–temperature abiotic calcites: experimental studies on coprecipitation, stability, and fractionation, Rev. Aquat. Sci., 3, 217–254, 1990.

Mulitza, S., Dürkoop, A., Hale, W., Wefer, G., and Niebler, H. S.: Planktonic foraminiferaa as recorders of past surface–water stratification, Geology, 25, 335–338, 1997.

Mulitza, S., Arz, H., Kemle–von Mücke, S., Moos, C., Niebler, H. S., Pätzold, J. and Segl, M.: The South Atlantic Carbon Isotope Record of Planktic Foraminifera, in: Use of Proxies in Paleoceanography: Examples from the South Atlantic, edited by: Fischer, G. and Wefer, G., Springer–Verlag, Berlin Heidelberg, 427–445, 1999.

Murray, J: On the distribution of the pelagic Foraminifera at the surface and on the floor of the ocean, Natural Science, 11, 17–27, 1897.

Murray, J. W.: Ecology, and distribution of planktonic foraminifera, in: Biology of foraminfera, edited by: Lee, J. J. and Anderson, O. R., Academic Press, Harcourt, 255–284, 1991.

Niebler, H. S.: Assemblage of planktonic foraminifera for the last glacial maximum (LGM) in sediment cores from the South Atlantic, Department of Geosciences, Bremen University, doi:10.1594/PANGAEA.55260, 2004.

Norris, R. D.: Symbiosis and evolutionary innovation in the radiation of Paleocene planktic foraminifera, Paleobiology, 22, 461–480, 1996.

Nürnberg, D., Bijma, J. and Hemleben, C.: Assessing the reliability of magnesium in foraminiferal calcite as proxy for water mass temperature, Geochim. Cosmochim. Ac., 60, 803–814, 1996.

Ortiz, J. D., Mix, A. C., and Collier, R. W.: Environmental control of living symbiotic and asymbiotic foraminifera of the California Current, Paleoceanography, 10, 987–1009, 1995.

Parker, F. L.: Planktonic foraminiferal species in Pacific sediments, Micropaleontology, 8, 219–254, 1962.

Pflaumann, U., Duprat, J., Pujol, C., and Labeyrie, L. D.: SIMMAX: A modern analog technique to deduce Atlantic sea surface temperatures from planktonic foraminifera is deep-sea sediments, Paleoceanography, 11, 15–35, 1996.

Pflaumann, U., Sarnthein, M., Chapman, M., de Abreu, L., Funnell, B. M.; Hüls, M., Kiefer, T., Maslin, M. A.; Schulz, H., Swallow, J.; van Kreveld, S. A, Vautravers, M., Vogelsang, E., Weinelt, M.: Glacial North Atlantic: Sea surface conditions reconstructed by GLAMAP 2000, doi:10.1594/PANGAEA.692144. Supplement to: Pflaumann, U., Sarnthein, M., Chapman, M., de Abreu, L., Funnell,

B. M.; Hüls, M., Kiefer, T., Maslin, M. A.; Schulz, H., Swallow, J., van Kreveld, S. A, Vautravers, M., Vogelsang, E., Weinelt, M.: Glacial North Atlantic: Sea-surface conditions reconstructed by GLAMAP 2000, Paleoceanography, 18, 1065, doi:10.1029/2002PA000774, 2003.

Prell, W. L., Martin, A., Cullen, J., and Trend, M.: The Brown University Foraminiferal Data Base, IGBP PAGES/World Data Center-A for Paleoclimatology, Data Contribution Series # 1999-027, NOAA/NGDC Paleoclimatology Program, Boulder CO, USA, 1999.

Pujol, C. and Grazzini, C. V.: Distribution patterns of live planktic foraminifers as related to regional hydrography and productive systems of the Mediterranean Sea, Mar. Micropal., 25, 187–217, 1995.

Rohling, E. J. and Cooke, S.: Stable oxygen and carbon isotopes in foraminiferal carbonate shells in: Modern foraminifera, edited by: Gupta, B. S. K., Dortrecht, Boston, London, 239–258, 1999.

Rosenthal, Y.: Elemental proxies for reconstructing cenozoic seawater paleotemperatures from calcareous fossils, in: Proxies in late Cenozoic paleoceanography, Developments in Marine Geology, Vol. 1, edited by: Hillaire–Marcel, C. and de Vernal, A. , Elsevier, Amsterdam, 765–797, 2007.

Rutherford, S., D´Hondt, S. and Prell, W.: Environmental controls on the geographic distribution of zooplankton diversity, Nature, 400, 749–753, 1999.

Sautter, L. R. and Thunell, R. C.: Seasonal succession of planktonic foraminifera: results from a four–year time–series sediment trap experiment in the northeast Pacific, J. Foramin. Res., 19, 253–267, 1989.

Sautter, L. R. and Thunell, R. C.: Planktonic foraminiferal response to upwelling and seasonal hydrographic conditions: sediment trap results from San Pedro Basin, Southern California Bight, J. Foramin. Res., 21, 347–363, 1991.

Shackleton, N. J.: Oxygen isotope analysis and Pleistocene temperature reassessed, Nature, 215, 15–17, 1967.

Shackleton, N. J. and Opdyke, N. D.: Oxygen isotope and palaeomagnetic stratigraphy of equatorial Pacific core V28–238: oxygen isotope temperatures and ice volumes on a 105 and 106 year scale, Quaternary Res., 3, 39–55, 1973.

Schiebel, R., Bijma, J., and Hemleben, C.: Population dynamics of the planktic foraminifer *Globigerina bulloides* from the eastern North Atlantic, Deep–Sea Res. I, 44, 1701–1713, 1997.

Schmidt, D. N., Renaud, S. and Bollmann, J.: Response of planktic foraminiferal size to late Quaternary climate change, Paleoceanography, 18, 10.1029/2002PA000831, 2003.

Schmidt, D. N., Renaud, S., Bollmann, J., Schiebel., R. and Thierstein, H. R.: Size distribution of Holocene planktic foraminifer assemblages: Biogeography, ecology and adaptation, Mar. Micropal., 50, 319–338, 2004.

Sexton, P. F., Wilson, P. A. and Pearson, P. N.: Palaeoecology of late middle Eocene planktic foraminifera and evolutionary implications, Mar. Micropal., 60, 1–16, 2006.

Spencer–Cervato, C. and Thierstein, H. R.: Fist appearance of *Globorotalia truncatulinoides*: cladocenensis and immigration, Mar. Micropaleontol, 30, 267–291, 1997.

Spindler, M., Hemleben, C., Salomons, J. B., and Smit, L. P.: Feeding behavior of some planktonic foraminifers in laboratory cultures, J. Foramin. Res., 14, 237–249, 1984.

Thiede, J.: Distribution of foraminifera in coastal waters of an upwelling area, nature, 253, 712–714, 1975.

Thunell, R. C., Honjo, S.: Seasonal and interannual changes in the planktonic foraminiferal production in the North Pacific, Nature, 328, 335–337, 1987.

Tolderlund, D. S. and Bé, A. W. H.: Seasonal distribution of planktonic Foraminfera in the western North Atlantic, Micropalaeontology, 17, 297–329, 1971.

Volkmann, R.: Planktic foraminifers in the outer Laptev Sea and the Fram Strait - modern distribution and ecology, J. of Foramin. Res., 30,, 157–176, 2000.

Waelbroeck, C., Labeyrie, L., Duplessy, J. C., Guiot, J., Labracherie, M., Leclair, H. and Duprat, J.: Improving past sea surface temperature estimates based on planktonic fossil faunas, Paleoceanography, 13, 272–283, 1998.

Watkins, J. M., Mix, A. C., and Wilson, J.: Living planktic foraminifera: tracers of circulation and productivity regimes in the central equatorial Pacific, Deep-Sea Res. II, 43, 1257–1282, 1996.

Žarić, S., Donner, B., Fischer, G., Mulitza, S., and Wefer, G.: Sensitivity of planktic foraminifera to sea surface temperature and export production as derived from sediment trap data, Mar. Micropal., 55, 75–105, 2005.

Published as: Fraile, I., Schulz, M., Mulitza, S. and Kucera, M., 2008. Predicting the global distribution of planktonic foraminifera using a dynamic ecosystem model. Biogeosciences, 5, 891–911.

Chapter 2

Predicting the global distribution of planktonic foraminifera using a dynamic ecosystem model

Abstract

We present a new planktonic foraminifera model developed for the global ocean mixed-layer. The main purpose of the model is to explore the response of planktonic foraminifera to different boundary conditions in the geological past, and to quantify the seasonal bias in foraminifera-based paleoceanographic proxy records.

This model is forced with hydrographic data and with biological information taken from an ecosystem model to predict monthly concentrations of the most common planktonic foraminifera species used in paleoceanography: N. pachyderma (sinistral and dextral varieties), G. bulloides, G. ruber (white variety) and G. sacculifer. The sensitivity of each species with respect to temperature (optimal temperature and range of tolerance) is derived from previous sediment-trap studies.

Overall, the spatial distribution patterns of most of the species are in agreement with core-top data. N. pachyderma (sin.) is limited to polar regions, N. pachyderma (dex.) and G. bulloides are the most common species in high productivity zones, while G. ruber and G. sacculifer are more abundant in tropical and subtropical oligotrophic waters. For N. pachyderma (sin) and N. pachyderma (dex.), the season of maximum production coincides with that observed in sediment-trap records. Model and sediment-trap data for G. ruber and G. sacculifer show, in general, lower concentrations and less seasonal variability at all sites.

A sensitivity experiment suggest that, within the temperature-tolerance range of a species, food availability may be the main parameter controlling its abundance.

2.1 Introduction

Planktonic foraminifera are widely used for paleoceanographic reconstructions. The spatial distribution of planktonic foraminifera species is controlled by physiological requirements, feeding preferences and temperature (e.g., Bé and Hamilton,

1967; Bé and Tolderlund, 1971). Shells of planktonic foraminifera extracted from marine sediments serve as an archive of chemical and physical signals that can be used to quantify past environmental conditions, such as temperature (e.g., Pflaumann et al., 1996; Malmgren et al., 2001), ocean stratification (e.g., Mulitza et al., 1997), atmospheric CO_2 concentration (Pearson and Palmer, 2000) and biological productivity (Kiefer, 1998). Past sea-surface temperatures can be estimated by either quantifying differences between modern and fossil species assemblages (e.g., CLIMAP, 1976; Pflaumann et al., 1996; Malmgren et al., 2001), or by analyzing the isotopic or trace-element composition of the calcite in the shell (e.g., Rohling and Cooke, 1999; Lea, 1999). In general, all estimation procedures are based on a correlation between modern environmental condition and assemblage composition or shell chemistry.

Seasonal changes in the flux of planktonic foraminifera are strongly influenced by environmental factors, such as sea-surface temperature, the stratification of the water column, and food supply (e.g., Bijma et al., 1990; Ortiz et al., 1995; Watkins et al., 1996; Watkins and Mix, 1998; Eguchi et al., 1999; Schnack-Schiel et al., 2001; King and Howard, 2003a; Morey et al., 2005; Žarić et al., 2005). The seasonality of foraminiferal production is an important factor which has to be taken into account in paleoceanographic interpretations (e.g., Deuser and Ross, 1989; Wefer, 1989; Mulitza et al., 1998; Ganssen and Kroon, 2000; King and Howard, 2001; Pflaumann et al., 2003; Waelbroeck et al., 2005). Any change in the timing of the seasonal maximum of foraminiferal flux may lead to a bias in estimated paleotemperature. Mulitza et al. (1998) have shown how temperature sensitivity can alter the proxy record in the sediment. Moreover, this differences in seasonality make reconstructed temperatures based on planktonic foraminifera assemblages difficult to compare with those derived by other sea-surface temperature proxies. For example, Niebler et al. (2003) suggested that discrepancies between temperature reconstructions based on foraminifera and alkenones might be due to different ecological and thus seasonal preferences of alkenone producing algae and planktonic foraminifera. Climate change could induce variations in the seasonal succession of the planktonic foraminifera and such variations need to be quantified to correctly interpret corresponding proxy-based reconstructions.

To study the seasonal variations of planktonic foraminifera species we have developed a numerical model for planktonic foraminifera at a species level. Previously, Žarić et al. (2006) developed an statistical model based on hydrographic and productivity data. In contrast to the model of Žarić et al. (2006), we present a dynamic model which, considering ecological processes, calculates the growth rate of the foraminifera population between successive time steps. This study shows model predictions for spatial and temporal distribution patterns of the five most important modern planktonic foraminifera used as SST proxies.

2.2 Model setup

The geographical distribution and population density of each planktonic foraminifera species depend on biotic (e.g., food, symbionts) and abiotic factors (e.g., light, temperature). To supply the foraminifera model with ecological information, we run the foraminifera module within an ecosystem model.

2.2.1 Ecosystem model

The employed marine ecosystem model (Moore et al., 2002) is configured for the global mixed-layer of the ocean. It predicts the distribution of zooplankton, diatoms, diazotrophs and a generic group of phytoplankton (so-called 'small phytoplankton'). The model considers sinking and non-sinking detrital pools, and carries nitrate, ammonium, phosphate, iron and silicate as nutrients.

The ecosystem model is driven by hydrographic data that are derived from a general ocean circulation model and from climatologies. The forcing data include local processes of turbulent mixing, vertical velocity at the base of the mixed layer, and seasonal mixed-layer entrainment/detrainment. Horizontal advection is not included; thus, there is no lateral exchange between grid points. Since our main interest is the ecosystem in the mixed layer, processes below the surface layer are ignored.

Previously, this two-dimensional model has been validated against a diverse set of field observations from several JGOFS (Joint Global Ocean Flux Study) and historical time series locations (Moore et al., 2002), satellite observations, and global nutrient climatologies (Moore et al., 2002b). The full list of model terms, parametrizations, resolution, equations and behavior in the global domain is described in detail in Moore et al. (2002,b) and the code is available at
http://usjgofs.whoi.edu/mzweb/jkmoore/areadme.html.

2.2.2 PLAFOM

The planktonic foraminifera model determines the global distribution of the following 5 species: *Neogloboquadrina pachyderma* (sinistral and dextral coiling varieties), *Globigerina bulloides*, *Globigerinoides ruber* (white variety) and *Globigerinoides sacculifer*. These species have often been considered to be sensitive to sea-surface temperature, and therefore their assemblage can be used to estimate past sea-surface temperatures by means of transfer functions.

Each species has a different food preference (Hemleben et al., 1989; Watkins et al., 1996; Schiebel et al., 1997; Watkins and Mix, 1998; Arnold and Parker, 1999). In general, spinose species prefer animal prey such as copepods (Spindler et al., 1984;

Caron and Bé, 1984; Hemleben et al., 1989) while non-spinose species are largely herbivorous (Anderson et al., 1979; Spindler et al., 1984; Hemleben et al., 1985, 1989), although in some specimens muscle tissue has been found in food vacuoles (Anderson et al., 1979; Hemleben et al., 1989). Many species also contain algal symbionts that may provide nutrition (Caron et al., 1981; Gastrich, 1987; Ortiz et al., 1995). On a seasonal scale, it is generally assumed that food is the predominant factor affecting the distribution of planktonic foraminifera under favorable temperatures (Ortiz et al., 1995). Planktonic foraminifera appear to respond to the redistribution of nutrients and phytoplankton very quickly, increasing in number of individuals within several days (Schiebel et al., 1995). Information about food availability is obtained from the ecosystem model. In the model, the food sources may be either zooplankton, small phytoplankton, diatoms or organic detritus.

For compatibility with the ecosystem model, the foraminifera model calculates foraminiferal abundance of each species via carbon biomass, the same as the ecosystem model. Since our study is directed to paleotemperature reconstructions, our main interest is in species relative abundances rather than in assessing the absolute biomass.

Accordingly, for each species the change in foraminifera concentration is calculated as follows:

$$\frac{dF}{dt} = (GGE \cdot TG) - ML \tag{2.1}$$

where F is the foraminifera carbon concentration, and GGE (gross growth efficiency) is the portion of grazed matter that is incorporated into foraminifera biomass, which we assume to be constant regardless of the food source. TG and ML represent total grazing and mass loss, respectively.

Growth (TG)

The growth rates are determined by available food using a modified form of Michaelis-Menton kinetics (Eq. 2.2),

$$TG = \sum_{n=1}^{4} p_n \cdot \left[G_{\max_n} \cdot \alpha \cdot F \cdot \left(\frac{C_n}{(C_n + g)} \right) \right] \tag{2.2}$$

where $G_{\max}$ is the maximum grazing rate, g is the half saturation constant for grazing, α is the relative efficiency for grazing in relation to temperature (calibrated from relative abundances), C_n represents the concentration of each type of food (diatoms (D), small phytoplankton (SP), zooplankton (Z) or detritus (DR)), and p is the preference for this food (assumed to be invariant in time). The values and units

of all parameters are summarized in Table 2.1. Food requirements vary for the different foraminifera species. Many species of planktonic foraminifera consume a wide variety of zooplankton and phytoplankton prey, and they are capable of a reasonably flexible adaptation to varying trophic regimes. The food of *N. pachyderma* (sinistral and dextral varieties) consist almost exclusively phytoplankton, commonly diatoms (Hemleben et al., 1989). *G. bulloides* presents biological characteristics that place it on the border between spinose and non-spinose species; while most spinose species carry algal symbionts, *G. bulloides* does not (Gastrich, 1987; Hemleben et al., 1989; Schiebel et al., 1997). It is abundant in periods of high phytoplankton productivity (Prell and Curry, 1981; Reynolds and Thunell, 1985; Hemleben et al., 1989) and feeds on algal prey (Lee et al., 1966). *G. bulloides* is common in mid-latitude and subpolar waters, but it is also present in the subtropical waters of the Indian Ocean. It is generally more abundant in eutrophic waters with high phytoplankton productivity and for this reason it is commonly used as a productivity proxy (Hemleben et al., 1989; Sautter and Thunell, 1989; Ortiz et al., 1995; Guptha and Mohan, 1996; Watkins and Mix, 1998). *G. ruber* exhibits two varieties; a pink and a white form. The pink variety is limited to the Atlantic Ocean, and we have therefore only modeled the white variety. *G. ruber* (white) is a spinose species generally found in tropical to subtropical water masses. It hosts dinoflagellate endosymbionts, and feeds mostly on zooplankton, although it has lower zooplankton dependence than other spinose species (Hemleben et al., 1989). The characteristics of bearing spines, utilization of zooplankton prey and symbiotic association are typical of foraminifera adapted to oligotrophic waters. *G. sacculifer* is also a spinose species hosting dinoflagellate endosymbionts. Culture experiments with *G. sacculifer* confirm that it depends on zooplankton food (Bé et al., 1981). It is also adapted to low productivity areas, mainly the centers of the oceanic gyres. Watkins et al. (1996) suggested that the adaptation to oligotrophic waters is possible because these foraminifera obtain nutrition from their symbionts. However, the seasonal maximum abundance occurs when productivity in these regions is maximal. To account for adaptation to low productivity regions, we limited the growth of *G. ruber* and *G. sacculifer* to regions in which maximum nutrient and chlorophyll concentration does not exceed a threshold value. This is done multiplying "total grazing" (Eq. 2.2) by a hyperbolic tangent function which, using maximum nitrate and chlorophyll concentration as input, identifies low productivity zones.

Maximum grazing rate for the foraminifera ($G_{\max}$) varies with the food source. Zooplankton carbon concentration is generally much lower than phytoplankton carbon concentration. For this reason, when zooplankton is the food source $G_{\max}$, is set higher than if phytoplankton or detritus are the food source. Thus, under typical food availability conditions, carnivore species can grow as fast as herbivore species.

Based on the observation that most planktonic foraminifera distribution patterns are latitudinal and correlate with temperature, we assume that temperature is the most important physical parameter controlling the distribution of planktonic foraminifera. This is supported by the experimental work of Bijma et al. (1990), which showed evidence for direct temperature control over vital processes. These authors demonstrated that a correlation exists between in vitro temperature tolerance limits and the known natural limits of the species used in their experiments. The tolerance limits of most species are most likely progressive since a departure from optimal growth conditions causes a gradual reduction of vital processes (Arnold and Parker, 1999). Žarić et al. (2005, 2006) compiled planktonic foraminiferal fluxes from sediment-trap observations across the World Ocean. They analyzed species sensitivity to temperature by relating fluxes and relative abundances of seven species to sea-surface temperature. Based on this work, we approximate the temperature relation with a normal distribution. Therefore each species exhibits an optimal SST and an SST tolerance range. The growth rate (Eq. 2.1) is limited by temperature through the parameter α (Eq. 2.3).

$$\alpha = \left[n \cdot \exp\left[-0.5 \cdot \left(\frac{(T_s - T_{\mathrm{opt}})}{\sigma} \right)^2 \right] \right]^{\left(\frac{1}{k}\right)} \tag{2.3}$$

The relationship with temperature assumes that the foraminifera concentration at any site is normally distributed, with an optimum temperature where the relative abundance is highest. Away from this optimum temperature the relative abundance decreases until a critical temperature beyond which the species does not occur. This pattern, with a central peak and symmetrical tails, can be approximated by Gaussian distribution (Eq. 2.3). The value of α varies between 0 (out of limit of tolerance) and 1 (optimal temperature).

The parameter n is a arbitrary parameter that scales the values of α between 0 and 1. T_{opt} and T_s are the optimum and actual temperatures, respectively, and σ is the tolerance range of a species. Species with small σ are more sensitive to temperature. The values of all parameters for each species are summarized in Table 2.1. Of the five species, *G. ruber* (white) and *G. sacculifer* (both tropical species), together with *N. pachyderma* (sin.) exhibit the narrowest SST tolerance range. *N. pachyderma* (sin.) is absent above 23.7°C (Žarić et al., 2005). *N. pachyderma* (sin.) is a polar species and survives even within sea ice (Antarctic), where it feeds on diatoms (Dieckman et al., 1991; Spindler, 1996). *N. pachyderma* (dex.) and *G. bulloides* are present almost throughout the entire oceanic SST range; however, *N. pachyderma* (dex.) exhibits a clear preference for intermediate temperatures. For *G. bulloides*, temperature does not seem to be a controlling factor. It is generally more abundant in eutrophic waters with high phytoplankton productivity, and for this reason it is commonly used as

a productivity proxy (Hemleben et al., 1989; Sautter and Thunell, 1989; Ortiz et al., 1995; Guptha and Mohan, 1996; Watkins and Mix, 1998). It has the second largest temperature tolerance, after *N. pachyderma* (dex.), and does not show a unimodal distribution when flux is plotted versus temperature (Žarić et al., 2005). *G. bulloides* comprises at least six different genetic types and exhibits a polymodal distribution pattern (Darling et al., 1999, 2000; Stewart et al., 2001; Kucera and Darling, 2002; Darling et al., 2003). Žarić et al. (2005) showed that in the tropical Indian Ocean, *G. bulloides* is present at higher temperatures than in the Atlantic and Pacific Ocean. In this region, highest abundances of *G. bulloides* occur at SSTs at which Atlantic as well as Pacific samples show reduced fluxes. Since our study is applied at a global scale, the temperature calibration is based on the preferred temperatures of *G. bulloides* in the Pacific and Atlantic Ocean. In Eq. 2.5 we modified the normal distribution for *N. pachyderma* (dex.) and *G. bulloides* to accept wider limits under high food availability through the parameter k (see Table 2.1).

Mass loss (ML)

The mass loss (mortality) equation comprises of three terms representing losses due to natural death rate (respiration loss), predation by higher trophic levels and competition (Eqs. 4–8).

$$\mathrm{ML} = predation + death\ rate + competition \tag{2.4}$$

$$predation = pl \cdot \exp\left(-4000 \cdot \left[\frac{1}{T_{sk}} - \frac{1}{T_{mk}}\right]\right) \cdot (F_p)^2 \tag{2.5}$$

with

$$F_p = \max((F - 0.01), 0) \tag{2.6}$$

$$death\ rate = rl \cdot F_p \tag{2.7}$$

$$competition = \sum \left[F_p \cdot \frac{cl_{ij} \cdot F_i \cdot d}{F_i \cdot d + 0.1}\right] \tag{2.8}$$

Since our model does not include lateral advection, a minimum threshold is needed to preserve the foraminifera population over the winter at high latitudes or during periods with insufficient food supply in regions with high seasonal variability. We set the minimum foraminifera biomass at 0.01 mmolC/m^3. When the populations reach this minimum level the mortality term is set to zero (Eq. 2.6). Predators specialized on planktonic foraminifera are not known, and therefore, the mortality

Table 2.1: *Model parameters.*

Species	*N. pachyderma* (sin.)	*N. pachyderma* (dex.)	*G.bulloides*	*G.ruber* (white)	*G. sacculifer*
σ	4.0	6.0	6.0	4.0	4.0
T_{opt}	3.8	15.0	12.0	23.5	28
k	1	1.2^{SP}	1.25^{D}	1	1
$p(SP)$	0.3	0.2	0.15	0.0	0.0
$p(D)$	0.7	0.8	0.45	0.2	0.1
$p(Z)$	0.0	0.0	0.15	0.6	0.7
$p(DR)$	0.0	0.0	0.25	0.2	0.2
$p\prime(SP)$	–	0.4	0.2	–	0.0
$p\prime(D)$	–	0.6	0.8	–	0.3
$p\prime(Z)$	–	0.0	0.0	–	0.6
$p\prime(DR)$	–	0.0	0.0	–	0.1
$G_{\max}(SP, D, DR)$	1.08	1.08	1.08	1.08	1.08
$G_{\max}(Z)$	2.16	2.16	2.16	2.16	2.16
g	0.66	0.66	0.66	0.66	0.66
$cl_{\textit{N. pachyderma}(\mathrm{sin.}),j}$	–	0.2	0	0	0
$cl_{\textit{N. pachyderma}(\mathrm{dex.}),j}$	–	–	0.1	1	0
$cl_{\textit{G. bulloides}}$	–	0.5	–	1	1
$cl_{\textit{G. ruber}(\mathrm{white}),j}$	–	0.8	0.5	–	0.8
$cl_{\textit{G. sacculifer},j}$	–	0	0.5	0.8	–
d	–	0.05	0.5	1	1
pl	1	4	5	5	4
rl	0.06	0.06	0.06	0.06	0.06
GGE	0.3	0.3	0.3	0.3	0.3

σ = standard deviation of optimal temperature
T_{opt} = optimal temperature (°C)
k = parameter for the range on temperature depending on the food availability
$p(SP)$ = preference for grazing on small phytoplankton
$p(D)$ = preference for grazing on diatoms
$p(Z)$ = preference for grazing on zooplankton
$p(DR)$ = preference for grazing on detritus
$p\prime$ = preference for grazing when main food source is missing
$G_{\max}(SP)$ = maximum grazing rate when grazing on small phytoplankton (per day)
$G_{\max}(D)$ = maximum grazing rate when grazing on diatoms (per day)
$G_{\max}(Z)$ = maximum grazing rate when grazing on zooplankton (per day)
$G_{\max}(DR)$ = maximum grazing rate when grazing on detritus (per day)
g = half-saturation constant for grazing
GGE = portion of grazed matter that is incorporated into foraminifera biomass (Gross Growth Efficiency)
pl = quadratic mortality rate coefficient
rl = respiration loss (per day)
cl_{ij} = effect of competition of the species i upon the species j
d = *e*-folding constant, which controls the steepness of the
Michaelis-Menton equation for competition C = food type (SP, D, Z or DR)
SP = small phytoplankton [mmolC/m^3]
D = diatoms [mmolC/m^3]
Z = zooplankton [mmolC/m^3]
DR = detritus [mmolC/m^3]

equation does not explicitly depend upon predator abundance. To represent predation, we choose a quadratic form which depends on foraminiferal biomass itself (Eq. 2.5). This may be interpreted either as predation by a higher trophic level not being explicitly modeled (Steele and Henderson, 1992; Edwards and Yool, 2000). The parameter pl represents the quadratic mortality-rate coefficient, which is used to scale mass loss to grazing. From a bioenergetic perspective, predation is also temperature dependent. Food consumption rates typically increase with increasing temperature; therefore higher trophic levels will exert more predation pressure with increasing temperature (M. Peck, personal communication). The parameter b is used to scale the temperature function between 0 and 1. Note that T_{sk} represents the absolute SST, and the maximum SST (T_{mk}) assumed in the model corresponds to 303.15 K (30°C). Death rate refers to natural physiological biomass losses, including respiration (Eq. 2.7). It is a linear term of 6% per day (rl), the same value used by Moore et al. (2002) for zooplankton.

The presence and activity of one species influences negatively the resource availability for another species, leading to the assumption that competition occurs between different species of foraminifera inhabiting the same regions (Eq. 2.8). In this equation, F_i is the concentration of the foraminiferal species exerting competition, cl_{ij} represents the maximum competition pressure of the species i upon the species j (varying from 0 to 1) and d is the *e*-folding constant, which controls the steepness of the Michaelis-Menton-type equation.

2.2.3 Standard model experiment: grid, forcing and boundary conditions

The foraminifera model is run within the ecosystem model for the global surface ocean, with a longitudinal resolution of 3.6°, a varying latitudinal resolution (between 1 – 2°, with higher resolution near the equator), and a temporal resolution of one month. This corresponds to the resolution of the underlying ecosystem model (Moore et al., 2002,b).

We used the same forcing as Moore et al. (2002). Mixed-layer temperatures are taken from the World Ocean Atlas 1998 (Conkright et al., 1998), surface shortwave radiation from the ISCCP cloud-cover-corrected dataset (Bishop and Rossow, 1991; Rossow and Schiffer, 1991) and climatological mixed-layer depths from Monterey and Levitus (1997). The minimum mixed-layer depth is set at 25 m. The vertical velocity at the base of mixed layer is derived from the NCAR-3D ocean model (Gent et al., 1998). The turbulent exchange rate at the base of the mixed layer is set to a constant value of 0.15 m/day. Sea-ice coverage was obtained from the EOSDIS NSIDC satellite data (Cavalieri et al., 1990). Atmospheric iron flux was obtained

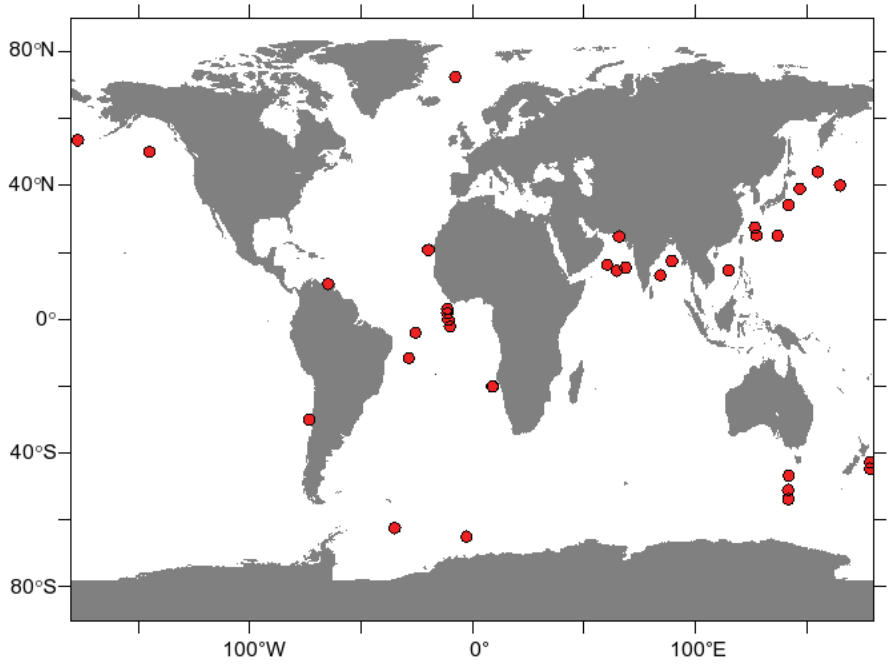

Figure 2.1: *Locations of the sediment-trap stations used to compare measured and modeled foraminiferal fluxes. See Table 2.2 for details.*

from the dust deposition model study of Tegen and Fung (1994, 1995). More details about the forcing can be found in Moore et al. (2002).

Bottom boundary conditions are the same as for the zooplankton component of the ecosystem model. For all foraminifera species we assumed a uniform distribution inside the mixed layer, whereas below the mixed layer the concentration was calculated as a function of the surface concentration and the mixed-layer depth. When the mixed-layer is thin, the foraminiferal concentration below the mixed-layer is set to 75% of the surface concentration. With increasing mixed-layer depth, the concentration below decreases linearly, until reaching the value 0 at a mixed layer depth of 100 m. This is a realistic limit, as the maximum production of the species in question occurs within this depth range (Bé, 1977; Duplessy et al., 1981; Murray, 1991; Watkins and Mix, 1998).

2.2.4 Comparison to core-top data

Since our main interest is to understand the distribution of planktonic foraminifera at geological timescales, we used the Brown University Foraminiferal Database (Prell et al., 1999) to compare our model results with sedimentary faunal assemblages. This database contains core-top planktonic foraminifera counts from 1264 cores across the world ocean. We extended this database with the dataset by Pflaumann et al. (1996), which contains planktonic foraminifera counts for 738 surface sediment samples from the North and South Atlantic; and with another 57 core-top samples from the eastern Indian Ocean (Martinez et al., 1998). For comparison, the relative abundances were recalculated using only the five foraminifera species under consideration. Additionally, the number of individuals was transformed to biomass (mgC/m^3) to take into account the size differences of each species. For this transformation, we calculated the volume occupied by the cytoplasm approximating the shape of all the species to a sphere and assuming that all the volume is occupied by the cytoplasm. For the mean size of each species we used sediment-trap data from Peeters et al. (1999). We assumed the carbon content of the cytoplasm is $0.089\,pgC/\mu m^3$ (Michaels et al., 1995), the same in all species.

To assess the deviation between observed and modeled species distributions, we calculated the root mean squared error (RMSE). For this, the data from each each core-top sample was compared to the nearest model grid point. No averaging was applied to the core-top data. This is justified because the observational data base is identical for all species and our interest is only to test model performance for the five species.

2.2.5 Comparison to sediment-trap data

Several sediment-trap studies were used to compare measured and modeled foraminiferal fluxes (Table 2.2). Sediment traps show a high temporal resolution and record the flux continuously over several months or years. Because of the sinking speed of foraminiferal shells (150 – 1300 m/day depending on their weight and size; Takahashi and Bé, 1984), the sediment-trap samples are not significantly affected by dissolution, lateral advection or bioturbation, and therefore can be related directly to modern surface hydrography (e.g., Tedesco and Thunell, 2003; Marchant et al., 2004; Mohiuddin et al., 2004; Žarić et al., 2005). However, due to the short duration of the collecting periods those data may represent local processes of a particular year rather than a long term mean. We used the global database compiled by Žarić et al. (2005, 2006). This database contains planktonic foraminiferal fluxes calculated from various sediment-trap investigations across the world ocean. To compare the modeled and observed annual distribution of the different planktonic foraminifera

species we used those datasets with a minimum collecting period of one year and at least monthly resolution. We extended the database of Žarić et al. (2005, 2006) by adding trap data from the northwest Pacific (Oda and Yamasaki, 2005; Xu et al., 2005), Bering Sea (Asahi and Takahashi, 2007), South China Sea (Tian et al., 2005) and Arabian Sea (Schulz et al., 2002). Table 2.2 summarizes locations, details and references of the sediment-trap studies used in this study. Fig. 2.1 illustrates locations of the sediment traps.

sediment-trap studies yield fluxes based on individual shells [ind. $m^{-2}\,day^{-1}$] whereas the model provides concentrations [$mmolC/m^3$]. To compare model output with observations, we assume that the flux through the water column is proportional to the surface concentration. The objective of our study is to detect relative changes in the seasonal distribution, rather than to assess foraminiferal biomass.

2.2.6 Sensitivity analysis of the parameters

To determine values for biological parameters is difficult as, unlike many chemical or physical parameters, they cannot strictly be regarded as constants. The free parameters have been tuned based on ecological knowledge about different species of foraminifera. In an attempt to assess the sensitivity of the model to the chosen values, we developed a sensitivity analysis of the parameters. The procedure used was similar to other marine plankton models (e.g., Fasham et al., 1990). We kept the parameters that are common to the ecosystem model constant, and modified only the values chosen for the foraminifera module. We run the model with each parameter altered by half and twice the standard value respectively to determine which parameters have the most effect (Table 2.3). In case of the parameter p (preference for the food type), we decreased the main food source was decreased by 50%, sharing this part between the other food sources (scaled relative to the original p in one experiment, a; and sharing equally between the other food sources during the experiment b). To test the effect of competiton we carried out three experiments: first, reducing experienced competition by 50%, a second experiment swithching it off completely and the last experiment increasing competition by 50%. For parameter choice, we compared modelled annual mean realtive abundances and core-top data. The sensitivity was quantified by calculating the change of RMSE between sensitivity experiment and standard run. Sensitivities of the species to each parameter are given in Table 2.3.

Table 2.2: *Locations, trap and water depths, sieve size and data sources of the planktonic foraminifera faunas (Žarić et al. (2005) and additional data).*

Trap Location	Latitude[° N]	Longitude[° E]	Trap depth [m]	Water depth [m]	Sieve size [μm]	References
Ocean Station Papa	50.00	−145.00	3800	4240	≥125	Reynolds and Thunell (1985) Sautter and Thunell (1989) Wong et al. (1999)
Peru-Chile Current	−30.01	−73.18	2318	4345	≥150	Marchant et al. (1998) Hebbeln et al. (2000)
N′ North Atlantic	72.38	−7.71	500;1000;2300	2624	≥125	Jensen (1998)
	69.69	0.48	500;1000	3254	≥125	Peinert et al. (2001)
Cape Blanc	20.76	−19.74	2195	3646	≥150	Fischer and Wefer (1996)
	21.15	−20.68	732;3552	4103	≥150	Fischer et al. (1996) Žarić et al. (2005)
W′ equatorial Atlantic	−4.00	−25.57	652;1232;4991	5330	≥150	Fischer and Wefer (1996)
	−7.52	−28.04	631; 5031	5570	≥150	Fischer (unpubl. data) Žarić et al. (2005)
W Atlantic	−11.57	−28.53	719; 4515	5472	≥150	Fischer (unpubl. data) Žarić et al. (2005)
Walvis Ridge	−20.05	9.16	599;1648	2202	≥150	Fischer and Wefer (1996)
	−20.13	8.96	1717	2263	≥150	Žarić et al. (2005)
Weddell Sea	−62.44	−34.76	863	3880	≥125	Donner and Wefer (1994)
	−64.91	−2.55	256;4456	5032	≥125	
Arabian Sea	16.33	60.49	1028; 3026	4016	≥150	Curry et al. (1992)
	14.49	64.76	733; 2909	3901	≥150	Guptha and Mohan (1996)
	15.48	68.74	1401; 2775	3774	≥125	Haake et al. (1993)
	24.65	65.81	590	1166	≥125	Schulz et al. (2002)
Bay of Bengal	17.45	89.60	967; 1498; 2029	2263	≥150	Guptha and Mohan (1996)
	13.15	84.35	950; 2286	3259	≥150	Guptha et al. (1997)
Northwest Pacific	25.00	136.99	917;1388;4336;4758	5107	≥125	Mohiuddin et al. (2002)
	39.01	147.00	1371; 1586; 4787	5339	≥125	
NW′ North Pacific	50.02	165.03	3260	5570	≥125	
	43.97	155.05	2957	5370	≥125	Kuroyanagi et al. (2002)
	40.00	165.00	2986	5483	≥125	
Subantarctic Zone	−46.76	142.07	1060;3850	4540	≥150	King and Howard (2003a,b)
	−51.00	141.74	3080	3780	≥150	Trull et al. (2001)
	−53.75	141.76	830; 1580	2280	≥150	
Chatman Rise	−42.70	178.63	300;1000	1500	≥150	King and Howard (2003a,b)
	−44.62	178.62	300;1000	1500	≥150	Nodder and Northcote (2001)
Cariaco Basin	10.50	−64.67	275	1400	≥125	Tedesco and Thunell (2003)
Japan Trench	34.16	141.98	1174;3680	8942	≥125	Oda and Yamasaki (2005)
	34.17	141.97	1174;3700	8941	≥125	
Ryukyu Islands	27.38	126.73	1000	1627	≥125	Xu et al. (2005)
	25.07	127.58	3000	3771	≥125	
Bering Sea	53.30N	−177	3198	3788	≥125	Asahi and Takahashi (2007)
	49	−174	4812	5406	≥125	
South China Sea	14.60	115.11	1208	4270	≥125	Tian et al. (2005)

Table 2.3: *Sensitivity analysis to the parameter values: Reduction of parameter values and resulting change of RMSE between the model and core-top relative abundances (RMSE sensitivity experiment minus RMSE standard run)*

Experiment	Parameter change	*N. pachyderma* (sin.)	*N. pachyderma* (dex.)	*G.bulloides*	*G.ruber* (white)	*G. sacculifer*
1	p_{main} (-50%)	–0.3	4.6	–2.9	–4.7	0.6
2	p_{main} (-50%)	–0.3	4.6	–2.9	–4.7	0.6
3	d (-50%)	–	4.0	–0.2	–1.9	–0.7
4	d (-100%)	–	4.6	0.8	6.4	1.9
5	d $(+50\%)$	–	3.4	–0.5	–5.3	0.7
6	$G_{\max}$ (-50%)	2.9	3.6	–1.9	–5.6	–0.5
7	$G_{\max}$ $(+50\%)$	–0.0	4.1	0.7	–6.2	0.6
8	σ (-50%)	1.1	2.1	4.1	–7.1	–1.0
9	σ $(+50\%)$	7.4	5.2	–0.1	–4.0	1.3

Experiments:
1 = Reduction of main food preference, $p(SP, D, ZOorDR)$, by 50%; sharing this part between the other food sources (scaled in relation to original p)
2 = Reduction of main food preference, $p(SP, D, ZOorDR)$, by 50%; sharing this part equally between the other food sources
3 = Reduction of experienced competition by 50%
4 = Suppression of competition
5 = Increase of experienced competition by 50% 6 = Decrease of maximum grazing rate, $G_{\max}$ by 50%
7 = Increase of maximum grazing rate, $G_{\max}$ by 50%
8 = Decrease of temperature tolerance range, σ by 50%
9 = Increase of temperature tolerance range, σ by 50%

2.3 Results

2.3.1 Spatial distribution patterns

Modeled global distribution patterns of the five foraminifera species are shown together with the corresponding core-top data in Figs. 2.2 – 2.6. The model results are expressed as relative abundances as derived from the biomass data. Relative abundances for core-top data consider only the five species included in the model. The global distribution of *N. pachyderma* (sin.) shows the lowest RMSE, around 9%, while for the remaining the species the error varies between 22% and 25%.

N. pachyderma (sin.) is a cold-water species, and dominates planktonic foramini-

feral assemblages in polar waters (Pflaumann et al., 1996; Bauch et al., 2003; Kucera et al., 2005). Previous work has shown that it can survive within Antarctic sea ice (Dieckman et al., 1991; Spindler, 1996; Schnack-Schiel et al., 2001). It is usually used as a proxy for cold water conditions (Bauch et al., 1997). Core-top, as well as modeled assemblages, show the highest relative abundances (up to 100%) in polar waters (Fig. 2.2).

N. pachyderma (dex.) is typical of subpolar to transitional water masses. In the surface sediment samples, *N. pachyderma* (dex.) shows a very high relative abundance in the North Atlantic Ocean, the Benguela upwelling system, parts of the Southern Ocean and in the equatorial upwelling of the Pacific Ocean. It is also present, although at lower abundance, in the upwelling systems off northwest Africa. The model output shows very high concentrations in the Peru-Chile current and the eastern boundary upwelling systems, as well as south of Iceland, and moderate abundances at mid latitudes (Fig. 2.3).

Like *N. pachyderma* (dex.), *G. bulloides* typically occurs in subpolar and transitional water masses (Bradshaw, 1959; Tolderlund and Bé, 1971; Bé, 1977), and is also found in upwelling areas (Duplessy et al., 1981; Thunell and Honjo, 1984; Hemleben et al., 1989). Temperature does not seem to be a controlling factor in the distribution of this species, although the exact relationship between environmental parameters and geographical distribution of *G. bulloides* may be masked by the fact that this species group comprises several distinct genotypes (Darling et al., 1999, 2000; Stewart et al., 2001; Kucera and Darling, 2002; Darling et al., 2003). Generally, the abundance of *G. bulloides* is related to high productivity areas (Prell and Curry, 1981; Bé et al., 1985; Hemleben et al., 1989; Giraudeau, 1993; Watkins and Mix, 1998; Žarić et al., 2005). *G. bulloides* shows a high relative abundance in the surface sediment samples of the North Atlantic Ocean, the upwelling systems off northwest and southwest Africa, the Southern Ocean, the northern Indian Ocean, and to a lesser extent, the upwelling region off Baja California. The model results show high concentrations of *G. bulloides* in the subpolar waters of both hemispheres, in the eastern boundary currents of the southern hemisphere and in some locations of the Arabian Sea (Fig. 2.4).

The seafloor record shows high relative abundance of *G. ruber* (white) in the central North and South Atlantic as well as the South Pacific and less pronounced relative abundance in the South Indian Ocean up to 40° S. The model output shows a similar pattern with high relative abundances in tropical and subtropical waters of the Atlantic, Pacific and Indian Oceans, and very low relative abundances in upwelling areas (Fig. 2.5).

G. sacculifer shows a clear preference for high temperatures (optimum of 28°C) and is absent (or in concentrations $\leq$10%) below 23°C (Žarić et al., 2005). Core-top

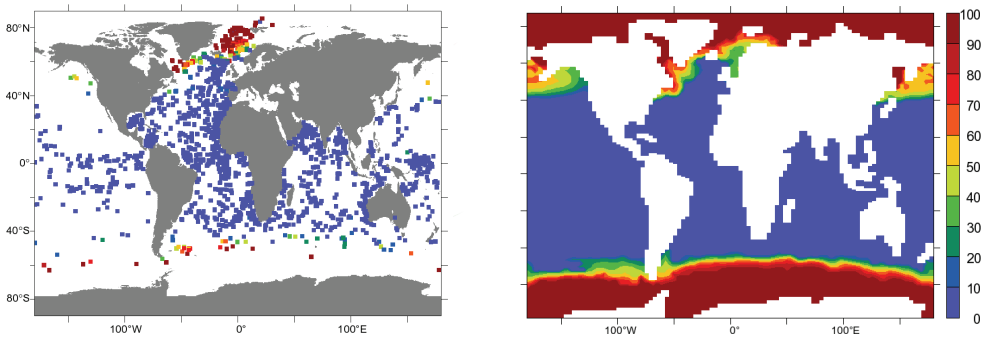

Figure 2.2: *N. pachyderma (sin.) relative abundances (%) from core-top (left) foraminiferal assemblages (Pflaumann et al., 1996; Martinez et al., 1998; Prell et al., 1999) and model output (right). Relative abundances consider only the species included in the model. RMSE is 9%.*

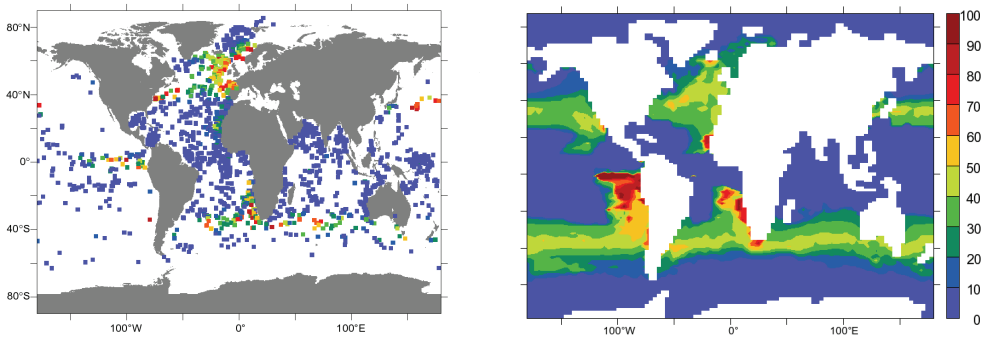

Figure 2.3: *N. pachyderma (dex.) relative abundances (%) from core-top (left) foraminiferal assemblages (Pflaumann et al., 1996; Martinez et al., 1998; Prell et al., 1999) and model output (right). Relative abundances consider only the species included in the model. RMSE is 22%.*

data show this species is limited to tropical waters, reflecting its narrow temperature tolerance (Fig. 2.6). The highest abundances occur in surface sediments from the equatorial Pacific and central Indian Ocean. The relative abundance in most of the core-top data from the upwelling region of the Arabian Sea is 10%. The annual mean distribution pattern of *G. sacculifer* in the model is limited to tropical waters, with highest concentrations in the equatorial Pacific. The model correctly simulates absence or low concentrations (10%) in eastern upwelling systems as well as in the upwelling area of the Arabian Sea.

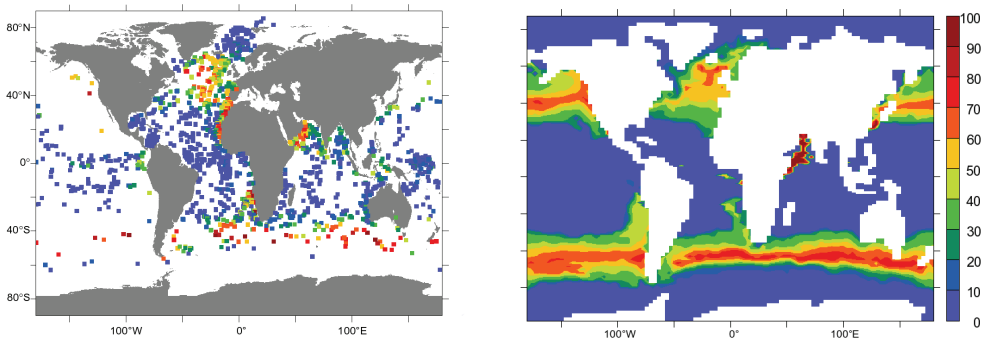

Figure 2.4: *G. bulloides relative abundances (%) from core-top (left) foraminiferal assemblages (Pflaumann et al., 1996; Martinez et al., 1998; Prell et al., 1999) and model output (right). Relative abundances consider only the species included in the model. RMSE is 25%.*

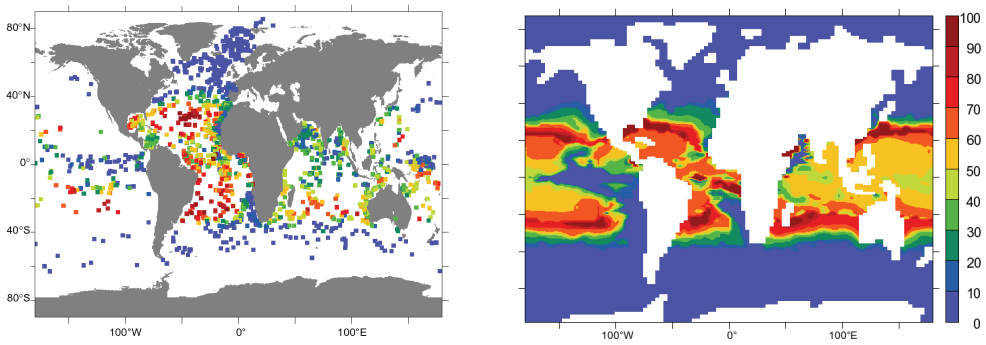

Figure 2.5: *G. ruber (white) relative abundances (%) from core-top (left) foraminiferal assemblages (Pflaumann et al., 1996; Martinez et al., 1998; Prell et al., 1999) and model output (right). Relative abundances consider only the species included in the model. RMSE is 25%.*

2.3.2 Temporal distribution patterns

We used several sediment-trap datasets to assess the modeled seasonal variations in foraminifera abundance. We limit the following comparison between the model output and the sediment-trap data to a few examples (Figs. 2.7 – 2.11).

In most of the cases, the sediment-trap data exhibit very pronounced interannual variability. In contrast, the model is forced with climatological data (i.e., long-term averages), and is therefore unable to reproduce interannual variability. For that rea-

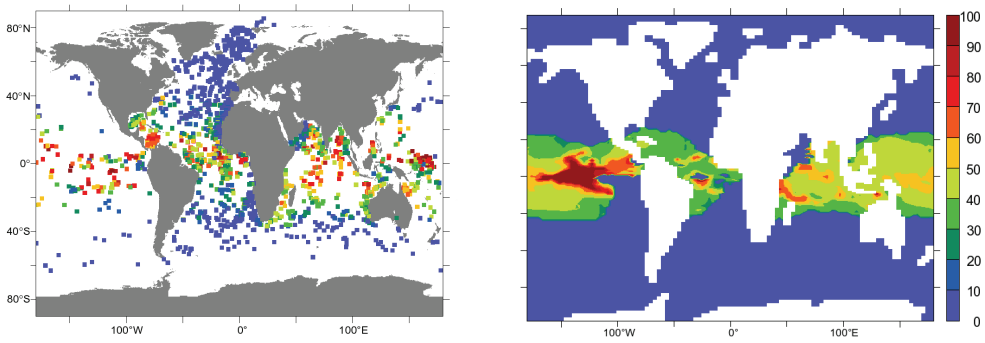

Figure 2.6: *G. sacculifer relative abundances (%) from core-top (left) foraminiferal assemblages (Pflaumann et al., 1996; Martinez et al., 1998; Prell et al., 1999) and model output (right). Relative abundances consider only the species included in the model. RMSE is 23%.*

son, we focused on the season with maximum production. In order to compare modeled and observed time series, we picked the season when maximum foraminiferal production occurs (Table 2.4). When sediment-trap were deployed for more than one year we considered the season in which most maxima occur.

Interannual variability of *N. pachyderma* (sin.) in all the locations is very high (Fig. 2.7), but the timing of the signal agrees between observed and predicted data.

The flux of *N. pachyderma* (dex.) increases during summer (July-October) in northern North Atlantic (Fig. 2.8a). The seasonal pattern of predicted concentrations corresponds well with the trap record.

Sediment-trap data located at Subantarctic Zone show an increase of the *N. pachyderma* (dex.) population during the summer (January-February). In accordance with the sediment-trap data, the model results also show the highest concentrations during the summer (Fig. 2.8b).

Examples for *G. bulloides* are shown in Fig. 2.9.

At Walvis Ridge, the sediment-trap data reveals a strong seasonality, where maxima occurs in fall (September-November) and in spring (May-June). The model successfully captures this bimodal pattern, with the main bloom occurring in spring. The second example represents a station north of the Kuroshio current in the northwest Pacific (Fig. 2.9b). At this location the model predicts a small peak during winter (December-January) and the maximum during early summer (May-June). The time-series record also presents this bimodal pattern; nevertheless, model and sediment-trap show better correspondence during the second year.

In general, *G. ruber* (white) show, less variability in the sediment-trap data (Fig. 2.10).

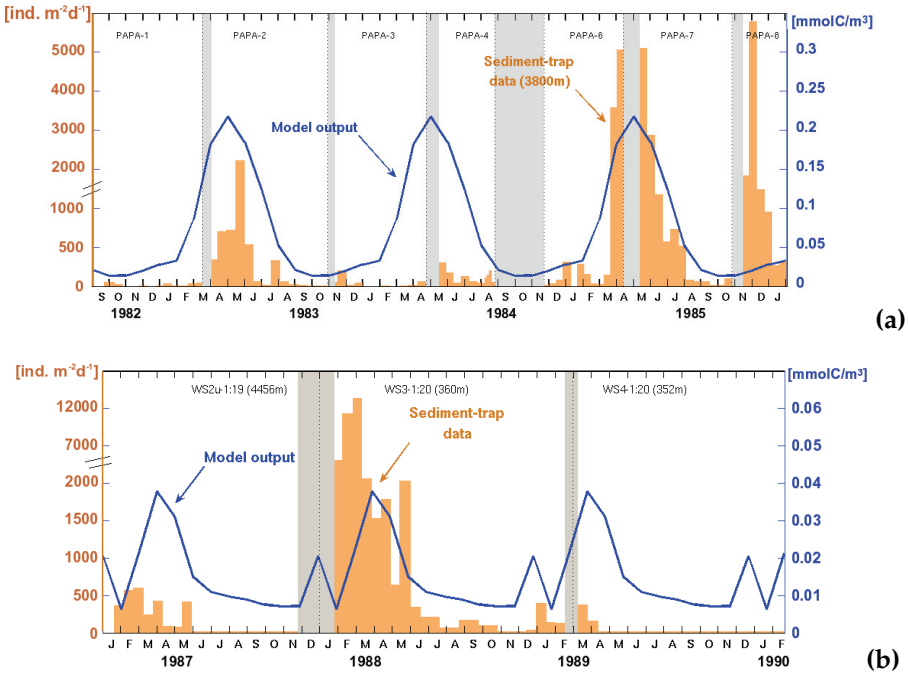

Figure 2.7: *Comparison of measured fluxes of N. pachyderma (sin.) in sediment traps (orange bars) vs. modeled abundances (blue lines). Note the difference in units between sediment-trap data [ind. m^{-2} day^{-1}] and model output [mmolC/m^3], which does not hamper with the assessment of the season of maximum foraminiferal production. Grey bars indicate gaps in sediment-trap data.* **(a)** *Ocean Station PAPA, in northwest Pacific, 50° N 145° W (Reynolds and Thunell, 1985; Sautter and Thunell, 1989; Wong et al., 1999);* **(b)** *Weddell Sea, 64.91° S 2.55° W, in the Southern Ocean (Donner and Wefer, 1994).*

Seasonal variations in the flux of *G. ruber* (white) off Cape Blanc, in the Canary Current, are shown for a period of four years (Fig. 2.10a). The first three years were characterized by a maximum in *G. ruber* flux during fall (September-October). During fall of 1991, however, the peak most likely occurred after the end of the sediment-trap deployment. The model predicts a longer bloom (high concentrations from June to December), but the maximum in September coincides with sediment-trap data. The data recorded by the sediment-trap located at the western equatorial Atlantic does not show a clear pattern (Fig. 2.10b). The first sampling year is characterized by a bimodal pattern, with high fluxes in the austral summer and winter, whereas during the second year the winter bloom was missing. At this site, the model predicts a unimodal pattern with highest fluxes from September to October.

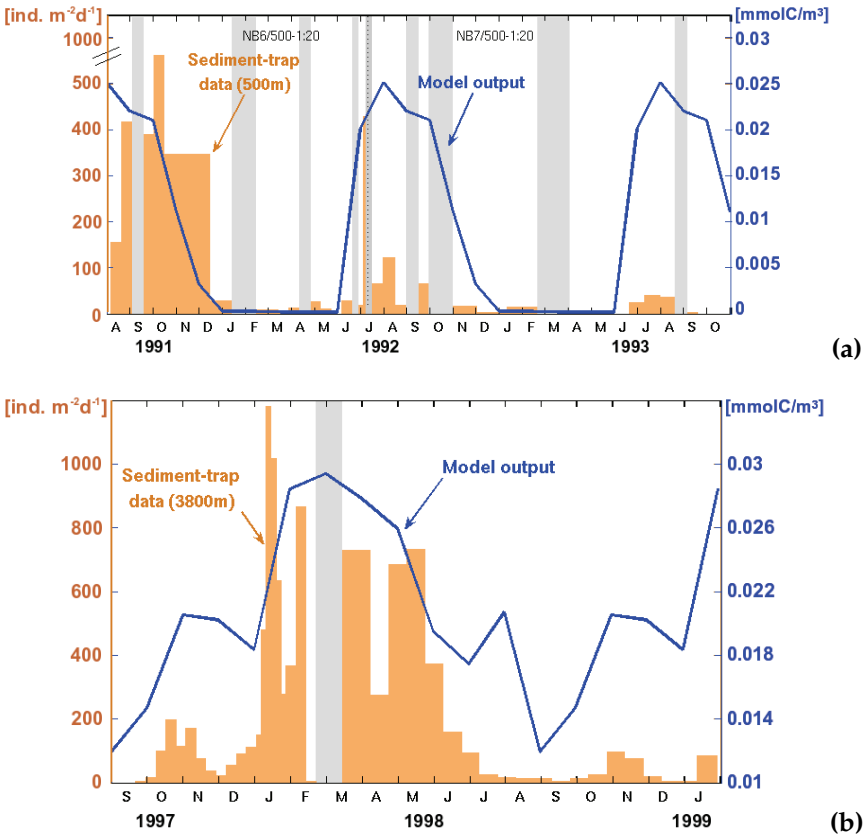

Figure 2.8: *Comparison of measured fluxes of N. pachyderma (dex.) in sediment traps (orange bars) vs. modeled abundances (blue lines). Symbols and layout of the graphs are the same as in Fig. 2.7.* **(a)** *northern North Atlantic, 69.69° N 0.48° E (Jensen, 1998);* **(b)** *Subantarctic Zone, 46.76° S 142.07° E (Trull et al., 2001; King and Howard, 2003a,b).*

G. sacculifer shows low fluxes in all sediment-trap data used for model validation. In most of the sites where sediment traps were deployed, the model predicts very low concentrations (Fig. 2.11).

When the model reaches the threshold value set for the minimum population size (0.01 mmolC/m^3), the hydrographic component of the model starts to dominate over the population dynamic itself. Therefore, in most of the locations, the model output is too low for comparison. We present examples from the Bay of Bengal and the Arabian Sea (Fig. 2.11). At both sites, the model predicts little variability in the population of *G. sacculifer*.

Table 2.4: *Season with maximum foraminiferal production at each site in Fig. 2.1. Empty cells denote if species is absent either in sediment-trap data or the model output.*

	N. pachyderma (sin.)		*N.pachyderma* (dex.)		*G. bulloides*		*G. ruber* (white)		*G. sacculifer*	
Trap Location	Model	sediment-trap	Model	sediment-trap	Model	sediment-trap	Model	sediment-trap	Model	sediment-trap
Ocean Station Papa	spring	spring	fall	fall	summer	spring	-	-	-	-
Peru-Chile Current	-	-	fall	spring	spring	summer	-	-	-	-
N' North Atlantic	summer	summer	summer	summer	-	-	-	-	-	-
Cape Blanc	-	-	-	-	winter	spring	fall	fall	-	-
W' equatorial Atlantic	-	-	-	-	-	-	spring	winter / spring	fall	fall / spring
W Atlantic	-	-	-	-	-	-	spring	winter	fall	fall / winter
Walvis Ridge	-	-	spring	spring	spring	fall / spring / winter	-	-	-	-
Weddell Sea	summer	summer	-	-	-	-	-	-	-	-
Arabian Sea	-	-	-	-	summer	summer	-	-	fall	summer
Bay of Bengal	-	-	-	-	-	-	winter	winter	summer	summer
Northwest Pacific	-	-	fall	summer	spring	winter / spring	spring	summer	-	-
NW' North Pacific	-	-	fall	fall	spring	spring	-	-	-	-
Subantarctic Zone	summer	summer	summer	summer	-	-	-	-	-	-
Chatman Rise	-	-	summer	summer	-	-	-	-	-	-
Cariaco Basin	-	-	-	-	-	-	spring	spring	-	-
Japan Trench	-	-	-	-	spring	spring	spring	spring	-	-
Ryukyu Islands	-	-	-	-	spring	fall / winter	-	-	-	-
Bering Sea	summer	fall	-	-	-	-	-	-	-	-
South China Sea	-	-	-	-	-	-	winter	winter	-	-

2.3.3 Spatio-temporal distribution pattern

We analyzed the model prediction for the temporal variation of *G. bulloides* in the North Atlantic. Fig. 2.12 shows the model output of *G. bulloides* concentrations throughout the year in the North Atlantic. The maximum concentrations occur around 40° N during spring (March-April) and around 60° N during summer (June-July), following the phytoplankton bloom in the model.

2.3.4 Sensitivity experiment: spatio-temporal distribution patterns with constant temperature

We ran the foraminifera module with a constant temperature of 12°C everywhere to test the sensitivity of *G. bulloides* to other environmental parameters (mainly food availability). The chosen temperature corresponds to the optimal temperature of

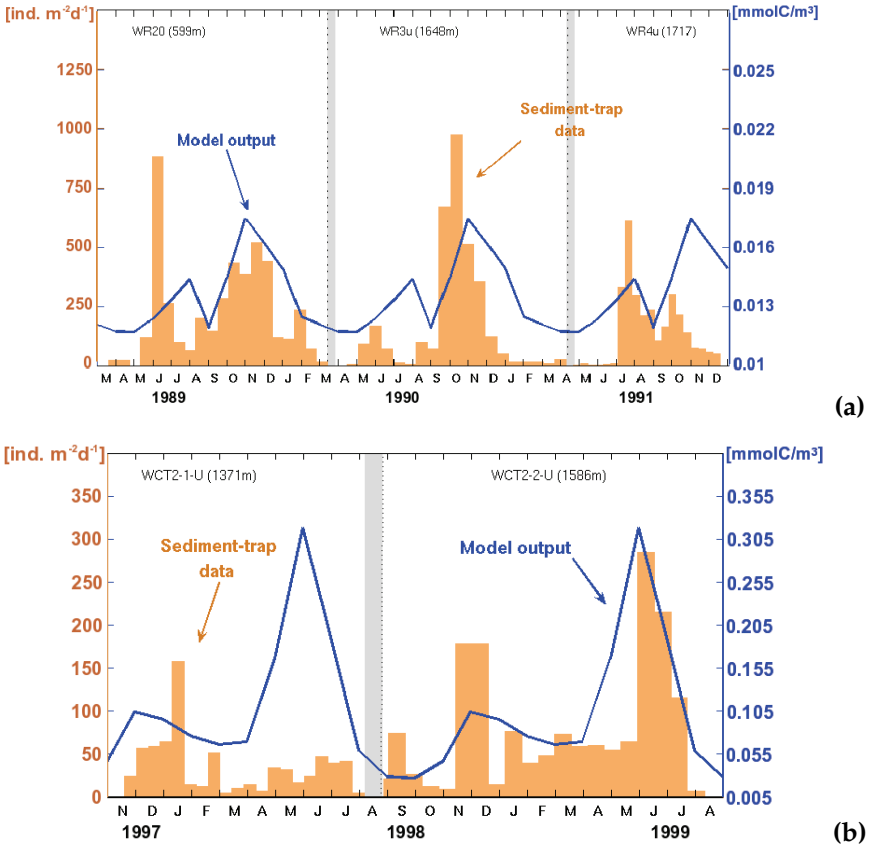

Figure 2.9: *Comparison of measured fluxes of G. bulloides in sediment traps (orange bars) vs. modeled abundances (blue lines). Symbols and layout of the graphs are the same as in Fig. 2.7.* **(a)** *Walvis Ridge, 20.05° S 9.16° E (Fischer and Wefer, 1996; Žarić et al., 2005);* **(b)** *northwest Pacific, 39.01° N 147.00° E (Mohiuddin et al., 2002).*

this species in the model. Fig. 2.13 shows the spatio-temporal distribution of *G. bulloides* in the North Atlantic for this experimental run. In general, absolute concentrations of *G. bulloides* are higher than in the standard run (Fig. 2.12). However, seasonal pattern does not change substantially from the standard run: During spring the model predicts the highest concentrations in the southern region (around 40°) while during summer, the bloom shifts to higher latitudes.

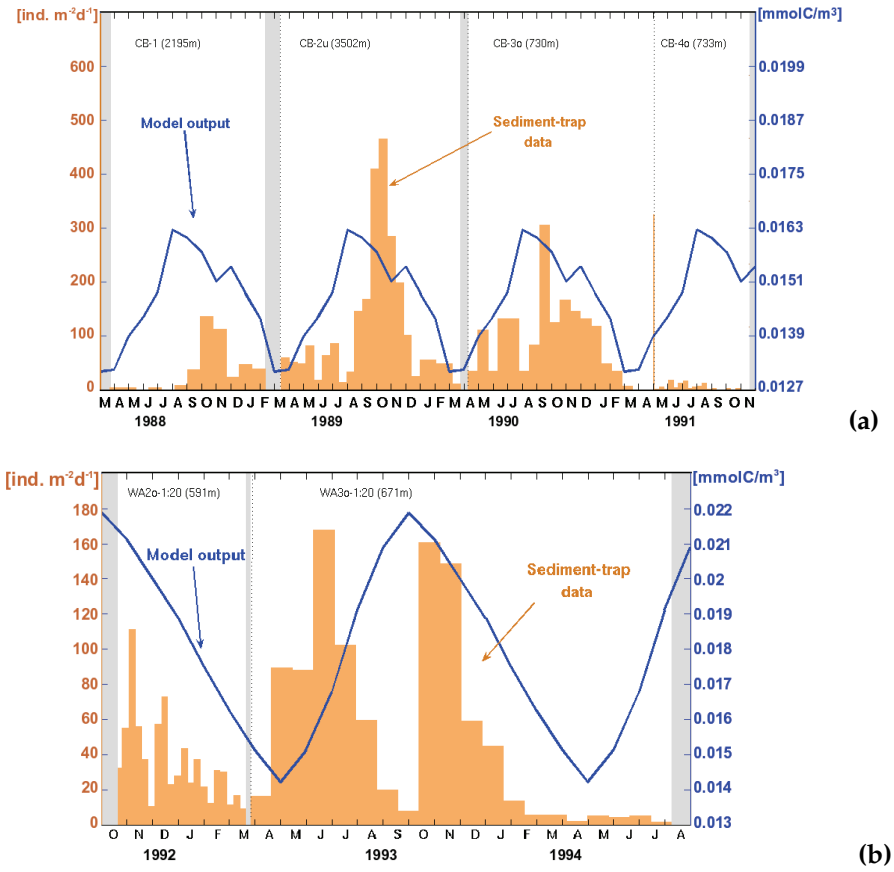

Figure 2.10: *Comparison of measured fluxes of G. ruber (white) in sediment-traps (orange bars) vs. modeled abundances (blue lines). Symbols and layout of the graphs are the same as in Fig. 2.7.* **(a)** *Cape Blanc, 21.15° N 20.69° W (Fischer and Wefer, 1996; Fischer et al., 1996; Žarić et al., 2005);* **(b)** *western equatorial Atlantic, 7.51° S 28.03° W (Fischer and Wefer, 1996; Fischer et al., 1996; Žarić et al., 2005).*

2.4 Discussion

2.4.1 Comparison with core-top data

In general, the global distribution patterns of foraminifera species predicted by the model are very close to those expected from core-top data.

The core-top data reflect the integrated flux through the water column, while our model reflects the situation in the mixed layer. As a consequence, some of the

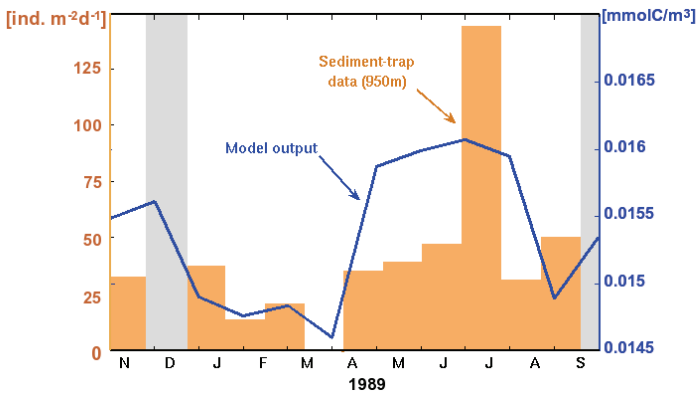

Figure 2.11: *Comparison of measured fluxes of G. sacculifer in sediment-traps (orange bars) vs. modeled abundances (blue lines). Symbols and layout of the graphs are the same as in Fig. 2.7.* **(a)** *central Bay of Bengal, 13.15° N 89.35° E (Guptha et al., 1997).*

discrepancies between model and core-top distributions could be due to the different depth habitats of the species. However, the five species simulated in our model live for most of their life cycle in the upper part of the water-column, thus we expect only a small error at a global scale. In addition, fossil faunal assemblages may be altered by selective dissolution (Berger, 1968; Thunell and Honjo, 1981; Le and Thunell, 1996; Dittert and Henrich, 1999), and by displacement through subsurface currents or bioturbation processes (Bé, 1977; Bé and Hutson, 1977; Boltovskoy, 1994). Since we can not take into account any of these factors, these processes may explain some of the discrepancies between core-top data and the model results.

The global distribution pattern of *N. pachyderma* (sin.) is very similar to that in the core-top data (Fig. 2.2). Distinct *N. pachyderma* (sin.) genotypes were identified by Darling et al. (2004) in the Arctic and Antarctic polar/subpolar waters. Those cryptic species seem to have different environmental preferences (Bauch et al., 2003). Accordingly, the temperature tolerance of the populations in the southern hemisphere is larger than that of North Atlantic population (Darling et al., 2006). For the calibration we did not take different genotypes into account. This causes a discrepancy at the edge of the distribution in the North Atlantic, where the temperature tolerance range is narrower. In fact, the model output agrees slightly better with the core-top data in the Southern Ocean, where the Root Mean Square Error is 8.7% compared to 9.3% in the northern hemisphere. This result reflects the fact that our parametrization is mainly based on the temperature tolerance of the southern population. However, the difference between hemispheres is not large, and treating the different genotypes of *N. pachyderma* (sin.) as a single ecological group in the

model seems justified.

For *N. pachyderma* (dex.) the model was able to predict the high relative abundances (up to 90%) found in core-top data from the eastern equatorial Pacific and Benguela upwelling systems (Fig. 2.3). In contrast, in the upwelling system off NW Africa, the model predicts too high relative abundances of *N. pachyderma* (dex.), while those in North Atlantic (40° - 70° N) were underestimated. A noticeable discrepancy arises in the equatorial Pacific, north of the eastern boundary upwelling region, where the model underestimates the relative abundance of *N. pachyderma* (dex.). In this region, the surface temperature in the model is higher than that typical for *N. pachyderma* (dex.) (minimum temperatures above 22°C). It is therefore possible that *N. pachyderma* (dex.) from these core-tops represent a population living below the mixed layer, as has been described in previous studies (Murray, 1991; Pujol and Grazzini, 1995; Kuroyanagi and Kawahata, 2004), or that they are expatriated specimens from the upwelling region.

The model-generated global pattern of *G. bulloides* for the Atlantic, Pacific and Southern Oceans agrees well with core-top data (Fig. 2.4). The model, however, underestimates the abundance of *G. bulloides* in the northern Indian Ocean. This underestimation could be due to the different *G. bulloides* genotypes. The two warm water types are found mainly in tropical/subtropical regions, whereas cold water types are found in transitional to subpolar waters (Kucera and Darling, 2002). Žarić et al. (2005) studied the sensitivity of several planktonic foraminifera species to sea-surface temperature and concluded that the population of *G. bulloides* present in the tropical Indian Ocean comprises mainly the warm-water genotype. Since the parametrization of the model is done at a global scale without specifically considering the warm water type, the increased relative abundance of warm-water *G. bulloides* in the tropical Indian Ocean cannot be captured by the model. The high concentrations simulated in the Arabian Sea are due to an unrealistically high phytoplankton concentration in the ecosystem model. In addition, the modification of the normal distribution by the introduction of the food-dependent relation (through the parameter k in Eq. 2.3) allows *G. bulloides* to grow in tropical waters. The model underestimates relative abundances of *G. bulloides* in the upwelling regions off northwest Africa, Peru-Chile and Benguela as a result of the overestimation of *N. pachyderma* (dex.) concentration. This could be due to the higher turnover-rate of *G. bulloides* in comparison to that of *N. pachyderma* (dex.), which is not included in this model.

The simulated global distribution pattern of *G. ruber* (white) is in good agreement with the core-top data. Only in the northern Indian Ocean are abundances somewhat overestimated (Fig. 2.5). This may be due to the underestimation of *G. bulloides* in the model as we compare relative abundances.

Both core-top data and model output show that the distribution of *G. sacculifer*

is limited to tropical areas (Fig. 2.6). The model favorably captures the distribution patterns in the Atlantic and eastern Pacific Oceans. The predicted relative abundances of *G. sacculifer* in the Indian and western Pacific Oceans are underestimated in the model. The observed distribution shows a wider spatial range than in the model. This could be due to competition exerted by *G. ruber*. The abundance of this species is overestimated in the mentioned regions and therefore competition is exerting a stronger influence on the other species.

2.4.2 Comparison with sediment-trap data

The comparison between model predictions and sediment-trap records bears several difficulties. Most of time series only represent short sampling periods (single or a few years). Sediment traps that were deployed for more than one year show pronounced interannual variability that is not captured by the model due to the climatological forcing. Moreover, the majority of sediment-traps have been deployed close to the coast (Fig. 2.1), where environmental conditions and ecological successions are more complex than in the open ocean. The lack of sediment-trap data in open-ocean settings is an obstacle for a global scale comparison. Nevertheless, in general, the seasonal pattern of species concentrations in the model is similar to the sediment-trap records (Table 2.4).

Simulated variations of *N. pachyderma* (sin.) correlate well with sediment-trap data. In 80% of the cases, the preadicted season of maximum production coincides with observational data. In the model *N. pachyderma* (sin.) lives in polar/subpolar waters, and the maximum production of this species occurs during a short period in summer, together with the phytoplankton bloom. For *N. pachyderma* (dex.), the season of maximum production varies between locations. However, model prediction and sediment-trap data coincide in 75% of the cases (Table 2.4). For the stations in Peru-Chile current and northwest Pacific, model prediction and sediment-trap data differ substantially. However, in the former location, the sampling period is limited to a single year and the data shows an irregular pattern without a distinct seasonal peak, whereas in the northwest Pacific the interannual variability in sediment-trap data is very high. It is likely that at these particular locations the sediment traps do not reflect the mean long-term flux pattern.

For most of the locations, the season of maximum production of *G. bulloides* simulated by the model does not coincide with the observations. At Ocean Station PAPA (northeast Pacific) the modeled seasonal peaks are delayed with respect to sediment-trap data, whereas in the Peru-Chile current and off Cape Blanc, the peak occurs too early. At the Walvis Ridge, close to the coastal upwelling zone, the model predicts successfully the bimodal pattern (Fig. 2.9a). However, when considering

the absolute flux maximum in each year, the season when it occurs varies throughout the sediment-trap record. At Ryukyu Islands (northwest Pacific) two sediment traps were deployed during the same period, but maximum production seasons recorded in both traps are different. The differences observed in the sediment-trap data highlights difficulties in comparing model predictions and observational data.

The season of maximum production of *G. ruber* (white) in the model corresponds to the recorded data in 6 of 8 stations. However, in the western Atlantic, the model produces highest concentrations too early in the year (Table 2.4). On the other hand, the variations in the sediment-trap data are very small and seem to occur randomly.

Only very few data are available to compare seasonal variations of *G. sacculifer*. Model and sediment-trap data show, in general, lower concentrations than the other four species and little seasonal variability in all sites. This is not surprising considering that *G. sacculife*r is limited to tropical waters, with small seasonal temperature range.

2.4.3 Sensitivity analysis

In an attempt to assess the sensitivity of the model to the chosen parameter values, we performed a sensitivity analysis of the parameters. The procedure used was similar to other marine plankton models (e.g., Fasham et al., 1990). We kept the parameters that are common to the ecosystem model constant, and modified only the values chosen for the foraminifera module. We run the model with each parameter altered by half and twice the standard value respectively to determine which parameters have the most effect (Table 2.3).

The sensitivity was quantified by calculating the change of RMSE between the sensitivity experiment and the standard run. The results (Table 2.3) indicate that none of the parameters lead to uniform changes for all species. The model seems to be more robust for *G. sacculifer* than for other species. In several experiments, the error between model and core-top data decreases. This occurs because the standard parametrization is based on ecological data compiled from literature rather than "tuned" to obtain a better fit. Removing competition generates a general increase of RMSE. Not surprisingly, the temperature tolerance range (σ) seems to be the most sensitive parameter.

2.4.4 Model experiment with constant mixed-layer temperature

When the foraminifera model is run with a constant temperature of 12°C, *G. bulloides* in the North Atlantic still showed highest concentrations at low latitudes during spring and maximum concentrations at higher latitudes in June, linked to the sea-

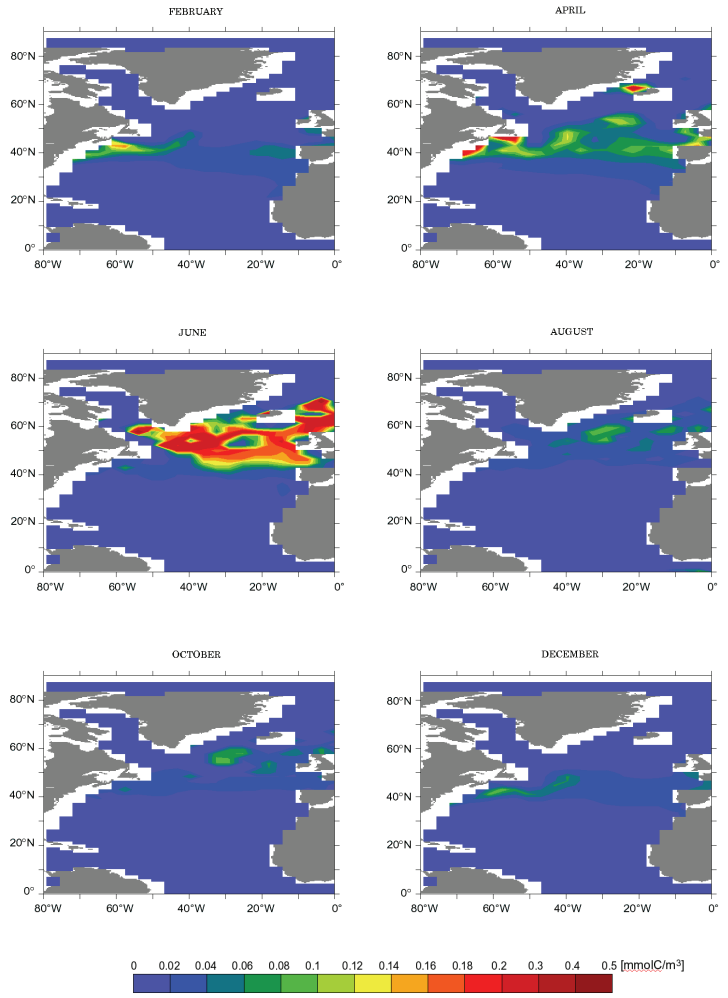

Figure 2.12: *Modeled monthly concentrations of G. bulloides in the North Atlantic in the standard run.*

sonal migration of the phytoplankton bloom (Fig. 2.13). This indicates that temperature is not the only controlling factor, but that food supply plays an important role in the temporal distribution pattern of this species. The experiment confirms the results of Ganssen and Kroon (2000), who from isotopic studies on North Atlantic surface sediments, concluded that *G. bulloides* reflects temperatures of a northward migrating spring bloom.

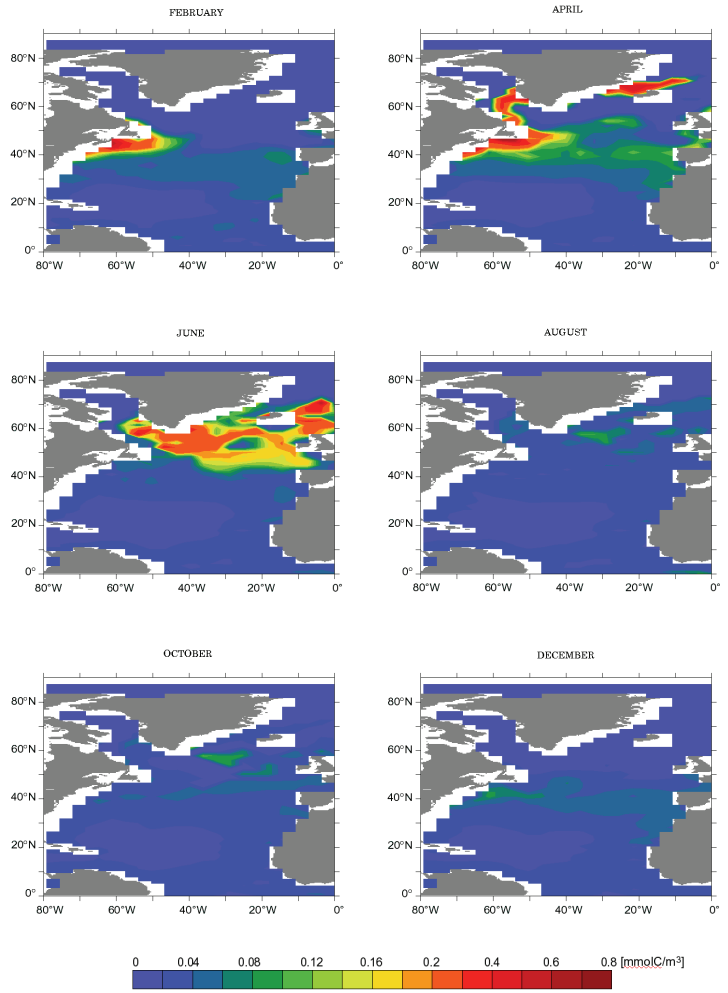

Figure 2.13: *Modeled monthly concentrations of G. bulloides in an experiment with constant mixed layer temperature of 12 °C.*

2.5 Summary and conclusions

A global model has been developed that predicts monthly planktonic foraminifera concentrations for *N. pachyderma* (sin.), *N. pachyderma* (dex.), *G. bulloides*, *G. ruber* (white) and *G. sacculifer*. It is a nonlinear dynamic model simulating growth rate of foraminifera populations using information from an underlying ecosystem model

(Moore et al., 2002).

The model aims at predicting the distribution of planktonic foraminifera at geological timescales. Overall, the global distribution patterns of the predicted species are similar to core-top data.

Modeled seasonal variations overall agree with sediment-trap records for most of the locations, although the comparison is hampered by interannual variability not captured by the model.

A sensitivity experiment using a constant temperature of 12°C indicates that food availability (primary production in the case of *G. bulloides*) is an important factor controlling the distribution of some species.

Our model provides a tool that will contribute to better assessing how changing environmental conditions in the geological past affected the distribution of foraminifera in space and time.

Quantitative data and a better knowledge of ecological process from laboratory and field studies are essential for further improvement of the current model. Results may also be improved by including additional information, such as different classes of zooplankton, or by explicitly resolving depth.

Acknowledgments We appreciate the contributions and helpful comments of R. Schiebel, M. Peck, A. Beck, A. Bisset, and 4 referees who improved the manuscript. Thanks also to M. Prange and T. Laepple for analytical assistance and G. Fischer for providing sediment-trap data. Special thanks to A. Manschke for computer support. This project was supported by the DFG (Deutsche Forschungsgemeinschaft) as part of the European Graduate Collegue "Proxies in Earth History" (EUROPROX).

Published as: Fraile, I., Schulz, M., Mulitza, S. and Kucera, M., 2008. Predicting the global distribution of planktonic foraminifera using a dynamic ecosystem model. Biogeosciences, 5, 891–911.

Bibliography

Anderson, O. R., Spindler, M., Be, A. W. H., and Hemleben, C.: Trophic activity of planktonic foraminifera, J. Mar. Biol. Assoc. U.K., 59, 791–799, 1979.

Arnold, A. J. and Parker, W. C.: Biogeography of planktonic Foraminifera, in: Modern Foraminifera, edited by: Gupta, B. S. K., Dortrecht, Boston, London, 103–122, 1999.

Asahi, H. and Takahashi, K.: A 9-year time-series of planktonic foraminifer fluxes and environmental change in the Bering sea and the central subarctic Pacific Ocean, 1990–1999, Prog. Oceanogr., 72, 343–363, 2007.

Bauch, D., Carstens, J. and Wefer, G.: Oxygen isotope composition of living *Neogloboquadrina pachyderma* (sin.) in the Arctic Ocean, Earth. Planet. Sc. Lett., 146, 47–58, 1997.

Bauch, D., Darling, K., Simstich, J., Bauch, H. A., Erlenkeuser, H. and Kroon, D.: Palaeoceanographic implications of genetic variation in living North Atlantic *Neogloboquadrina pachyderma*, Nature, 424, 299–302, 2003.

Bé, A. W. H. and Hamilton, W. H.: Ecology of Recent planktonic foraminifera, Micropal., 13, 87–106, 1967.

Bé, A. W. H. and Tolderlund, D. S.: Distribution and ecology of living planktonic foraminifera in surface waters of the Atlantic and Indian Oceans, in The Micropalaeontology of Oceans, edited by: Funnell, B. M. and Riedel, W. R., 105–149, Cambridge University Press, 1967.

Bé, A. W. H.: An ecological, zoogeographic and taxonomic review of recent planktonic foraminifera, in: Oceanic Micropalaeontology, edited by: Ramsay, A. T. S., 1–100, Academic Press Inc., London, 1977.

Bé, A. W. H. and Hutson, W. H.: Ecology of planktonic foraminifera and biogeographic patterns of life and fossil assemblages in the Indian Ocean, Micropal., 23, 369–414, 1977.

Bé, A. W. H., Caron, D. A., and Anderson, O. R.: Effects of feeding frequency on life processes of the planktonic foraminifer *Globigerinoides sacculifer* in laboratory culture, J. Mar. Biol. Assoc. U.K., 61, 257–277, 1981.

Bé, A. W. H., Bishop, J. K. B., Sverdlove, M. S., and Gardner, W. D.: Standing stock, vertical distribution and flux of planktonic Foraminifera in the Panama Basin, Mar. Micropal., 9, 307–333, 1985.

Berger, W. H.: Planktonic foraminifera: selective solution and paleoclimatic interpretation, Deep-Sea Res., 15, 31–43, 1968.

Bijma, J., Faber, W. W. J., and Hemleben, C.: Temperature and salinity limits for growth and survival of some planktonic foraminifers in laboratory cultures, J. Foramin. Res., 20, 95–116, 1990.

Bishop, J. K. B. and Rossow, W. B.: Spatial and temporal variability of global surface solar irradiance, J. Geophys. Res., 96, 16 839–16 858, 1991.

Boltovskoy, D.: The sedimentary record of pelagic biogeography, Prog. Oceanogr., 34, 135–160, 1994.

Bradshaw, J. S.: Ecology of living planktonic foraminifera in the North and equatorial Pacific Ocean, Cushman Foundation for Foraminiferal Research Contribution, 10, 25–64, 1959.

Caron, D. A., Bé, A. W. H. and Anderson, O. R.: Effects on variations in light intensity on life processes of the planktonic foraminifera Globigerinoides sacculifer in laboratory culture, J. Mar. Biol. Assoc. U.K., 67, 323–341, 1981.

Caron, D. A. and Bé, A. W. H.: Predicted and observed feeding rates of the spinose planktonic foraminifer *Globigerinoides sacculifer*, B. Mar. Sci., 35, 1–10, 1984.

Cavalieri, D., Gloerson, P., and Zwally, J.: DMSP SSM/I daily polar gridded sea ice concentrations, October 1998 to September 1999, edited by: Maslanik, J. and Stroeve, J., National Snow and Ice Data Center, Boulder, CO, Digital media, 1990.

CLIMAP Project Members: The surface of the ice-age earth, Science, 191, 1131–1137, 1976.

Conan, S. M. H., and Brummer, G. J. A.:Fluxes of planktic foraminifera in response to monsoonal upwelling on the Somalia Basin margin, Deep-Sea Res. II, 47, 2207-2227, 2000.

Conkright, M., Levitus, S., OBrien, T., Boyer T., Antonov, J. and Stephens: World Ocean Atlas 1998 CD-ROM Data Set Documentation, Tech. Rep. 15, NODC Internal Report, Silver Spring, MD, 16 pp., 1998.

Cullen, J. L.: Microfossil evidence for changing salinity patterns in the Bay of Bengal over the last 20,000 years, Palaeogeogr. Palaeocl., 35, 315–356, 1981.

Curry, W. B., Ostermann, D. R., Guptha, M. V. S., and Ittekkot, V.: Foraminiferal production and monsoonal upwelling in the Arabian Sea: evidence from sediment traps, in: Upwelling Systems: Evolution Since the Early Miocene, edited by: Summerhayes, C. P., Prell, W. L., and Emeis, K. C., 93–106, The Geological Society, London, 1992.

Darling, K. F., Wade, C. M., Kroon, D., Leigh Brown, A. J., and Bijma, J.: The diversity and distribution of modern planktonic foraminiferal small subunit ribosomal RNA genotypes and their potential as tracers of present and past ocean circulations, Paleoceanography, 14, 3–12, 1999.

Darling, K. F., Wade, C. M., Stewart, I. A., Kroon, D., Dingle, R., and Leigh Brown, A. J.: Molecular evidence for genetic mixing of Arctic and Antarctic subpolar populations of planktonic foraminifers, Nature, 405, 43–47, 2000.

Darling, K. F., Kucera, M., Wade, C. M., von Langen, P., and Pak, D.: Seasonal distribution of genetic types of planktonic foraminifer morphospecies in the Santa Barbara Channel and its paleoceanographic implications, Paleoceanography, 18, 1032, doi:10.1029/2001PA000723, 2003.

Darling, K. F.,Kucera, M., Pudsey, C. J. and Wade, C. M.: Molecular evidence links cryptic diversification in polar plankton to Quaternary climate dynamics, Proc. Natl. Acad. Sci., U. S. A., 101, 7657-7662, 2004.

Darling, K. F., Kucera, M., Kroon, D., and Wade, C. M.: A resolution for the coiling direction paradox in *Neogloboquadrina pachyderma*, Paleoceanography, 21, 2011, doi:10.1029/2005PA001189, 2006.

Deuser, W. G. and Ross, E. H.: Seasonally abundant planktonic foraminifera of the Sargasso Sea: succession, deep-water fluxes, isotopic compositions, and paleoceanographic implications, J. Foramin. Res., 19, 268–293, 1989.

Dieckmann, G. S., Spindler, M., Lange, M. A., Ackley, S. F., and Eicken, H.: Antarctic sea ice: a habitat for the foraminifer *Neogloboquadrina pachyderma*, J. Foramin. Res., 21, 182–189, 1991.

Dittert, N. and Henrich, R.: Carbonate dissolution in the South Atlantic Ocean: evidence from ultrastructure breakdown in *Globigerina bulloides*, Deep-Sea Res. I, 47, 603–620, 1999.

Donner, B. and Wefer, G.: Flux and stable isotope composition of *Neogloboquadrina pachyderma* and other planktonic foraminifers in the Southern Ocean (Atlantic sector), Deep-Sea Res. I, 41, 1733–1743, 1994.

Duplessy, J. C., Delibrias, G., Turon, J. L., Pujol, C., and Duprat, J.: Deglacial warming of the Northeastern Atlantic Ocean: correlation with the paleoclimatic evolution of the European continent, Palaeogeogr. Palaeocl., 35, 121–144, 1981.

Edwards, A. M. and Yool, A.: The role of higher predation in plankton population models, J. Plankton Res., 22, 1085–1112, 2000.

Eguchi, N. O., Kawahata, H., and Taira, A.: Seasonal Response of Planktonic Foraminifera to Surface Ocean Condition: Sediment Trap Results from the Central North Pacific Ocean, J. Oceanogr., 55, 681–691, 1999.

Fasham, M. J. R., Ducklow, H. W. and McKelvie, S. M.: A nitrogen-based model of plankton dynamics in the oceanic mixed layer, J. Mar. Res., 48, 591–639, 1990.

Fischer, G. and Wefer, G.: Long-term Observation of Particle Fluxes in the Eastern Atlantic: Seasonality, Changes of Flux with Depth and Comparison with the Sediment Record, in: The South Atlantic: Present and Past Circulation, edited by: Wefer, G., Berger, W. H., Siedler, G., and Webb, D. J., 325–344, Springer-Verlag, Berlin Heidelberg, 1996.

Fischer, G., Donner, B., Ratmeyer, V., Davenport, R., and Wefer, G.: Distinct year-to-year particle flux variations off Cape Blanc during 1988–1991: Relation to δ^{18}O-deduced sea-surface temperatures and trade winds, J. Mar. Res., 54, 73–98, 1996.

Ganssen, G. M. and Kroon, D.: The isotopic signature of planktonic foraminifera from NE Atlantic surface sediments: implications for the reconstruction of past oceanic conditions, J. Geol. Soc., 157, 693–699, 2000.

Gastrich, M. D.: Ultrastructure of a new intracellular symbiotic alga found within planktonic foraminifera, J. Phycol., 23, 623-632, 1987.

Gent, P. R., Bryan, F. O., Danabasoglu, G., Doney, S. C., Holland, W. R., Large, W. G., and McWilliams, J. C.: The NCAR climate system model global ocean component, J. Climate, 11, 1287–1306, 1998.

Giraudeau, J.: Planktonic foraminiferal assemblages in surface sediments from the southwest African continental margin, Mar. Geol., 110, 47–62, 1993.

Guptha, M. V. S. and Mohan, R.: Seasonal variability of the vertical fluxes of *Globigerina bulloides* (d Orbigny) in the northern Indian Ocean, Mitt. Geol.-Paläont. Inst. Univ. Hamburg, 79, 1–17, 1996.

Guptha, M. V. S., Curry, W. B., Ittekkot, V., and Muralinath, A. S.: Seasonal variation in the flux of planktic foraminifera: Sediment trap results from the Bay of Bengal, northern Indian Ocean, J. Foramin. Res., 27, 5–19, 1997.

Haake, B., Ittekkot, V., Rixen, T., Ramaswamy, V., Nair, R. R., and Curry, W. B.: Seasonality and interannual variability of particle fluxes to the deep Arabian Sea, Deep-Sea Res. I, 40, 1323–1344, 1993.

Hebbeln, D., Marchant, M., and Wefer, G.: Seasonal variations of the particle flux in the Peru-Chile current at 30° S under normal and El Niño conditions, Deep-Sea Res. II, 47, 2101–2128, 2000.

Hemleben, C., Spindler, M., Breitinger, J., and Deuser, W. G.: Field and laboratory studies of the ontogeny and ecology of *Globorotalia truncatulinoides* and *G. hirsuta* in the Sargasso Sea, J. Foramin. Res., 15, 254–272, 1985.

Hemleben, C., Spindler, M., and Anderson, O. R.: Modern Planktonic Foraminifera, Springer-Verlag, New York, 1989.

Jensen, S.: Planktische Foraminiferen im Europaischen Nordmeer: Verbreitung und Vertikalfluss sowie ihre Entwicklung während der letzten 15000 Jahre, Berichte SFB 313, Univ. Kiel, 75, 105 pp., 1998.

Kiefer, T.: Produtivität und Temperaturen im subtropischen Nordatlantik: zyklische und abrupte Veränderungen im späten Quartär, Berichte – Reports, Geol.-Paläont. Inst., Univ. Kiel, 90, 1–127, 1998.

King, A. L. and Howard, W. R.: Seasonality of foraminiferal flux in sediment traps at Chatham Rise, SW Pacific: implications for paleotemperature estimates, Deep-Sea Res. I, 48, 1687–1708, 2001.

King, A. L. and Howard, W. R.: Planktonic foraminiferal flux seasonality in Subantarctic sediment traps: A test for paleoclimate reconstructions, Paleoceanography, 18, 1019, doi:1010.1029/2002PA000839, 2003a.

King, A. L. and Howard, W. R.: Seasonal Subantarctic Planktonic Foraminiferal Flux Data, available from the IGBP PAGES/World Data Center for Paleoclimatology (http://www.ngdc.noaa.gov/paleo), Data Contribution Series # 2003-022., NOAA/NGDC Paleoclimatology Program, Boulder CO, 2003b.

Kucera, M. and Darling, K. F.: Cryptic species of planktonic foraminifera: their effect on paleoceanographic reconstructions, Philos. Tr. Roy. Soc. A, 360, 695–718, 2002.

Kucera, M., Rosell-Mele, A., Schneider, R., Waelbroeck, C., and Weinelt, M.: Reconstruction 15 of sea-surface temperatures from assemblages of planktonic foraminifera: multi-technique approach based on geographically constrained calibration data sets and its application to glacial Atlantic and Pacific Oceans, Quat. Sci. Rev., 24, 951998, 2005.

Kuroyanagi, A., Kawahata, H., Nishi, H., and Honda, M. C.: Seasonal changes in planktonic foraminifera in the northwestern North Pacific Ocean: sediment trap experiments from subarctic and subtropical gyres, Deep-Sea Res. II, 49, 5627–5645, 2002.

Kuroyanagi, A. and Kawahata, H.: Vertical distribution of living planktonic foraminifera in the seas around Japan, Mar. Micropal., 53, 173–196, 2004.

Le, J. and Thunell, R. C.: Modelling planktic foraminiferal assemblage changes and application to sea surface temperature estimation in the western equatorial Pacific Ocean, Mar. Micropal., 28, 211–229, 1996.

Lea, D. W.: Trace elements in foraminiferal calcite, in: Modern foraminifera, edited by: Gupta, B. S. K., Dortrecht, Boston, London, 259–277, 1999.

Lee, J. J., McEnery, M. E., Pierce, S., Freudenthal, H. D. and Muller, W. A.: Tracer experiments in feeding littoral foraminifera, J. Protozool., 13, 659-670, 1966.

Malmgren, B. A., Kucera, M., Nyberg, J., and Waelbroeck, C.: Comparison of statistical and artificial neural network techniques for estimating past sea surface temperature from planktonic foraminifer census data, Paleoceanography, 16, 520–530, 2001.

Marchant, M., Hebbeln, D., and Wefer, G.: Seasonal flux patterns of planktic foraminifera in the Peru-Chile Current, Deep-Sea Res. I, 45, 1161–1185, 1998.

Martinez, J. I., Taylor, L., Deckker, P., and Barrows, T. (1998), Planktonic foraminifera from the eastern Indian Ocean: distribution and ecology in relation to the Western Pacific Warm Pool (WPWP), *Mar. Micropaleontol.*, 34, 121–151.

Marchant, M., Hebbeln, D., Giglio, S., Coloma C., and Gonzalez, H.: Seasonal and interannual variability in the flux of planktic foraminifers in the southern Humboldt Current System off central Chile, Deep-Sea Res. II, 51, 2441–2455, 2004.

Martinez, J. I., Taylor, L., Deckker, P., and Barrows, T.: Planktonic foraminifera from the eastern Indian Ocean: distribution and ecology in relation to the Western Pacific Warm Pool (WPWP), Mar. Micropal., 34, 121–151, 1998.

Michaels, A. F., Caron, D. A., Swanberg, N. R., and Howse, F. A.: Planktonic sarcodines (Acantharia, Radiolaria, Foraminifera) in surface waters near Bermuda: abundance, biomass and vertical flux, J. Plankton Res., 17, 131–163, 1995.

Mohiuddin, M. M., Nishimura, A., Tanaka, Y., and Shimamoto, A.: Regional and interannual productivity of biogenic components and planktonic foraminiferal fluxes in the northwestern Pacific Basin, Mar. Micropal., 45, 57–82, 2002.

Mohiuddin, M. M., Nishimura, A., Tanaka, Y., and Shimamoto, A.: Seasonality of biogenic particle and planktonic foraminifera fluxes: response to hydrographic variability in the Kuroshio Extension, northwestern Pacific Ocean, Deep-Sea Res. I, 51, 1659–1683, 2004.

Monterey, G. and Levitus, S.: Seasonal variability ofmixed layer depth for the world ocean, NOAA Atlas NESDIS 14, US Government Printing Office, Washington, D.C., 1997.

Moore, J. K., Doney, S. C., Kleypas, J. A., Glover, D. M., and Fung, I. Y.: An intermediate complexity marine ecosystem model for the global domain, Deep-Sea Res. II, 49, 403–462, 2002a.

Moore, J. K., Doney, S. C., Glover, D. M., and Fung, I. Y.: Iron cycling and nutrient-limitation patterns in surface waters ofthe World Ocean, Deep-Sea Res. II, 49, 463–507, 2002b.

Morey, A. E., Mix, A. C., and Pisias, N. G.: Planktonic foraminiferal assemblages preserved in surface sediments correspond to multiple environment variables, Quat. Sci. Rev., 24, 925–950, 2005.

Mulitza, S., Dürkoop, A., Hale, W., Wefer, G., and Niebler, H. S.: Planktonic foraminiferaa as recorders of past surface-water stratification, Geology, 25, 335–338, 1997.

Mulitza, S., Wolff, T., Pätzold, J., Hale, W., and Wefer, G.: Temperature sensitivity of planktic foraminifera and its influence on the oxygen isotope record, Mar. Micropal., 33, 223–240, 1998.

Murray, J. W.: Ecology, and distribution of planktonic foraminifera, in: Biology of foraminfera, edited by: Lee, J. J. and Anderson, O. R., Academic Press, Harcourt, 255–284, 1991.

Niebler, H. S., Arz, H. W., Donner, B., Mulitza, S., Pätzold, J., and Wefer, G.: Sea surface temperatures in the equatorial and South Atlantic Ocean during the last glacial maximum (23–19 ka), Paleoceanography, 18, 1069, doi:1010.1029/2003PA000902, 2003.

Nodder, S. D. and Northcote, L. C.: Episodic particulate fluxes at southern temperate mid-latitudes (42–45° S) in the Subtropical Front region, east of New Zealand, Deep-Sea Res. I, 48, 833–864, 2001.

Oda, M. and Yamasaki, M.: Sediment trap results from the Japan Trench in the Kuroshio domain: seasonal variations in the planktic foraminiferal flux, J. Foramin. Res., 35, 315–326, 2005.

Ortiz, J. D., Mix, A. C., and Collier, R. W.: Environmental control of living symbiotic and asymbiotic foraminifera of the California Current, Paleoceanography, 10, 987–1009, 1995.

Pearson, P. N. and Palmer, M. R.: Atmospheric carbon dioxide concentrations over the past 60 million years, Nature, 406, 695–699, 2000.

Peeters, F., Ivanova, E., Conan, S., Brummer, G. J., Ganssen, G., Troelstra, S., and van Hinte, J.: A size analysis of planktic foraminifera from the Arabian Sea, Mar. Micropal., 36, 31–63, 1999.

Peinert, R., Antia, A. N., Bauerfeind, E., Haupt, O., Krumbholz, M., Peeken, I., Bodungen, B. V., Ramseier, R., Voss, M., and Zeitzschel, B.: Particle Flux Variability in the Polar and Atlantic Biogeochemical Provinces of the Nordic Seas, in: The Northern North Atlantic: A Changing Environment, edited by: Schäfer, P., Ritzrau, W., Schlüter, M., and Thiede, J., 53–68, Springer, Berlin, 2001.

Pflaumann, U., Duprat, J., Pujol, C., and Labeyrie, L. D.: SIMMAX: A modern analog technique to deduce Atlantic sea surface temperatures from planktonic foraminifera is deep-sea sediments, Paleoceanography, 11, 15–35, 1996.

Pflaumann, U., Sarnthein, M., Chapman, M., d'Abreu, L., Funnell, B., Huels, M., Kiefer, T., Maslin, M., Schulz, H., Swallow, J., van Kreveld, S., Vautravers, M., Vogelsang, E., and Weinelt, M.: Glacial North Atlantic: Sea-surface conditions reconstructed by GLAMAP 2000, Paleoceanography, 18, 1065, doi:1010.1029/2002PA000774, 2003.

Prell, W. L. and Curry, W. B.: Faunal and isotopic indices of monsoonal upwelling: Western Arabian Sea, Oceanologica Acta, 4, 91–95, 1981.

Prell, W. L., Martin, A., Cullen, J., and Trend, M.: The Brown University Foraminiferal Data Base, IGBP PAGES/World Data Center-A for Paleoclimatology, Data Contribution Series # 1999-027, NOAA/NGDC Paleoclimatology Program, Boulder CO, USA, 1999.

Pujol, C. and Grazzini, C. V.: Distribution patterns of live planktic foraminifers as related to regional hydrography and productive systems of the Mediterranean Sea, Mar. Micropal., 25, 187–217, 1995.

Reynolds, L. and Thunell, R. C.: Seasonal succession of planktonic foraminifera in the subpolar North Pacific, J. Foramin. Res., 15, 282–301, 1985.

Rohling, E. J. and Cooke, S.: Stable oxygen and carbon isotopes in foraminiferal carbonate shells in: Modern foraminifera, edited by: Gupta, B. S. K., Dortrecht, Boston, London, 239–258, 1999.

Rossow, W. B. and Schiffer, R. A.: ISCCP cloud data products, B. Am. Meteorol. Soc., 72, 2–20, 1991.

Sautter, L. R. and Thunell, R. C.: Seasonal succession of planktonic foraminifera: results from a four-year time-series sediment trap experiment in the northeast Pacific, J. Foramin. Res., 19, 253–267, 1989.

Schiebel, R., Hiller, B., and Hemleben, C.: Impacts of storms on recent planktic foraminiferal test production and $CaCO_3$ flux in the North Atlantic at 47.8° N, 20.8° W (JGOFS), Mar. Micropal., 26, 115–129, 1995.

Schiebel, R., Bijma, J., and Hemleben, C.: Population dynamics of the planktic foraminifer *Globigerina bulloides* from the eastern North Atlantic, Deep-Sea Res. 44, 1701–1713, 1997.

Schiebel, R., Waniek, J., Bork, M., and Hemleben, C.: Planktic foraminiferal production stimulated by chlorophyll redistribution and entrainment of nutrients, Deep-Sea Res. I, 48, 721–740, 2001.

Schnack-Schiel, S. B., Dieckmann, G. S., Gradinger, R., Melnikov, I. A., Spindler, M., and Thomas, D. N.: Meiofauna in sea ice of the Weddell Sea (Antarctica), Polar Biol., 24, 724–728, 2001.

Schulz, H., Von Rad, U., and Ittekkot, V.: Planktic foraminifera, particle flux and oceanic productivity off Pakistan, NE Arabian Sea: modern analogues and application to the paleoclimatic record, in: The Tectonic and Climatic Evolution of the Arabian Sea Region, edited by: Clift, P. D., Kroon, D., Gaedicke, C., and Craig, J., Geol. Soc. Spec. Publ., 195, 499–516, 2002.

Spindler, M., Hemleben, C., Salomons, J. B., and Smit, L. P.: Feeding behavior of some planktonic foraminifers in laboratory cultures, J. Foramin. Res., 14, 237–249, 1984.

Spindler, M. and Dieckmann, G. S.: Distribution and Abundance of the Planktic Foraminifer *Neogloboquadrina pachyderma* in Sea Ice of the Weddell Sea (Antarctica), Polar Biol., 5, 185–191, 1986.

Spindler, M.: On the salinity tolerance of the planktonic foraminifer *Neogloboquadrina pachyderma* from Antarctic sea ice, Polar Biol., 9, 85–91, 1996.

Steele, J. H. and Henderson, E. W.: The role of predation in plankton models, J. Plankton Res., 14, 157–172, 1992.

Stewart, I. A., Darling, K. F., Kroon, D., Wade, C. M., and Troelstra, S. R.: Genotypic variability in subarctic Atlantic planktic foraminifera, Mar. Micropal., 43, 143–153, 2001.

Takahashi, K. and Bé, A. W. H.: Planktonic foraminifera: factors controlling sinking speed, Deep-Sea Res., 31, 1477–1500, 1984.

Tedesco, K. A. and Thunell, R. C.: Seasonal and interannual variations in planktonic foraminiferal flux and assemblage composition in the Cariaco Basin, Venezuela, J. Foramin. Res., 33, 192–210, 2003.

Tegen, I. and Fung, I. Y.: Modeling of mineral dust in the atmosphere: sources, transport, and optical thickness, J. Geophys. Res., 99, 22 897–22 914, 1994.

Tegen, I. and Fung, I. Y.: Contribution to the atmospheric mineral aerosol load from land surface modification, J. Geophys. Res., 100, 18 707–18 726, 1995.

Thunell, R. C. and Honjo, S.: Calcite dissolution and the modification of planktonic foraminiferal assemblages, Mar. Micropal., 6, 169–182, 1981.

Thunell, R. C. and Reynolds, L. A.: Sedimentation of planktonic foraminifera: seasonal changes in species flux in the Panama Basin, Micropaleontology, 30, 243–262, 1984.

Tian, J., Wang, P., Chen, R., and Cheng, X.: Quaternary upper ocean thermal gradient variations in the South China Sea: Implications for east Asian monsoon climate, Paleoceanography, 20, 4007, doi:10.1029/2004PA001115, 2005.

Tolderlund, D. S. and Bé, A. W. H.: Seasonal distribution of planktonic Foraminfera in the western North Atlantic, Micropalaeontology, 17, 297–329, 1971.

Trull, T. W., Bray, S. G., Manganini, S. J., Honjo, S., and Francois, R.: Moored sediment trap measurements of carbon export in the Subantarctic and Polar Frontal Zones of the Southern Ocean, south of Australia, J. Geophys. Res., 106, 31 489–31 510, 2001.

Waelbroeck, C., Mulitza, S., Spero, H., Dokken, T., Kiefer, T., and Cortijo, E.: A global compilation of late Holocene planktonic foraminiferal δ^{18}O: relationship between surface water temperature and δ^{18}O, Quat. Sci. Rev., 24, 853–868, 2005.

Watkins, J. M., Mix, A. C., and Wilson, J.: Living planktic foraminifera: tracers of circulation and productivity regimes in the central equatorial Pacific, Deep-Sea Res. II, 43, 1257–1282, 1996.

Watkins, J. M. and Mix, A. C.: Testing the effects of tropical temperature, productivity, and mixed-layer depth on foraminiferal transfer functions, Paleoceanography, 13, 96–105, 1998.

Wefer, G.: Particle Flux in the Ocean: Effects of Episodic Production, in: Productivity of the Ocean: Present and Past, edited by: Berger, W. H., Smetacek, V. S., and Wefer, G., 139–154, John Wiley and Sons, New York, 1989.

Wong, C. S., Whitney, F. A., Crawford, D. W., Iseki, K., Matear, R. J., Johnson, W. K., Page, J. S., and Timothy, D.: Seasonal and interannual variability in particle fluxes of carbon, nitrogen and silicon from time series of sediment traps at Ocean Station PAPA, 1982–1993: relationship to changes in subarctic primary productivity, Deep-Sea Res. II, 46, 2735–2760, 1999.

Xu, X., Yamasaki, M., Oda, M., and Honda, M. C.: Comparison of seasonal flux variations of planktonic foraminifera in sediment traps on both sides of the Ryukyu Islands, Japan, Mar. Micropal., 58, 45–55, 2005.

Žarić, S., Donner, B., Fischer, G., Mulitza, S., and Wefer, G.: Sensitivity of planktic foraminifera to sea surface temperature and export production as derived from sediment trap data, Mar. Micropal., 55, 75–105, 2005.

Žarić, S., Schulz, M., and Mulitza, S.: Global prediction of planktic foraminiferal fluxes from hydrography and productivity data, Biogeosciences, 3, 187–207, 2006.

Submitted to Marine Micropaleontology as: Fraile, I, Mulitza, S. and Schulz, M. – *"Modeling planktonic foraminiferal seasonality: Implications for SST reconstructions"*

Chapter 3

Seasonal bias in Foraminifera-based Proxy records

Abstract

A global foraminiferal model was used to determine the seasonal imprint of planktonic foraminifera on the sedimentary record. The model provides monthly concentrations of five planktonic foraminiferal species used in paleoceanographic reconstructions including N. pachyderma (sin. and dex.), G. bulloides, G. ruber (white) and G. sacculifer. The temperature imprint in foraminiferal shells varies according to the season of calcification, and the sedimentary records retain this seasonal imprint. Proxy records for a species will therefore be weighted towards the values during the season of maximum production for that species. Our model prediction reveals that, in general, at high latitudes, close to the geographical limit of occurrence of each species, the signal is biased towards summer conditions. In contrast, at lower latitudes the signal is biased towards winter or annual mean conditions. Temperatures derived from G. ruber (white) and G. sacculifer are most suitable for estimating annual mean SST in tropical waters, between 20°N/S, while G. ruber (white) when collected at mid-latitudes, near to 40° latitude, reflects mainly summer conditions.

We carried out sensitivity experiments to study the response of planktonic foraminiferal seasonality to changes in temperature. We forced the model decreasing the temperature globally by 2°C and 6°C. In most of the regions, due to the cooling, the season of maximum production shifted to a warmer season. Thus, the foraminiferal population as a whole recorded little change in the temperature. In tropical waters, where temperature seasonality is low, foraminiferal population recorded the entire temperature variation. These findings highlight the importance of considering changes in seasonality through time.

3.1 Introduction

Planktonic foraminifera are the most common source of paleoceanographic proxies. Their long geological history, good preservation in sediments and easy collection make foraminifera ideal bio-indicators of marine environmental changes (e.g., Barbieri et al., 2006). Assemblages of fossil planktonic foraminifera, size and

isotopic ratios or trace-element composition of foraminiferal calcite are used to quantify the sea-water temperature in which the foraminifera grew (e.g., Schmidt et al., 2004; Rohling and Cooke, 1999; Lea, 1999). The use of planktonic foraminifera as a basis for geochemical proxies relies upon the knowledge of the ecology of the signal carriers (e.g., Rohling et al., 2004). Sediment traps, plankton tows and laboratory cultures have contributed to the understanding of planktonic foraminiferal ecology, revealing that foraminifera have large seasonal variations in abundance, tied closely to surface water hydrography (Bé, 1960; Bé and Tolderlund, 1971; Deuser et al., 1981; Thunell and Reynolds, 1987; Sautter and Thunell, 1991). Because of that, the recorded temperature may reflect the integration of a flux pattern or a short time period of the year (Mix, 1987; Deuser, 1987; Mulitza et al., 1998). Thus, the temperature signature found in the sedimentary record lies between the annual mean water temperature and the temperature preferred by a species. Sediment-trap studies have shown that depending on species and sampling location, that recorded temperature signal can be associated to different seasons. For example, Tedesco et al. (2007), concluded that in the Cariaco Basin the sediment $\delta^{18}O$ record of *G. ruber* (pink) is most suitable for estimating past values of annual sea-surface temperature (SST), while *G. bulloides* provides information on conditions during the spring upwelling. *G. ruber* (white) is often considered to be a summer species. However, Tian et al. (2005) have shown that in the South China Sea the highest flux of *G. ruber* (white) occurs during winter. The difference in isotopic signature between species has also been suggested as a tool for the estimation of seasonality (Deuser and Ross, 1989). Niebler et al. (2003) pointed out that discrepancies between temperature reconstructions based on foraminifera and alkenones might be due to different ecological and thus seasonal preferences of alkenone producing algae and planktonic foraminifera.

The geographical distribution of a species and its abundance depends on the physico-chemical properties of the water and the species-specific ecological demands (e.g., Bé and Hamilton, 1967; Bé, 1977). The faunal biogeographical provinces are distributed along latitudinal zones, reflecting the strong relationship between SST and species abundances (e.g., Murray, 1897; Bé and Tolderlund, 1971; Bijma et al., 1990). Foraminifera may respond to environmental changes in terms of reproduction rates, leading to high production of specimens under favorable conditions and to their disappearance under strongly unfavorable environmental conditions (Barbieri et al., 2006; Kucera, 2007). The imprint of this seasonality is preserved in the sedimentary record (Wefer, 1989; Ganssen and Kroon, 2000; King and Howard, 2005; Schiebel and Hemleben, 2005). The seasonality of some species may change through time as climate changes, leading to a bias in estimated paleotemperature. This variation needs to be quantified in order to reduce uncertainties of foraminifera-based SST reconstructions.

In this study, we use the global planktonic foraminiferal model to compare the temperature signature recorded in five planktonic foraminifera species. We conduct sensitivity experiments to test the response of planktonic foraminifera to changes in SST.

3.2 Data and Methods

3.2.1 Description of the model

To study the seasonal variations of planktonic foraminifera species we used a dynamic foraminiferal model (Fraile et al., 2008). This model is forced with a global hydrographic dataset (e.g. temperature, mixed layer depth) and with biological information taken from a ecosystem model (Moore et al., 2002) to predict the growth rate of five foraminifera species: *N. pachyderma* (sinistral and dextral varieties), *G. bulloides*, *G. ruber* (white variety) and *G. sacculifer*. These species are mostly found in the euphotic zone, and reflect the sea surface environment (Bé, 1982). Previously, this model has been validated against a diverse set of field observations from several core-tops and sediment traps. The full list of model terms, parametrizations, equations and behavior in the global domain is described in detail in Fraile et al. (2008).

3.2.2 Sediment-trap data

Using the model prediction and in situ observations from sediment trap, we calculated the theoretical annual temperature signal recorded by the mean population of a species (T_r). We used planktonic foraminifera flux data from a global sediment-trap dataset (Žarić et al., 2005) to compare model results with observational data. The dataset contains time series of planktonic foraminiferal species flux from 42 different sites. We added two more time series from the northern North Atlantic, at 69.69°N 0.48°W and 72.38°N 7.71°W (Jensen, 1998). We only used sediment-trap data with a minimum sampling period of one year. When the sampling period exceeded one year, the data were split to single years and they were used as independent time-series records. T_r for sediment-trap data was calculated using SST derived from the Integrated Global Ocean Services System Products Bulletin (IGOSS) (Reynolds and Smith, 1994), the same SST as Žarić et al. (2005) for the sediment-trap studies. The locations and original data sources of the sediment traps used for this analysis are listed in Table 3.1.

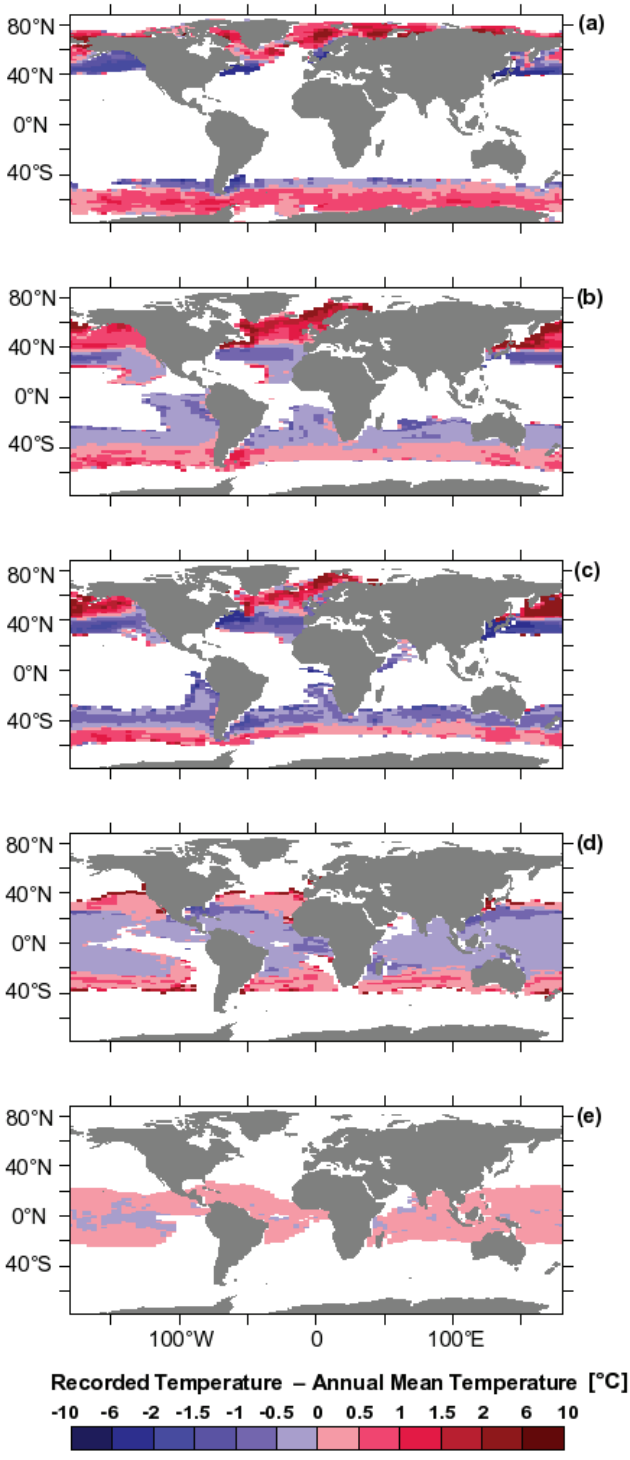

Figure 3.1: *Difference between recorded temperature and annual mean SST (WOA98) ($T_r - T_a$). T_r is based on the monthly concentrations predicted with PLAFOM.*
(a) *N. pachyderma (sin.),*
(b) *N. pachyderma (dex.),*
(c) *G. bulloides,*
(d) *G. ruber (white),*
(e) *G. sacculifer.*

3.2.3 Experimental design

We carried out a standard and three sensitivity experiments to test the response of the five planktonic foraminifera species to changes in SST: In the standard run we forced the model with climatological SST from the World Ocean Atlas WOA98 (Conkright et al., 1998). In the first two sensitivity experiments we decreased SST globally by 2°C and 6°C respectively. In the third experiment we raised the amplitude of temperature seasonality by 25 %, that is, we increased summer temperature and decreased winter temperature. Temperature can exert direct influence on foraminifera, or can also entail changes in the ecosystem model and affect the foraminifera indirectly. In order to differentiate both effects, these imposed temperature changes have been applied separately to the foraminifera and ecosystem models.

3.3 Results

3.3.1 Influence of seasonality and temperature sensitivity on temperature estimates

For both, observational and modeled data, we calculated the annual temperature signal recorded by the mean population of a species (T_r), as

$$T_r = \frac{\sum_{m=1}^{12} (C_m \times T_m)}{\sum_{m=1}^{12} C_m} \tag{3.1}$$

where C_m is monthly species concentration (or flux for sediment-trap data) and T_m denotes SST. At each site, T_r ranges between the mean water temperature and mean preferred temperature by the species (Mix, 1987). Taking into account monthly concentrations of the species (modeled with PLAFOM) and monthly SST from the WOA98 (Conkright et al., 1998), we estimated T_r that corresponds to the theoretical flux-weighted mean temperature signal found in sediments. In order to determine the effect of seasonality, the difference between the annual mean temperature (T_a) and the recorded temperature (T_r) is shown in Fig. 3.1. Positive values indicate that the species live during the warm season, and therefore, the recorded temperature is above the annual mean. Negative values indicate that the temperature signal is biased towards the cold season. Depending on the latitude or oceanic region, the same species can reflect different seasonal signals. Since the model has no internal variability, a statistical significance of the differences cannot be assessed.

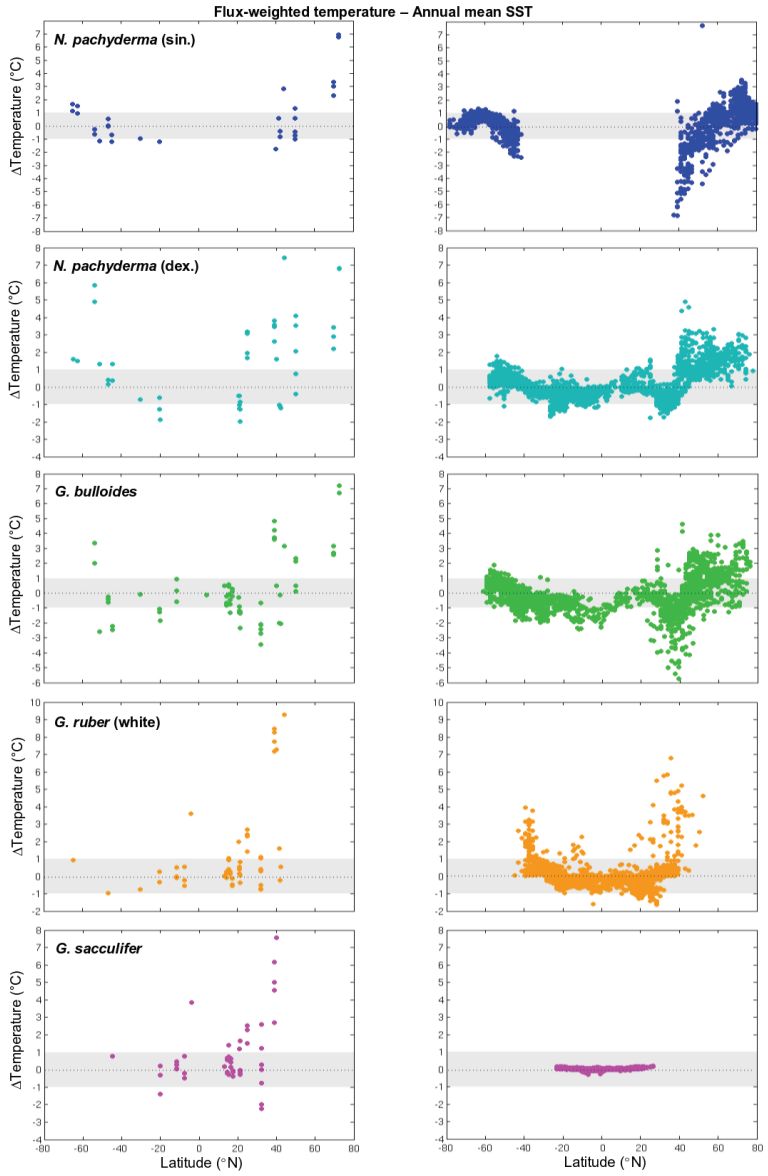

Figure 3.2: *Variation of $T_r - T_a$ with latitude from sediment-trap data (left) (Žarić et al., 2005) and model prediction (right). Positive values: T_r reflects "warm" conditions. Shadowing: T_r coincides with annual mean temperature within $\pm\ 1\ ^\circ C$.*

Our model simulation indicates that the temperature differences show that the flux-weighted annual temperatures derived from *N. pachyderma* (sin.) correspond to summer temperatures at high latitudes, but can also reflect temperatures of colder seasons when collected from lower latitudes (Fig 3.1). *N. pachyderma* (dex.) and *G. bulloides* show a very similar pattern: At high latitudes they record a summer signal; around 40° latitude, T_r is close to the annual mean temperature, and equatorwards of 40° the winter signal becomes more significant. For both species, in the northern hemisphere, the effect of seasonality appears more important. *G. ruber*, in general, records temperatures close to the annual mean. At the limit of its distribution, around 40° latitude, it records summer temperatures. Our model results suggest that the flux-weighted annual temperatures derived from *G. sacculifer* are within ± 1°C of the annual mean SST.

For both, model and sediment-trap data, the imprint of seasonal foraminiferal production varies with latitude (Fig. 3.2).

For all species, except *G. bulloides*, the general trend shown by the sediment-trap is the same: at low latitudes the temperature signal recorded in the shell is close to the annual mean ($\pm$ 1°C), while at high latitudes it is biased towards summer temperatures.

A similar pattern can be observed in the model-simulated reconstructions for most of the species. Our model indicates that *N. pachyderma* (sin.) records summer conditions at high latitudes (60° – 80°N), but around 40°N it can also record winter temperatures. Both sediment-trap data and model simulations illustrate that the temperature signal derived from *N. pachyderma* (dex.) is up to 5 – 7°C above the annual mean between 40 – 80° latitude. The flux-weighted annual temperature derived from *G. bulloides* does not show a strong change related to latitude. In the northern hemisphere, in particular, it can record temperatures above and below the annual mean. The latitudinal effect in the case of *G. ruber* appears very important: In tropical waters (20°S – 20°N) *G. ruber* (white) records annual mean SST, while in subtropical waters it provides information on summer conditions. The model predicts the *G. sacculifer* population is limited to tropical waters (20°N – 20°S), where seasonality has no effect on the recorded temperature.

3.3.2 Sensitivity analysis

Since the seasonality of foraminifera could have been different during for example, glacials, we carried out sensitivity experiments to test the response of planktonic foraminifera to changes in temperature. In the first experiment we decreased temperature globally by 2°C. The temperature change was only applied to the foraminiferal module, thus, the underlying ecosystem model was forced with modern SST. If

Table 3.1: *Locations and data sources of the planktonic foraminifera faunas (modified from Žarić et al., 2005).*

Trap Location		Latitude[° N]	Longitude[° E]	References
Ocean Station Papa		50.00	−−145.00	Reynolds and Thunell (1985)
				Reynolds and Thunell (1986)
				Sautter and Thunell (1989)
				Wong et al. (1999)
Peru-Chile Current		−−30.01	−−73.18	Marchant et al. (1998)
				Hebbeln et al. (2000)
Sargasso Sea		32.08	−−64.25	Deuser et al. (1981)
				Deuser (1987)
				Deuser and Ross (1989)
N′ North Atlantic	NB–6	72.38	−−7.71	Jensen (1998)
	NB–7	69.69	0.48	Peinert et al. (2001)
Cape Blanc	CB–1	20.76	−−19.74	Fischer and Wefer (1996)
	CB–2,3,4	21.15	−−20.68	Žarić et al. (2005)
W′ equatorial Atlantic	WA–1	−−4.00	−−25.57	Fischer and Wefer (1996)
	WA–2,3	−−7.52	−−28.04	Žarić et al. (2005)
W Atlantic	WAB–1	−−11.57	−−28.53	Fischer (unpubl. data)
				Žarić et al. (2005)
Walvis Ridge	WR–2,3	−−20.05	9.16	Fischer and Wefer (1996)
	WR–4	−−20.13	8.96	Žarić et al. (2005)
Weddell Sea	WS–1	−−62.44	−−34.76	Donner and Wefer (1994)
	WS3,4	−−64.91	−−2.55	
Arabian Sea	WAST	16.33	60.49	Curry et al. (1992)
	CAST	14.49	64.76	Guptha and Mohan (1996)
	EAST	15.48	68.74	Haake et al. (1993)
Bay of Bengal	NBBT	17.45	89.60	Guptha and Mohan (1996)
	CBBT	13.15	84.35	Guptha et al. (1997)
Northwest Pacific	WCT–1	25.00	136.99	Mohiuddin et al. (2002)
	WCT–2	39.01	147.00	
NW′ North Pacific	50N	50.02	165.03	
	KNOT	43.97	155.05	Kuroyanagi et al. (2002)
	40N	40.00	165.00	
Subantarctic Zone	SAZ–47	−−46.76	142.07	King and Howard (2003a,b)
	SAZ–51	−−51.00	141.74	Trull et al. (2001)
	SAZ–54	−−53.75	141.76	
Chatman Rise	SCR	−−44.62	178.62	King and Howard (2001)
				Nodder and Northcote (2001)

there is no change in the seasonality of foraminifera, then the expected temperature variation recorded by foraminifera will be 2°C . In our experiment, due to cooling, the maximum production month for most species shifted to a warmer season, and as a consequence the temperature variation retained in the sedimentary record was often significantly underestimated (Table 3.2). However, the estimates derived from *G. sacculifer*, as well as *N. pachyderma* (sin. and dex.) in the Arctic Ocean and in polar/subpolar waters, were able to reflect the entire temperature variation of 2°C. *G. ruber* underestimated the variation of temperature at all latitudes, more notable in the subtropical than in the tropical population (maximum bias of 0.4°C in sub-

Table 3.2: *Difference of recorded temperature for $\triangle T = -2^{\circ}C$. Mean temperature difference (sensitivity experiment minus standard experiment) recorded by the species and its standard deviation (σ). Empty cells indicate that the species is not living in this region. * denotes that temperature variation was significantly underestimated (t–test with 99% of confidance; ** 95% of confidance). $\triangle T$ applied only to the foraminifera model.*

	Ocean regions	*N.pachyderma* (sin.)		*N. pachyderma* (dex.)		*G. bulloides*		*G. ruber* (white)		*G. sacculifer*	
		mean	σ	mean	σ	mean	σ	mean	σ	mean	σ
Atlantic	Polar/Subpolar (60 °–90°)	–2	0.6	–1.9**	0.3	–1.7*	0.5	—		—	
	Temperate (40°–60°)	–1.9*	0.5	–1.9*	0.2	–1.8*	0.3	—		——	
	Subtropic (20°–40°)	—		–1.9*	0.3	–2	0.4	–1.6*	0.5	–2	< 0.1
	Tropic(0°–20°)	—		–2	0.3	–1.7*	0.6	–1.8*	0.3	–2	< 0.1
Pacific	Polar/Subpolar (60°–90°)	–1.9**	0.4	—		—		—		—	
	Temperate (40°–60°)	–1.6*	0.7	–1.8*	0.4	–1.7*	0.3	—		—	
	Subtropic (20°–40°)	—		–1.8*	0.3	–2	0.5	–1.7*	0.5	–2	< 0.1
	Tropic(0°–20°)	—		–1.9*	0.3	–1.6*	0.7	–1.9*	0.1	–2	< 0.1
Indian	Polar/Subpolar (60°–90°)	–2.5	0.4	—		—		—		—	
	Temperate (40°–60°)	–1.9*	0.2	–1.9*	0.2	–1.9*	0.2	—		—	
	Subtropic (20°–40°)	—		–1.8*	0.3	–1.9*	0.3	–1.8*	0.4	–2	< 0.1
	Tropic (0°–20°)	—		—		–1.9*	0.2	–1.9*	0.2	–2	< 0.1
Arctic (70°– 90°N)		–1.9	0.5	–2	0.3	–1.5*	0.5	—		—	

tropics compared to 0.2°C in subtropics).

We carried out another experiment in which the 2°C temperature reduction was only applied to the ecosystem model, while the foraminifera model used modern SST. Except for *G. bulloides*, the variations in the ecosystem model due to the temperature reduction did not influence the seasonality of foraminifera, and therefore the species were able to record the entire temperature variation (Table 3.3). Hence, for the subsequent analysis, we only consider the direct temperature control on foraminifera and not the indirect effect via the ecosystem.

In the second sensitivity experiment, decreasing SST globally by 6°C, *N. pachyderma* (sin.) disappeared from the Pacific and Indian sectors of the Southern Ocean (Table 3.4). *N. pachyderma* (dex.) recorded a variation of 5.5 – 5.9°C, and was the species that, after *G. sacculifer*, best documented the entire temperature change of 6°C. *G. bulloides* and *G. ruber* recorded the were closer to record the entire variation of 6°C at low latitudes than at high latitudes. The temperature change reflected by

Table 3.3: *Difference of recorded temperature for $\triangle T = -2^{\circ}C$. Mean temperature difference (sensitivity experiment minus standard experiment) recorded by the species and its standard deviation (σ). Empty cells indicate that the species is not living in this region. * denotes that temperature variation was significantly underestimated (t–test with 99% of confidance; ** 95% of confidance). $\triangle T$ applied only to the ecosystem model.*

	Ocean regions	*N.pachyderma* (sin.)		*N. pachyderma* (dex.)		*G. bulloides*		*G. ruber* (white)		*G. sacculifer*	
		mean	σ	mean	σ	mean	σ	mean	σ	mean	σ
Atlantic	Polar/Subpolar (60 °–90°)	–2	0.2	–2.1	0.2	–2	0.4	—		—	
	Temperate (40°–60°)	–2	0.2	–2	0.2	–1.9*	0.3	—		—	
	Subtropic (20°–40°)	—		–2	0.3	–1.9	0.4	–2	0.3	–2.1	< 0.1
	Tropic(0°–20°)	—		–2	0.3	–1.6*	0.5	–1.9*	0.1	–2	< 0.1
Pacific	Polar/Subpolar (60°–90°)	–2	0.1	—		—		—		—	
	Temperate (40°–60°)	–2	0.1	–2	0.2	–1.9*	0.3	—		—	
	Subtropic (20°–40°)	—		–2	0.3	–2	0.5	–2	0.3	–2.1	< 0.1
	Tropic(0°–20°)	—		–1.9*	0.3	–1.4*	0.6	–2	0.1	–2	< 0.1
Indian	Polar/Subpolar (60°–90°)	–2	0.1	—		—		—		—	
	Temperate (40°–60°)	–2	0.2	–2	0.2	–1.9*	0.2	—		—	
	Subtropic (20°–40°)	—		–1.9*	0.3	–1.9*	0.4	–2.1	0.2	–2.1	< 0.1
	Tropic(0°–20°)	—		—		–1.9**	0.2	–1.9*	0.1	–2	< 0.1
Arctic (70° – 90°N)		–1.9	0.4	–2	0.3	–2.1	0.5	—		—	

G. bulloides was around 5.2 – 5.7°C at polar/subpolar and temperate regions; while in the tropics and subtropics the temperature change was 5.4 – 6°C.

G. ruber (white), in the subtropics, underestimated the variation of temperature to a greater °than in the tropics (5.1 – 5.6°C compared to 5.7 – 5.8°C in the tropics). *G. sacculifer* reflected accurately the total temperature change.

The last sensitivity experiment consists on increasing the seasonality of temperature by 25%. This implies a cooling of winter temperature, while summer temperature increases. The variation of T_r in all cases was very small, less than 0.2°C, which has not measurable effect in paleotemperature estimations (Table 3.5).

Table 3.4: *Difference of recorded temperature for $\triangle T = -2^{\circ}C$. Mean temperature difference (sensitivity experiment minus standard experiment) recorded by the species and its standard deviation (σ). Empty cells indicate that the species is not living in this region. * denotes that temperature variation was significantly underestimated (t–test with 99% of confidance; ** 95% of confidance). $\triangle T$ applied only to the foraminifera model.*

	Ocean regions	*N.pachyderma* (sin.)		*N. pachyderma* (dex.)		*G. bulloides*		*G. ruber* (white)		*G. sacculifer*	
		mean	σ	mean	σ	mean	σ	mean	σ	mean	σ
Atlantic	Polar/Subpolar (60°–90°)	–5.3*	0.6	–5.8*	0.5	–5.3*	0.4	—		—	
	Temperate (40°–60°)	–5*	1.3	–5.5*	0.5	–5.4*	0.6	—		—	
	Subtropic (20°–40°)	—		–5.6*	0.4	–6	0.6	–5.1*	0.9	–6.1	< 0.1
	Tropic (0°–20°)	—		–5.9*	0.3	–5.7*	0.6	–5.7*	0.3	–6	< 0.1
Pacific	Polar/Subpolar (60°–90°)	—		—		—		—		—	
	Temperate (40°–60°)	–4.3*	1.6	–5.6*	1	–5.2*	0.7	—		—	
	Subtropic (20°–40°)	—		–5.5*	0.5	–5.7*	0.7	–5.3*	1	–6	< 0.1
	Tropic(0°–20°)	—		–5.8*	0.4	–5.6*	0.6	–5.8*	0.3	–6	< 0.1
Indian	Polar/Subpolar (60°–90°)	—		—		—		—		—	
	Temperate (40°–60°)	–5.6*	0.4	–5.8*	0.3	–5.7*	0.3	—		—	
	Subtropic (20°–40°)	—		–5.6*	0.3	–5.7*	0.4	–5.6*	0.9	–6	< 0.1
	Tropic (0°–20°)	—		–5.5*	0.4	–5.9*	0.2	–5.8*	0.2	–6	< 0.1
Arctic (70°– 90°N)		–5.1*	0.9	–5.9**	0.3	–5.1*	0.5	—		—	

3.4 Discussion

3.4.1 Latitudinal species distribution

Our study suggests that for all species, except *G. sacculifer*, the recorded temperature signal varies depending on the sampling location. In general, at high latitudes, close to the geographical limit of occurrence of each species, the signal is biased toward summer conditions, while at lower latitudes the signal shifts towards winter or annual mean temperatures. *G. ruber* (white) records temperatures close to annual mean when collected in tropical waters. However, near 40°, at the edge of its thermal distribution range, it reflects summer temperatures. The model prediction shows that the flux-weighted reconstructed temperatures derived from *G. sacculifer* are close to the annual mean SST, indicating that shells of *G. sacculifer* provide a good proxy to estimate annual mean temperatures. These is consistent with previ-

Table 3.5: *Difference of recorded temperature for increased temperature seasonality. Mean temperature difference (sensitivity experiment minus standard experiment) recorded by the species and its standard deviation (σ). Empty cells indicate that the species is not living in this region. $\triangle T$ applied only to the foraminifera model.*

	Ocean regions	*N.pachyderma* (sin.)		*N. pachyderma* (dex.)		*G. bulloides*		*G. ruber* (white)		*G. sacculifer*	
		mean	σ	mean	σ	mean	σ	mean	σ	mean	σ
Atlantic	Polar/Subpolar (60°–90°)	0.04	0.11	0.01	0.06	0.02	0.24	—		—	
	Temperate (40°–60°)	–0.05	0.27	0.05	0.12	0.01	0.13	—		—	
	Subtropic (20°–40°)	—		–0.05	0.08	–0.19	0.32	0.02	0.16	0.01	0.00
	Tropic (0°–20°)	—		–0.04	0.10	–0.09	0.31	–0.03	0.09	0.00	0.00
Pacific	Polar/Subpolar (60°–90°)	0.02	0.08	—		—		—		—	
	Temperate (40°–60°)	–0.13	0.31	0.11	0.21	0.02	0.10	—		—	
	Subtropic (20°–40°)	—		–0.06	0.10	–0.16	0.34	0.01	0.22	0.01	0.00
	Tropic (0°–20°)	—		–0.04	0.05	–0.16	0.31	–0.02	0.04	0.00	0.00
Indian	Polar/Subpolar (60°–90°)	0.07	0.04	—		—		—		—	
	Temperate (40°–60°)	–0.03	0.13	0.04	0.10	0.02	0.09	—		—	
	Subtropic (20°–40°)	—		–0.03	0.10	–0.09	0.13	0.02	0.15	0.01	0.00
	Tropic (0°–20°)	—		–0.06	0.16	0.00	0.14	–0.03	0.03	0.00	0.01
Arctic (70°– 90°N)		0.03	0.12	–0.01	0.10	0.03	0.24	—		—	

ous work of Curry et al. (1983), who concluded that the flux weighted $\delta^{18}O$ composition of sediment-trap samples was in agreement with annual mean hydrography in the area of Panama Basin. On the other hand, the model predicts the population of *G. sacculifer* is limited to tropical waters (20°N – 20°S), where annual temperature variations are relatively small. Instead, sediment-trap data shows fluxes of *G. sacculifer* shells up to 40 °N, where the effect of seasonality increases. These samples belong to the stations in the northwestern Pacific (WCT-2 and 40N in Table 3.1). At WCT-2, *G. sacculifer* contributed a small part (less than 1%) of the total foraminiferal flux (Mohiuddin et al., 2002). At 40N, Kuroyanagi et al. (2002) measured temperatures up to 24°C during late summer, while our climatological SST has a maximum of 20°C. This difference in temperature could be the reason why the model does not predict *G. sacculifer* at these latitudes.

In any case, using this foraminiferal model, we cannot simulate seasonal variations of *G. sacculifer* above 20° latitude.

3.4.2 Sensitivity of species to changes in SST

With global cooling of 2°C the foraminiferal maximum production can shift to warmer seasons; thus the mean population would record little change in isotopic or trace element composition (Mix, 1987). Our experiments show that, in most regions, the species are not able to record the entire cooling of 2°C and 6°C. The foraminifera-based signal underestimates the temperature variation up to 0.5°C for the 2°C cooling and up to 1.7°C for the 6°C cooling. At polar/subpolar waters the temperature decrease of 2°C is indeed recorded by *N. pachyderma* (sin.). In these regions the foraminiferal seasonal maxima occurs during summer; therefore it can not shift to warmer conditions. There are a few locations where foraminifera overestimated the variation of temperature; e.g. *N. pachyderma* (sin.) in the Indian sector on the Southern Ocean and *G. sacculifer* in suptropical waters of the Atlantic Ocean. At these locations foraminiferal maximum production occurs in summer. Upon cooling, the seasonal maximum does not shift in phase, but the amplitude of the peak decreases; while the population size during the winter season does not diminish (but remains close to the threshold value set in the model to keep a minimum population over the year). In this way, the relative weight of the winter population increases and the temperature signal reflects cooler conditions. It is however possible that this is a model artifact rather than a circumstance that can be found in nature.

In tropical waters of the Atlantic and Pacific Oceans, *N. pachyderma* (dex.) is linked to coastal upwelling zones, and follows the dynamic and seasonal succession of the upwelling region. SST decrease produces little or no change in the seasonality of this species.

For *G. bulloides*, considered as a productivity proxy (Hemleben et al., 1989; Sautter and Thunell, 1991; Prell, 1993; Watkins and Mix, 1998; Ortiz et al., 1995), temperature does not seem to be the controlling factor (Deuser et al., 1981; Thunell and Honjo, 1984; Žarić et al., 2005). Nevertheless, except in subtropical waters, the temperature variation recorded by the shell was underestimated. In tropical waters of the Pacific Ocean, the model predicts *G. bulloides* living close to the Peru upwelling system. The seasonal maximum of *G. bulloides* occurs during November-December with the end of the strong upwelling season (Marchant et al., 1998). The effect of decreasing SST by 2°C, is to bring temperature during these months closer to the optimal temperature of *G. bulloides*, and therefore the amplitude of the seasonal peak increases. Our simulation does not show a shift of the seasonal maximum, but due to increase in abundance during these months (beginning of austral sum-

mer), the relative weight of the summer signal increased, and T_r underestimated the prescribed variation. The same situation arises in tropical regions of the Atlantic Ocean, where *G. bulloides* is linked to the upwelling system of Benguela.

In both experiments, the temperature bias in *G. ruber* (white) population was stronger in the subtropics than in the tropics. In tropical waters, a decrease of 2°C still allows *G. ruber* to live during cold seasons. In contrast, in the subtropics, where the seasonality of temperature is higher, a 2°C decrease in winter shifts the maximum production to the summer. With the 6°C cooling the seasonal peak shifts to summer months in both regions, but since the amplitude of temperature seasonality is larger in the subtropics, the effect on the recorded signal is also more pronounced. *G. sacculifer*, when living in tropical waters, can record a temperature decrease of 2°C and 6°C. In tropical waters the seasonality of temperature is not very pronounced, and therefore shifts in foraminiferal production do not affect the annual proxy signal found in sediments.

Increasing the amplitude of temperature seasonality by 25% does not show effects in the recorded temperature signal. The differences between the standard and sensitivity experiment (0 – 0.16°C), although in some cases statistically significant, are not measurable in proxy records. *G. bulloides* is the only species underestimating T_r by 0.2°C in subtropical and tropical regions. For the remaining species, the differences are within the typical analytical uncertainty of $\pm$ 1°C (Anand et al., 2003; Dekens et al., 2002; Shen et al., 2007).

This foraminiferal model allows to project any climate change to the temperature signature of the population of each species reaching the sea floor. However, this model is limited to the global ocean mixed-layer, assuming that it is biologically homogeneous. Therefore, the effects in the temperature signature due to the depth habitat can not be assessed with this model.

3.5 Conclusions

The effect of seasonality at different latitudes has to be taken into account for the calibration and interpretation of foraminifera-based temperature reconstructions, as it may overprint the true climatic signal. The general patterns show that at low latitudes the temperature signal recorded by the shells reflects annual mean temperatures. On the other hand, at high latitudes, due to the fact that the highest seasonal flux occurs during summer, the recorded signal corresponds to summer conditions. For all species, the imprint of seasonality in the recorded temperature signal is more pronounced in the northern hemisphere than in the southern hemisphere.

Our experiments indicate that in regions where foraminiferal maximum production occurs during the warmest season (e.g. *N. pachyderma* (sin.) in polar waters), the species can record a cooling of 2°C. *G. sacculifer*, when living in tropical waters, reflects temperatures close to the annual mean. Therefore the absolute temperature variation is fully recorded. For the remaining species, the temperature signal reflected by the shells underestimates the temperature variation by up to 0.5°C when the global temperature is reduced by 2°C; and up 1.7°C when reduced by 6°C. Nevertheless, the underestimation is relatively small and in most cases is within the analytical uncertainty. Enhancing the amplitude of temperature seasonality by 25% has no measurable impact in the recorded temperature.

Our model prediction suggest that planktonic foraminiferal seasonality is strongly linked to temperature. In this study, we isolated the direct impact of temperature on foraminifera and its implications on the annual flux-weighted temperature signal. Climatic changes include alterations on broad-scale conditions, such mixed-layer depth, ice cover or solar radiation. Applying the same methodology to controlled past climatic conditions enables to quantify the seasonal bias in foraminifera-based proxy records.

Acknowledgments This project was supported by the DFG (Deutsche Forschungsgemeinschaft) as part of the European Graduate Collegue "Proxies in Earth History" (EUROPROX). We appreciate the contributions and helpful comments of A. Bisset and M. Prange. We also thank G. Fischer for providing sediment-trap data and A. Manschke for computer support.

Bibliography

Anand, P., Elderfield, H. and Conte, M. H., 2003. Calibration of Mg/Ca thermometry in planktonic foraminifera from a sediment trap time series. Paleoceanography, 18, 1050, doi:10.1029/2002PA000846.

Barbieri, R., Hohenegger, J., Pugliese, N., (Eds.), 2006. Foraminifera and Environmental Micropaleontology. Mar. Micropal. (special issue), 61, 1–3.

Bé, A. W. H.,1960. Ecology of Recent planktonic foraminifera: Part 2 – Bathymetric and seasonal distributions in the Sargasso Sea off Bermuda. Micropaleontology, 6, 373–392.

Bé, A. W. H., and Hamilton, W. H., 1967. Ecology of Recent planktonic foraminifera. Micropaleontology, 13, 87–106.

Bé, A. W. H., and Tolderlund, D. S., 1971. Distribution and ecology of living planktonic foraminifera in surface waters of the Atlantic and Indian Oceans. In: Funnell, B. M. and Riedel, W. R. (Eds.), The Micropaleontology of Oceans. Cambridge University Press, pp. 105–149.

Bé, A. W. H., 1977. An ecological, zoogeographic and taxonomic review of recent planktonic foraminifera. In: Ramsay, A.T.S. (Ed), Oceanic Micropaleontology, vol. 1. Academic Press, London, pp. 1–100.

Bé, A. W. H.,1982. Biology of planktonic foraminifera. In: T.W. Broadhead (Ed.), Foraminifera: Notes for a short course. The University of Tennessse, Knoxville, pp. 51–92.

Bijma, J., Faber, W. W. J., and Hemleben, C., 1990. Temperature and salinity limits for growth and survival of some planktonic foraminifers in laboratory cultures. J. Foramin. Res., 20, 95–116.

CLIMAP Project Members, 1976. The surface of the ice–age earth. Science, 191, 1131–1137.

Conkright, M., Levitus, S., OBrien, T., Boyer T., Antonov, J. and Stephens, 1998. World Ocean Atlas 1998 CD–ROM Data Set Documentation. Tech. Rep. 15, NODC Internal Report, Silver Spring, MD, pp. 1–16.

Curry, W. B., Thunell, R. C., and Honjo, S., 1983. Seasonal changes in the isotopic composition of planktonic foraminifera collected in Panama Basin sediment traps, Earth Planet. Sci. Lett., 64, 33–43.

Curry, W. B., Ostermann, D. R., Guptha, M. V. S., and Ittekkot, V., 1992 Foraminiferal production and monsoonal upwelling in the Arabian Sea: evidence from sediment traps. In: Summerhayes, C. P., Prell, W. L., and Emeis, K. C. (Eds.), Upwelling Systems: Evolution Since the Early Miocene, The Geological Society, London, pp. 93–106.

Dekens, P. S., Lea, D. W., Pak, D. K. and Spero, H. J., 2002. Core top calibration of Mg/Ca in tropical foraminifera: Refining paleotemperature estimation. Geochem. Geophys. Geosyst., 3, 1022, doi:10.1029/2001GC000200.

Deuser, W. G., Ross, E. H., Hemleben, C., and Spindler, M., 1981. Seasonal changes in species composition, numbers, mass, size, and isotopic composition of planktonic foraminifera settling into the deep Sargasso Sea. Palaeogeogr. Palaeocl., 33, 103–127.

Deuser, W. G, 1987. Seasonal variations in Seasonal variations in isotopic composition and deep–water fluxes of the tests of perennially abundant planktonic foraminifera of the Sargasso Sea: results from sediment–trap collections and their paleoceanographic significance. J. Foram. Res., 17, 14–27.

Deuser, W. G., and Ross, E. H., 1989. Seasonally abundant planktonic foraminifera of the Sargasso Sea: succession, deep–water fluxes, isotopic compositions, and paleoceanographic implications. J. Foramin. Res., 19, 268–293.

Donner, B. and Wefer, G., 1994 Flux and stable isotope composition of *Neogloboquadrina pachyderma* and other planktonic foraminifers in the Southern Ocean (Atlantic sector). Deep–Sea Res. I, 41, 1733–1743.

Fischer, G. and Wefer, G., 1996. Long–term Observation of Particle Fluxes in the Eastern Atlantic: Seasonality, Changes of Flux with Depth and Comparison with the Sediment Record. In: Wefer, G., Berger, W. H., Siedler, G., and Webb, D. J. (Eds.), The South Atlantic: Present and Past Circulation, Springer–Verlag, Berlin Heidelberg, pp. 325–344.

Fraile, I., Schulz, M., Mulitza, S. and Kucera, M., 2008. Predicting the global distribution of planktonic foraminifera using a dynamic ecosystem model. Biogeosciences, 5, 891–911.

Ganssen, G. M. and Kroon, D., 2000. The isotopic signature of planktonic foraminifera from NE Atlantic surface sediments: implications for the reconstruction of past oceanic conditions. J. Geol. Soc., 157, 693–699.

Guptha, M. V. S. and Mohan, R., 1996. Seasonal variability of the vertical fluxes of *Globigerina bulloides* (d'Orbigny) in the northern Indian Ocean. Mitt. Geol.–Paläont. Inst. Univ. Hamburg, 79, 1–17.

Guptha, M. V. S., Curry, W. B., Ittekkot, V., and Muralinath, A. S., 1997. Seasonal variation in the flux of planktic foraminifera: Sediment trap results from the Bay of Bengal, northern Indian Ocean. J. Foramin. Res., 27, 5–19.

Haake, B., Ittekkot, V., Rixen, T., Ramaswamy, V., Nair, R. R., and Curry, W. B., 1993. Seasonality and interannual variability of particle fluxes to the deep Arabian Sea. Deep–Sea Res. I, 40, 1323–1344.

Hebbeln, D., Marchant, M., and Wefer, G., 2000. Seasonal variations of the particle flux in the Peru–Chile current at 30° S under normal and El Niño conditions. Deep–Sea Res. II, 47, 2101–2128.

Hemleben, C., Spindler, M. and Anderson, O. R., 1989. Modern Planktonic Foraminifera. Springer–Verlag, New York, pp. 1–363.

Jensen, S., 1998. Planktische Foraminiferen im Europäischen Nordmeer: Verbreitung und Vertikalfluss sowie ihre Entwicklung während der letzten 15000 Jahre. Berichte SFB 313, Univ. Kiel, 75, pp. 1–105.

King, A. L. and Howard, W. R., 2001. Seasonality of foraminiferal flux in sediment traps at Chatham Rise, SW Pacific: implications for paleotemperature estimates. Deep–Sea Res. I, 48, 1687–1708.

King, A. L. and Howard, W. R., 2003a. Planktonic foraminiferal flux seasonality in Subantarctic sediment traps: A test for paleoclimate reconstructions. Paleoceanography, 18, 1019, doi:1010.1029/2002PA000839.

King, A. L. and Howard, W. R., 2003b. Seasonal Subantarctic Planktonic Foraminiferal Flux Data, available from the IGBP PAGES/World Data Center for Paleoclimatology (http://www.ngdc.noaa.gov/paleo), Data Contribution Series # 2003–022., NOAA/NGDC Paleoclimatology Program, Boulder CO.

King, A. L. and Howard, W. R., 2005. $\delta^{18}O$ seasonality of planktonic foraminifera from Southern Ocean sediment traps: Latitudinal gradients and implications for paleoclimate reconstructions. Mar. Micropal., 56, 1–24.

Kucera, M., 2007. Planktonic Foraminifera as Tracers of Past Oceanic Environments. In: C. Hillaire–Marcel and A. De Vernal (eds.), Developments in Marine Geology, Vol. 1, Proxies in late Cenozoic paleoceanography. Elsevier, pp. 213–262.

Kuroyanagi, A., Kawahata, H., Nishi, H., and Honda, M. C., 2002. Seasonal changes in planktonic foraminifera in the northwestern North Pacific Ocean: sediment trap experiments from subarctic and subtropical gyres. Deep–Sea Res. II, 49, 5627–5645.

Lea, D. W., 1999. Trace elements in foraminiferal calcite. In: Gupta, B. S. K. (Ed.), Modern foraminifera. Dortrecht, Boston, London, pp. 259–277.

Levitus, S., Boyer, T. Burgett, R. and M. Conkright, 1998. World Ocean Atlas 1998 (WOA98). Ocean Climate Laboratory, National Oceanographic Data Center. NODC_WOA98 data provided by the NOAA/OAR/ESRL PSD, Boulder, Colorado, USA, from their Web site at http://www.cdc.noaa.gov/.

Malmgren, B. A., Kucera, M., Nyberg, J. and Waelbroeck, C., 2001. Comparison of statistical and artificial neural network techniques for estimating past sea surface temperature from planktonic foraminifer census data. Paleoceanography, 16, 520–530.

Marchant, M., Hebbeln, D., and Wefer, G., 1998 Seasonal flux patterns of planktic foraminifera in the Peru–Chile Current. Deep–Sea Res. I, 45, 1161–1185.

Mix, A., 1987. The oxygen–isotope record of glaciation. In: Ruddiman, W.F. and Wright, H.E. (Eds.), North America and adjacent oceans during the last deglaciation. (The Geology of North America, Vol. K–3.). Geol. Soc. Am., Boulder CO, pp. 111–135.

Mohiuddin, M. M., Nishimura, A., Tanaka, Y., and Shimamoto, A., 2002. Regional and interannual productivity of biogenic components and planktonic foraminiferal fluxes in the northwestern Pacific Basin. Mar. Micropal., 45, 57–82.

Moore, J. K., Doney, S. C., Kleypas, J. A., Glover, D. M., and Fung, I. Y., 2002. An intermediate complexity marine ecosystem model for the global domain. Deep–Sea Res. II, 49, 403–462.

Mulitza, S., Wolff, T., Pätzold, J., Hale, W., and Wefer, G., 1998. Temperature sensitivity of planktic foraminifera and its influence on the oxygen isotope record. Mar. Micropal., 33, 223–240.

Murray, J., 1897. On the distribution of the pelagic foraminifera at the surface and on the floor of the oceans. Nat. Sci., 11, 17–27.

Niebler, H. S., Arz, H. W., Donner, B., Mulitza, S., Pätzold, J. and Wefer, G., 2003. Sea surface temperatures in the equatorial and South Atlantic Ocean during the last glacial maximum (23–19 ka). Paleoceanography 18, 1069, doi:1010.1029/2003PA000902.

Nodder, S. D. and Northcote, L. C., 2001. Episodic particulate fluxes at southern temperate mid–latitudes (42—-45° S) in the Subtropical Front region, east of New Zealand. Deep–Sea Res. I, 48, 833–864.

Ortiz, J. D., Mix, A. C., and Collier, R. W., 1995. Environmental control of living symbiotic and asymbiotic foraminifera of the California Current. Paleoceanography, 10, 987–1009.

Peinert, R., Antia, A. N., Bauerfeind, E., Haupt, O., Krumbholz, M., Peeken, I., Bodungen, B. V., Ramseier, R., Voss, M., and Zeitzschel, B., 2001. Particle Flux Variability in the Polar and Atlantic Biogeochemical Provinces of the Nordic Seas. In: Schäfer, P., Ritzrau, W., Schlüter, M., and Thiede, J. (des.), The Northern North Atlantic: A Changing Environment. Springer, Berlin, pp. 53–68.

Pflaumann, U., Duprat. J., Pujol, C. and Labeyrie, L. D., 1996. SIMMAX: A modern analog technique to deduce Atlantic sea surface temperatures from planktonic foraminifera is deep–sea sediments. Paleoceanography, 11, 15–35.

Prell, W.L., 1993. Variation of monsoonal upwelling: a response to changing solar radiation. In: J.E. Hansen and T. Takahasi (Eds.), Climatic Processes and Climate Sensitivity, Am. Geophys. Union, Geophys. Monogr., 29, pp. 48–57.

Reynolds, L. and Thunell, R. C., 1985. Seasonal succession of planktonic foraminifera in the subpolar North Pacific, J. Foramin. Res., 15, 282–301.

Reynolds, L. and Thunell, R. C., 1986. Seasonal production and morphologic variation of Neogloboquadrina pachyderma (Ehrenberg) in the northeast Pacific. Micropaleontology, 32, 1–18.

Reynolds, R. W. and Smith, T. M., 1994. Improved global sea surface temperature analysis. J. Climate, 7, 929–948.

Rohling, E. J. and Cooke, S., 1999. Stable oxygen and carbon isotopes in foraminiferal carbonate shells. In: Gupta, B. S. K. (Ed.), Modern foraminifera. Dortrecht, Boston, London, pp. 239–258.

Rohling, E.J., Sprovieri, M. , Cane, T., Casford, J.S.L., Cooke, S., Bouloubassi, I., Emeis, K.–C, Schiebel, R., Rogerson, M., Hayes, A., Jorissen, F.J. and Kroon, D., 2004. Reconstructing past planktic foraminiferal habitats using stable isotope data: a case history for Mediterranean sapropel S5. Mar. Micropal., 50, 89–123.

Sautter, L. R. and Thunell, R. C., 1989. Seasonal succession of planktonic foraminifera: results from a four–year time–series sediment trap experiment in the northeast Pacific. J. Foramin. Res., 19, 253–267.

Sautter, L. R., and Thunell, R. C., 1991. Planktonic foraminiferal response to upwelling and seasonal hydrographic conditions: sediment trap results from San Pedro Basin, Southern California Bight. J. Foramin. Res., 21, 347–363.

Schiebel, R. and Hemleben, D., 2005. Modern planktic foraminifera. Paläontologische Zeitschrift, 79, 135–148.

Schmidt, D. N., Renaud, S., Bollmann, J., Schiebel, R. and Thierstein, H. R., 2004. Size distribution of Holocene planktic foraminifer assemblages: biogeography, ecology and adaptation, Mar. Micropal., 50, 319–338.

Shen, C. C., Chiu, H. Y., Chiang, H. W., Chu, M. F., Wei, K. Y., Steinke, S., Chen, M. T., Lin, Y. S. and Lo, L., 2007. High precision measurements of Mg/Ca and Sr/Ca ratios in carbonates by cold plasma inductively coupled plasma quadrupole mass spectrometry. Chem. Geol., 236, 339–349.

Tedesco, K., Thunell, R., Astor, Y. and Muller–Karger, F., 2007. The oxygen isotope composition of planktonic foraminifera from the Cariaco basin, Venezuela: Seasonal and interannual variations. Mar. Micropal., 62, 180–193.

Thunell, R. C., Reynolds, L. A., 1984. Sedimentation of planktonic foraminifera: seasonal changes in species flux in the Panama Basin. Micropaleontology, 30, 243–262.

Thunell, R. C., Honjo, S., 1987. Seasonal and interannual changes in the planktonic foraminiferal production in the North Pacific. Nature, 328, 335–337.

Tian, J., Wang, P., Chen, R. and Cheng, X., 2005. Quaternary upper ocean thermal gradient variations in the South China Sea: Implications for east Asian monsoon climate. Paleoceanography, 20, 4007, doi:10.1029/2004PA001115.

Trull, T. W., Bray, S. G., Manganini, S. J., Honjo, S., and Francois, R., 2001. Moored sediment trap measurements of carbon export in the Subantarctic and Polar Frontal Zones of the Southern Ocean, south of Australia. J. Geophys. Res., 106, 31 489–31 510.

Watkins, J. M., and Mix, A. C., 1998. Testing the effects of tropical temperature, productivity, and mixed–layer depth on foraminiferal transfer functions. Paleoceanography, 13, 96–105.

Wefer, G., 1989. Particle Flux in the Ocean: Effects of Episodic Production. In: Berger, W. H., Smetacek, V. S., and Wefer, G. (Eds.), Productivity of the Ocean: Present and Past. John Wiley and Sons, New York, pp. 139–154.

Wong, C. S., Whitney, F. A., Crawford, D. W., Iseki, K., Matear, R. J., Johnson, W. K., Page, J. S., and Timothy, D., 1999. Seasonal and interannual variability in particle fluxes of carbon, nitrogen and silicon from time series of sediment traps at Ocean Station PAPA, 1982–1993: relationship to changes in subarctic primary productivity. Deep–Sea Res. II, 46, 2735–2760.

Žarić, S., Donner, B., Fischer, G., Mulitza, S., and Wefer, G., 2005. Sensitivity of planktic foraminifera to sea surface temperature and export production as derived from sediment trap data. Mar. Micropal., 55, 75–105.

Submitted to Paleoceanography as: Fraile, I., Schulz, M., Mulitza, S., Merkel, U., Prange, M. and Paul, A. – *"Modeling the seasonal distribution of planktonic foraminifera during the Last Glacial Maximum"*

Chapter 4

Seasonality of planktonic foraminifera during the Last Glacial Maximum

Abstract

We studied the seasonality of planktonic foraminifera during the Last Glacial Maximum using a foraminifera model coupled to an ecosystem model. The model suggests that the seasonality of planktonic foraminifera during the Last Glacial Maximum was different from today. This finding entails implications for foraminifera-based paleotemperature reconstructions. The change in the timing of maximum foraminiferal production could lead to a bias in estimated paleotemperature, if the change in seasonality is not taken into account.

In tropical waters, where temperature seasonality has a relatively small amplitude, the estimated sea-surface temperature is close to the annual mean. Thus, variations in foraminiferal seasonality do not cause a significant change in the recorded temperature. By contrast, changes in seasonality have the largest influence on the temperature signal at high and mid-latitudes. Our model prediction suggests that due to the temperature sensitivity of the considered species, during the Last Glacial Maximum, the largest production of foraminifera occurred during a warmer season of the year. In some regions, the maximum foraminiferal production month shifted by up to six months.

Our findings may help to reconcile low glacial planktonic $\delta^{18}O$ values with proxy evidence for deep-water formation in the Nordic Seas.

4.1 Introduction

Foraminiferal studies provide a fundamental contribution to our understanding of past and future ocean and climate systems. Many paleotemperature reconstructions rely on the analysis of foraminiferal test chemistry or assemblage composition. However, temperature estimates derived using species-specific paleotemperature equations are strongly affected by the seasonality of temperature-sensitive species (Mulitza et al., 1998; Tedesco et al., 2007). In order to accurately interpret the foraminiferal fossil record preserved within deep-sea sediments, early works focused on modern foraminiferal ecology (e.g., Bé and Hamilton, 1967; Bé and Told-

erlund, 1971; Hemleben et al., 1989). The development of automated time-series sediment traps (Honjo et al., 1980; Honjo and Doherty, 1988) has led to a better understanding of the fluxes of modern planktonic foraminifera, revealing that they have large seasonal variations in abundance tied closely to surface water hydrography (Bé, 1960; Bé and Tolderlund, 1971; Deuser et al., 1981; Thunell and Reynolds, 1987; Sautter and Thunell, 1991). Different foraminifera species have distinct seasonal patterns, the imprint of which is preserved in the sedimentary record (King and Howard, 2005; Schiebel and Hemleben, 2005). Thus, the temperature signature found in the sedimentary record lies between the annual mean water temperature and the preferred temperature of a particular species (Mix, 1987).

The seasonal distribution of some foraminiferal species can change through time as climate changes, leading to a bias in estimated paleotemperature. This variation needs to be quantified in order to better constrain the interpretation of foraminifera-based sea-surface temperature (SST) reconstructions. To study the seasonal variations of planktonic foraminifera species at glacial-interglacial timescales, we use a foraminiferal numerical model (Fraile et al., 2008). This planktonic foraminiferal model predicts monthly concentrations of the most important species used as source of paleoceanographic proxies. In order to test the response of planktonic foraminifera to climate changes, the model has been run for modern conditions and for the Last Glacial Maximum (LGM). This study shows model predictions for spatial and temporal distributions of five most frequently used foraminiferal species, and discusses the implications for paleotemperature reconstructions.

4.2 Methods

4.2.1 Foraminifera model and experiment setup

The model predicts monthly concentrations of the following planktonic foraminifera species: *N. pachyderma* (sinistral and dextral varieties), *G. bulloides*, *G. ruber* (white variety) and *G. sacculifer*. These species are mostly found in the euphotic zone, and reflect the sea-surface environment (Bé, 1982). The model is implemented into an ecosystem model (Moore et al., 2002), from which it takes information on food availability for the foraminifera. The ecosystem-foraminifera model is forced with physical and chemical boundary conditions. Initially, the model is integrated for two years, to allow an equilibrium state to be reached (Moore et al., 2002). The third year is then saved with a temporal resolution of one month. In the model standard setup, the forcing includes SST (World Ocean Atlas 1998, Conkright et al.,1998), surface shortwave radiation (Bishop and Rossow, 1991; Rossow and Schiffer, 1991), climatological mixed-layer depths (Monterey and Levitus, 1997), vertical velocity at

the base of mixed layer (Gent et al., 1998), turbulent exchange rate at the base of the mixed layer (constant value of 0.15 m/day; Moore et al., 2002), sea-ice coverage (Cavalieri et al., 1990) and atmospheric iron flux (Mahowald et al., 1999). The foraminifera model and its behavior in a global surface mixed-layer is described in detail in Fraile et al. (2008).

To compare the foraminiferal response to glacial-interglacial periods, we used the global coupled Community Climate System Model-version 3 (CCSM3) (Collins et al., 2006) to force the foraminifera model. We carried out experiments for two different environmental conditions: in the standard run the model was forced with present day conditions (PD), using the same forcing as described in Fraile et al. (2008), and in the second run with Last Glacial Maximum conditions (LGM).

We also performed sensitivity experiments to evaluate the influence of nutrients on foraminiferal populations. We carried out an experiment increasing the nutrient concentrations below the mixed layer by 3.2% for the LGM, equivalent to the increase resulting from a 120 m eustatic sea-level lowering (Fairbanks, 1989). Finally, we performed another experiment using the nutrient (nitrate and phosphate) distributions below the mixed layer as simulated by the University of Victoria Earth System - Climate Model (UVic ESCM) for the LGM (Weaver et al., 2001). For this experiment, we calculated the difference in nutrient concentration between preindustrial and LGM conditions within the UVic, and we applied this anomaly to our standard LGM run.

4.2.2 CCSM3 Climate Model simulations

The National Center for Atmospheric Research (NCAR) CCSM3 is a state-of-the-art coupled climate model. The global model is composed of four separate components representing atmosphere, ocean, land, and sea ice (Collins et al., 2006). Here, we use the low-resolution version of CCSM3 which is described in detail by Yeager et al. (2006). In this version, the resolution of the atmospheric component is given by T31 (3.75° by 3.75° transform grid) spectral truncation with 26 layers, while the ocean has a mean resolution of 3.6° by 1.6° (like the sea-ice model) with 25 levels. The latitudinal resolution of the oceanic model grid is variable, with finer resolution near the equator ($\approx 0.9°$).

We have performed two coupled climate simulations (preindustrial and LGM), the results of which were used to force the ecosystem and foraminifera model. The preindustrial simulation uses forcing appropriate for conditions before industrialization and follows the protocol established by the Paleoclimate Modelling Intercomparison Project, Phase 2 (PMIP–2; http:// www–lsce.cea.fr/pmip2/) (Bracon-

not et al., 2007). This forcing represents the average conditions of the late Holocene before the significant impact of humans, rather than a specific date, and it includes concentrations of greenhouse gases, changes in the spatial distributions of ozone, sulfate (only direct effect), and carbonaceous aerosols (Otto-Bliesner et al., 2006b). In addition to these forcing factors, changes in orbital parameters, ice sheets and a reduced global sea level are taken into account for the LGM (21,000 years before present) simulation following the PMIP-2 protocol. For continental ice-sheet extent and topography, the LGM ICE-5G reconstruction (Peltier, 2004) is used. The coastline is also taken from ICE-5G and corresponds to a sea-level lowering of ≈ 120 m such that new land is exposed.

Both climate simulations were integrated for more than 600 years so that the surface climatologies reached a statistical equilibrium and could be used for ecosystem-model forcing. The mean of the last 100 simulation years of the following parameters was used to force the ecosystem and foraminifera models: SST, mixed-layer depth, ice fraction, shortwave radiation and vertical velocity at the base of mixed-layer. The glacial cooling of the tropical surface ocean is up to 2°C. Stronger cooling (>5°C) takes place at high latitudes. The largest temperature drop can be found in the North Atlantic, where glacial temperatures are up to 10°C colder than pre-industrial values (Fig. 4.1). The North Atlantic temperature drop can partly be explained by a reduction of the meridional overturning circulation. In the LGM simulation, the overturning weakens by nearly one third from 14 Sv in the preindustrial run to about 10 Sv (not shown). The core depth of southward flowing North Atlantic Deep Water (i.e. the Deep Western Boundary Current) reduces from ~ 2500 m in the preindustrial simulation to ~ 1500 m in the glacial run. The peak northward heat transport in the North Atlantic ocean decreases by about 20% in the LGM. Further details of the model experiment will be presented elsewhere (Merkel et al., in prep.). We calculated the anomaly of the forcing variables (SST, mixed-layer depth, ice fraction, shortwave radiation and vertical velocity at the base of the mixed-layer) simulated by CCSM3 between LGM and preindustrial conditions, and we added this anomaly to the standard forcing data as an LGM forcing for the foraminiferal model. We used this approach in order to reduce deviations induced by the climate model errors. For example, in the North Atlantic, the SSTs simulated by CCSM3 for present day are up to 7°C too low compared to World Ocean Atlas data (Prange, 2008). Glacial SST anomalies correspond well with reconstructions (Fig. 4.1). In order to avoid potential inconsistencies between sea-ice fraction and SST, we set ice fraction to zero for temperatures above -1.5°C.

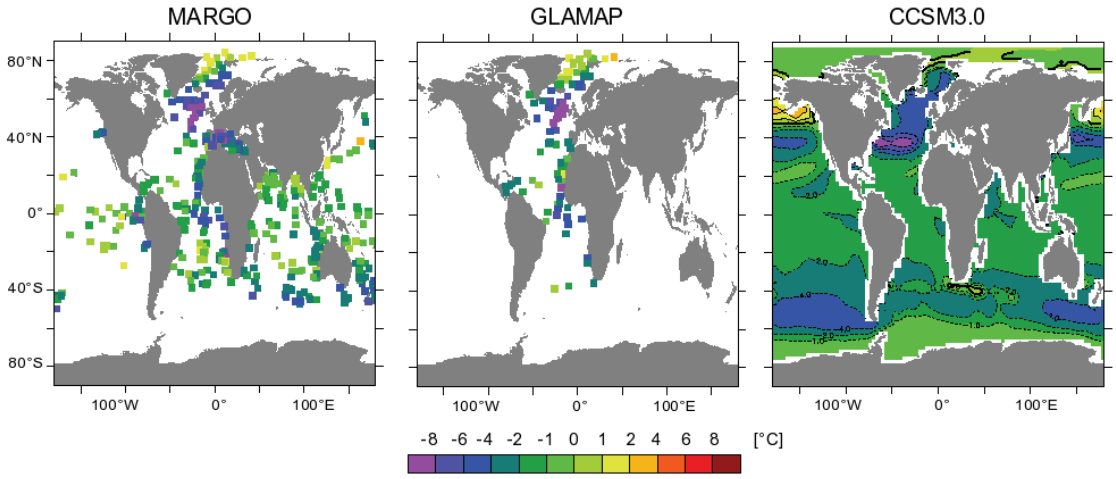

Figure 4.1: *Average annual SST anomaly between Last Glacial Maximum and modern conditions (LGM – WOA) estimated from planktonic foraminifera (MARGO dataset (left) (Weinelt et al., 2004); and GLAMAP 2000 compilation (center) (Pflaumann et al., 2003)), and SST anomaly (LGM – PI) simulated by CCSM3.0 (right).*

4.2.3 UVic Earth System - Climate Model simulations

For an experiment on foraminiferal sensitivity to changes in the nutrient distributions, we used the output from the UVic ESCM (version 2.8). Compared to CCSM3, the atmospheric component is simplified and consists of a vertically integrated two-dimensional energy-moisture balance model (Weaver et al., 2001). In addition to the atmosphere, ocean and sea ice components, it contains a land surface scheme (Cox, 1999), a dynamic global vegetation model (Cox et al. 2001; Meissner et al. 2003) and a marine biogeochemical component (Schmittner et al., 2005).

The horizontal resolution of the model is constant at 3.6° in the longitudinal and 1.8° in the latitudinal direction and thus comparable to CCSM3. In the ocean component, there are 19 levels in the vertical direction.with a thickness ranging from 50 m near the surface to 590 m near the bottom.

In both (preindustrial and LGM) simulations carried out with the UVic ESCM, the monthly wind stress to force the ocean and monthly winds for the advection of heat and moisture in the atmosphere are prescribed from the NCEP reanalysis climatology (Kalnay et al., 1996). The model is driven by the seasonal variation of insolation, appropriate to either preindustrial or LGM conditions. As in CCSM3, the ICE-5G reconstruction (Peltier, 2004) is used to prescribe the continental ice-sheet extent and topography for the LGM. Because of the computational efficiency

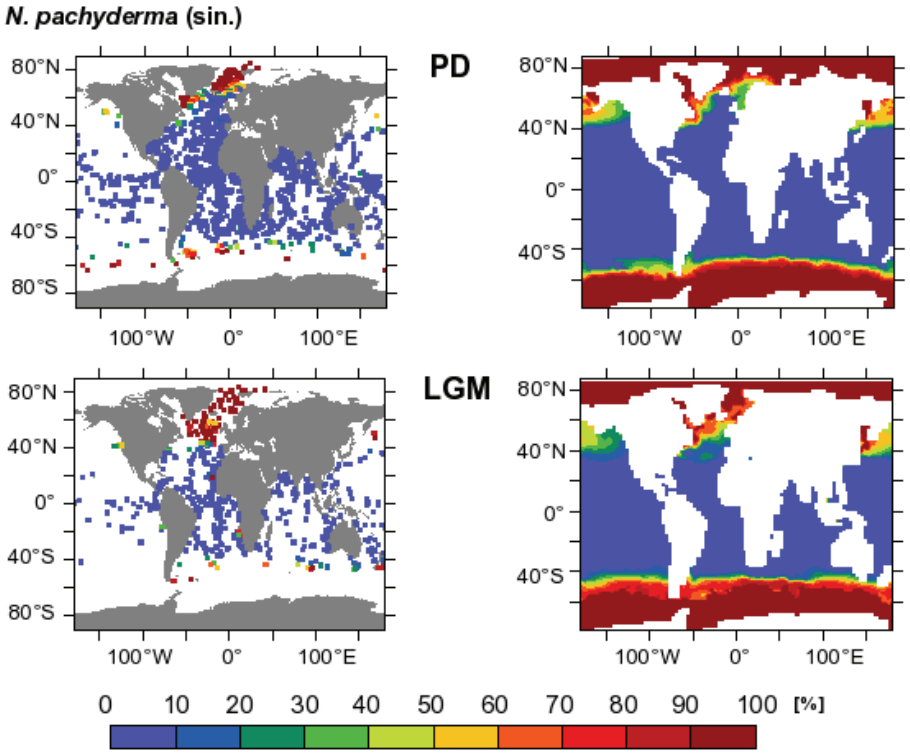

Figure 4.2: *Relative abundance of N. pachyderma (sin.) for modern conditions (upper panel) and during the LGM (lower panel) in the sedimentary record (left) and model prediction (right). Relative abundances consider only the five species included in the model. Modern sedimentary faunal assemblage data from Pflaumann et al. (1996); Prell et al. (1999); Martinez et al. (1998), and LGM data from MARGO and GLAMAP datasets (Barrows and Juggins, 2004; Kucera et al., 2004a,b; Niebler et al., 2004; Kucera et al., 2005; Pflaumann et al., 2003).*

of the UVic ESCM, the simulations could be integrated for more than 10,000 years and reached quasi-equilibrium conditions even in the deep ocean, with a cooling of the sea surface between ≈2°C in the tropics and ≈10°C in the high-latitude North Atlantic. For further details, see Paul et al., in prep.

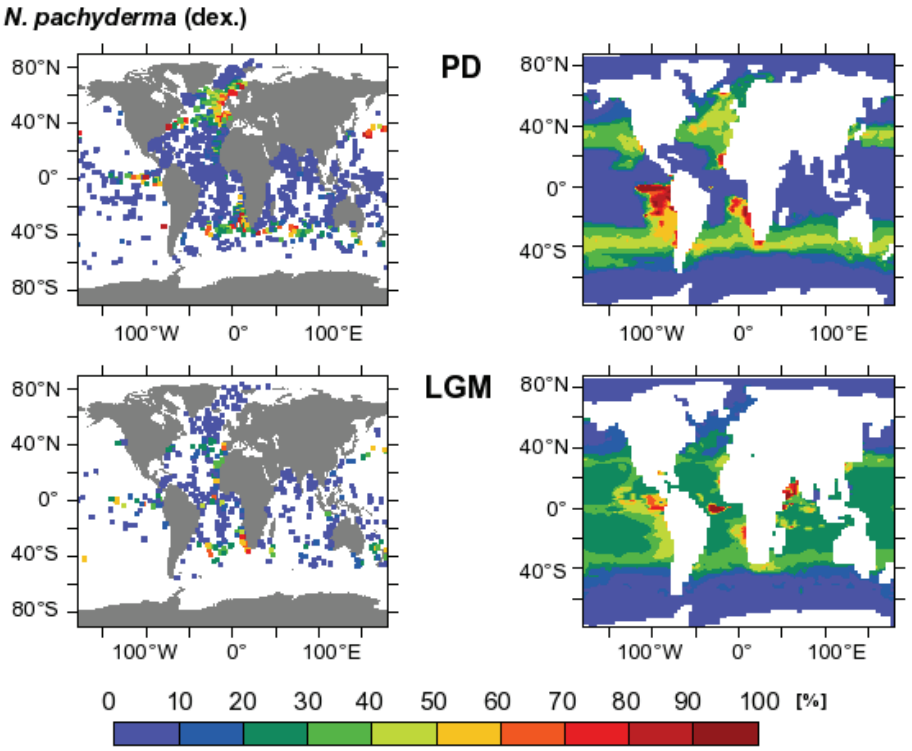

Figure 4.3: *Relative abundance of N. pachyderma (dex.) for modern (upper panel) and during the LGM (lower panel) in the sedimentary record (left) and model prediction (right). Symbols and layout of the graphs are the same as in Fig. 4.2.*

4.2.4 Sedimentary faunal assemblages

To compare our model prediction of planktonic foraminiferal distribution during the LGM with sediment data, we used planktonic foraminifera census data from the MARGO (Barrows and Juggins, 2004; Kucera et al., 2004a,b; Niebler et al., 2004; Kucera et al., 2005) and GLAMAP (Pflaumann et al., 2003) datasets. For present day we used core-top data from the Brown University Foraminiferal Database (Prell et al., 1999), extended with the dataset by Pflaumann et al. (1996) for the Atlantic, and with samples from the eastern Indian Ocean (Martinez et al., 1998). For comparison, the relative abundances were recalculated using only the five foraminifera species under consideration. The number of individuals was transformed into biomass (mgC/m^3) to take into account the size differences of each species. The transfor-

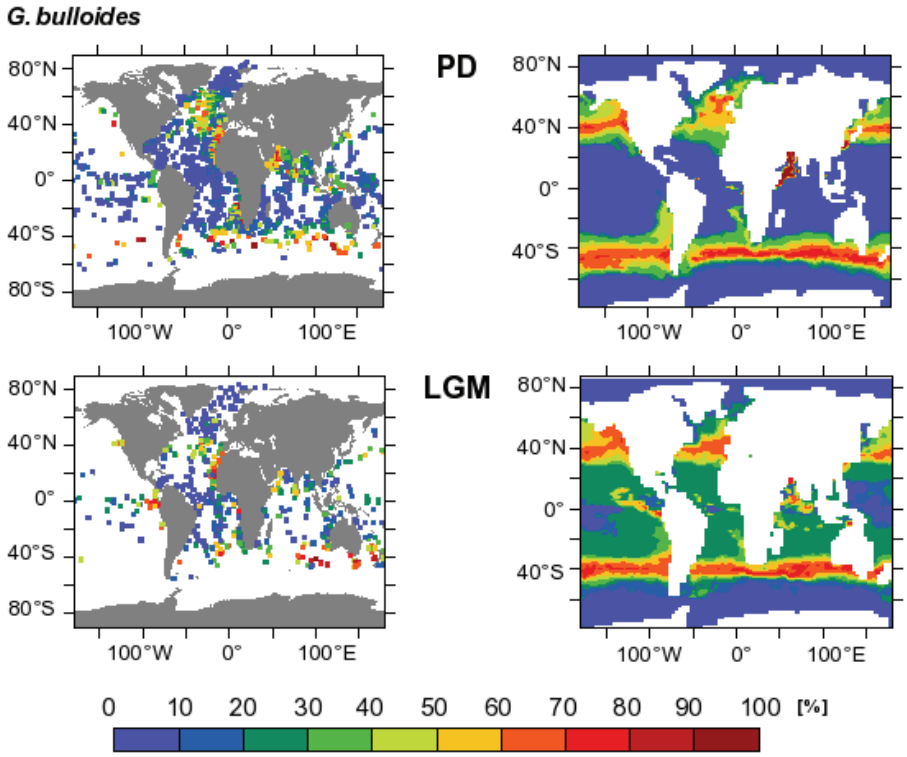

Figure 4.4: *Relative abundance of G. bulloides for modern (upper panel) and during the LGM (lower panel) in the sedimentary record (left) and model prediction (right). Symbols and layout of the graphs are the same as in Fig. 4.2.*

mation was made following the same procedure as in Fraile et al. (2008).

4.2.5 Flux-weighted temperature signal

Seasonal variations in the abundance of the species have been studied to evaluate their implications for proxy records. The isotopic (or trace-element) composition of a foraminiferal population in the sediment is the flux-weighted mean of all isotope values. Thus, theoretically, the temperature sensed by the mean population of a species (T_r) is the flux-weighted mean of all temperatures at the site. We calculated the theoretical mean SST recorded in each of the respective species (T_r):

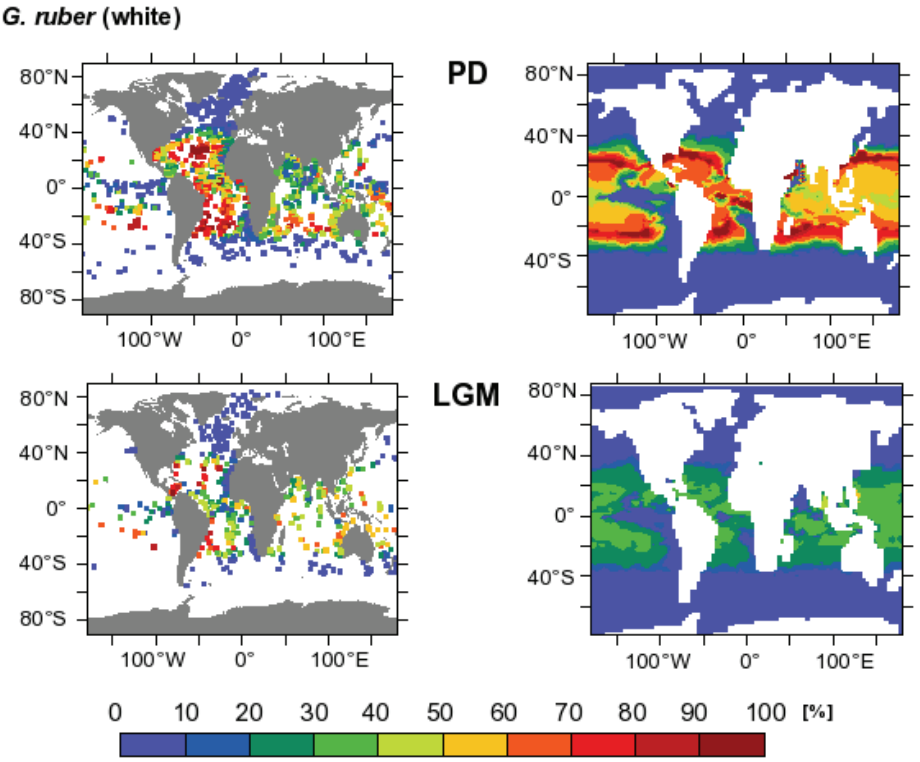

Figure 4.5: *Relative abundance of G. ruber (white) for modern (upper panel) and during the LGM (lower panel) in the sedimentary record (left) and model prediction (right). Symbols and layout of the graphs are the same as in Fig. 4.2*

$$T_r = \frac{\sum_{m=1}^{12} (C_m \times T_m)}{\sum_{m=1}^{12} C_m} \tag{4.1}$$

where C_m is monthly species concentration and T_m denotes SST. At each site, T_r ranges between the mean water temperature and mean preferred temperature by the species (Mix, 1987). Theoretically, T_r corresponds to the signal found in the sedimentary record.

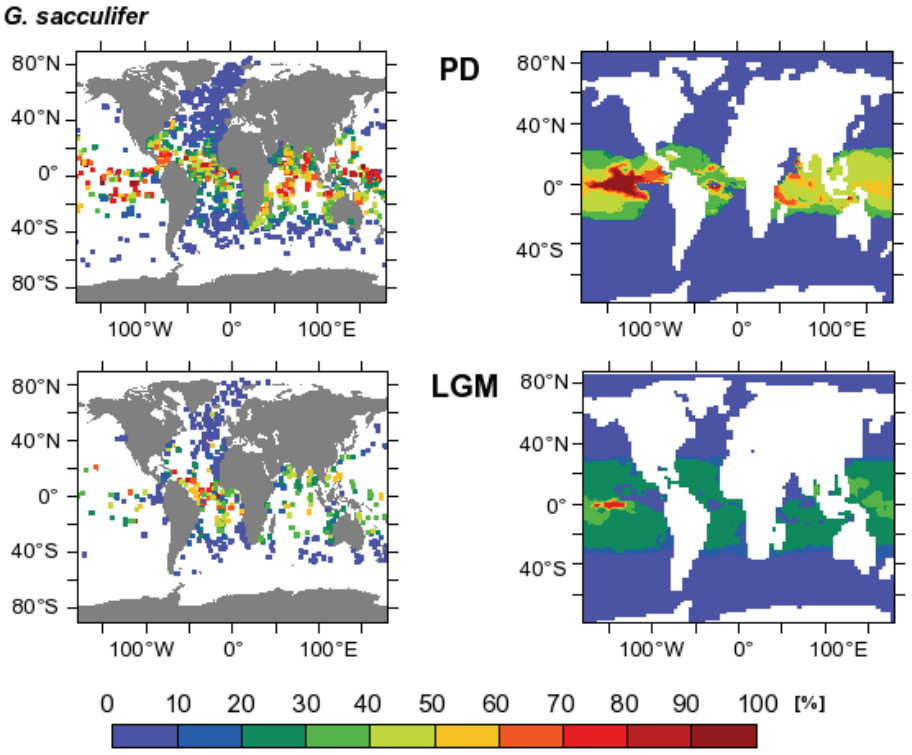

Figure 4.6: *Relative abundance of G. sacculifer for modern (upper panel) and during the LGM (lower panel) in the sedimentary record (left) and model prediction (right). Symbols and layout of the graphs are the same as in Fig. 4.2.*

4.3 Results

4.3.1 Relative abundances of the species during the LGM

The sensitivity experiment with increased nutrient concentrations below the mixed layer by 3.2% does not show a significant effect in foraminiferal concentration (total biomass variation $\leq 2\%$ for all species). Using the nutrient redistribution below the mixed layer simulated with UVic ESCM does not lead to major changes either (total biomass variation $\leq 3\%$ for all species). Therefore, to compare with sediment samples, nutrient concentrations below the mixed layer were kept the same as in Moore et al. (2002) for both modern and LGM runs. Figs. 4.2–4.6 illustrate annual mean relative abundances predicted by the model as compared to those measured

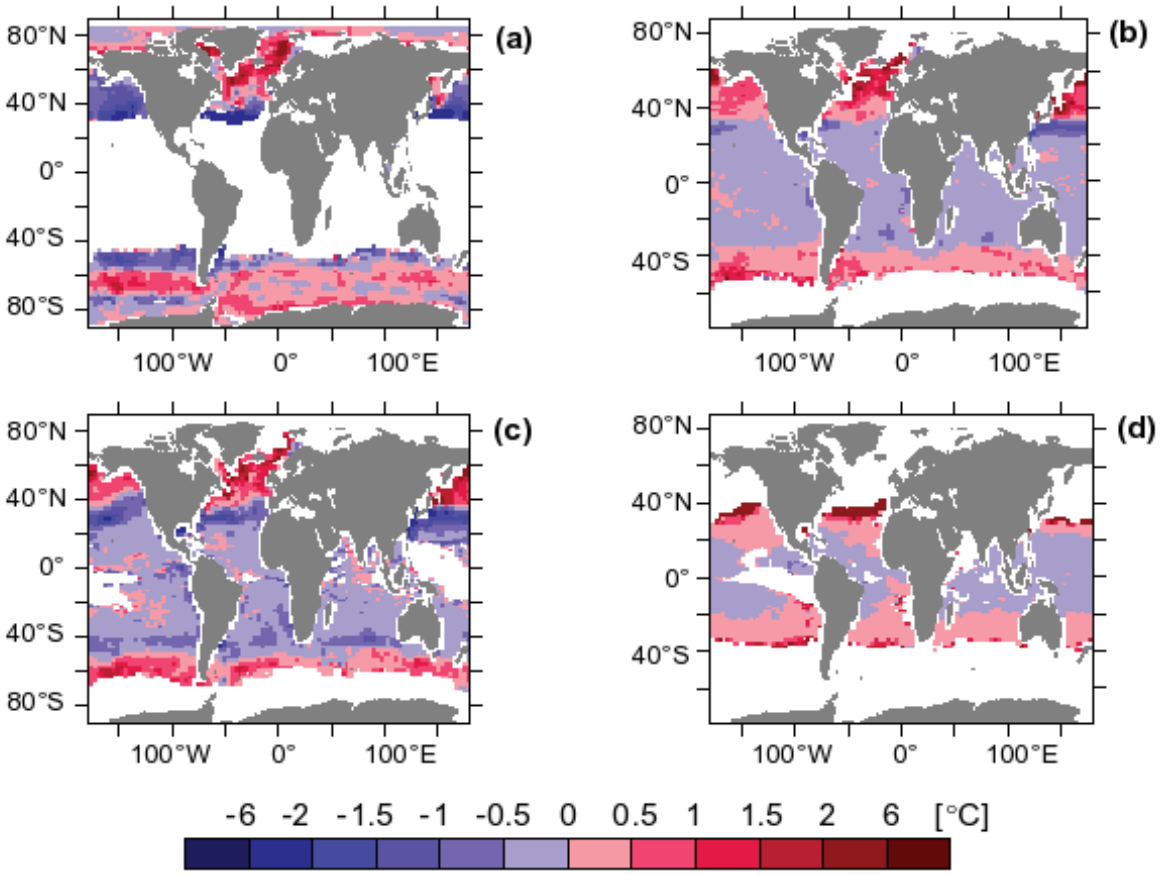

Figure 4.7: *Temperature signal recorded by the species (T_r) minus annual mean SST during LGM for* ***(a)*** *N. pachyderma (sin.),* ***(b)*** *N. pachyderma (dex.),* ***(c)*** *G. bulloides and* ***(d)*** *G. ruber (white). Values around zero: T_r corresponds to annual mean SST. Negative/positive values: T_r dominated by winter/summer conditions.*

in sediments for the five different species.

The global abundance pattern of *N. pachyderma* (sin.) in sediments, as well as in the model prediction, yield highest relative abundances (up to 100%) in polar waters (Fig. 4.2, upper panels). In comparison with present-day conditions, the area of dominance of *N. pachyderma* (sin.) during the glacial period is wider. In partic-

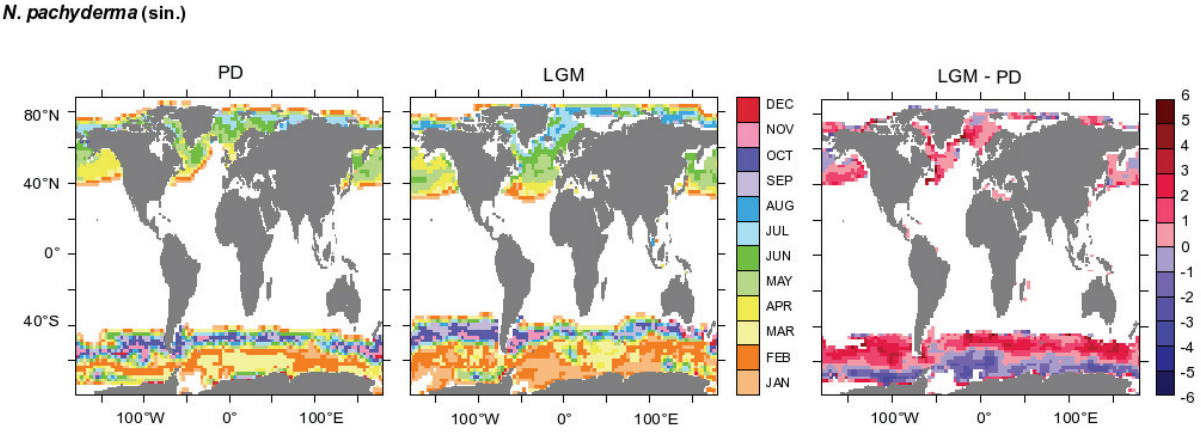

Figure 4.8: *Maximum production month of N. pachyderma (dex.) at present day (PD), Last Glacial Maximum (LGM) and the difference between both (in months). Positive values indicate that during the LGM, the maximum production was later in the year.*

ular, its distribution in the North Atlantic spreads southwards to lower latitudes. The lack of foraminiferal census data in the Southern Ocean hampers model evaluation in this region. Both model and sedimentary data indicate that *N. pachyderma* (dex.) and *G. bulloides* occurred in significant numbers in the major upwelling areas (Figs. 4.3–4.4 respectively, upper panels). Along 40°S, the model predicts a dominance of *G. bulloides* over the other four species, which is also reflected by the sediments south of Australia. The distribution of *N. pachyderma* (dex.) and *G. bulloides* during the LGM also extends towards lower latitudes compared to present day. However, the model overestimates their relative abundance in tropical waters, between 20°N and 20°S, where, away from upwelling regions, the relative abundances in the sediments are $\leq 10\%$. By contrast, the model predicts relative abundances between 20 – 40% during the LGM. As consequence, the predicted relative abundance of *G. ruber* (white) at these latitudes is too low (Fig. 4.5, upper panels). *G. sacculifer* is limited to tropical waters, but its abundance is also underestimated, more pronounced in the Atlantic Ocean than in the Pacific and Indian Oceans (Fig. 4.6, upper panels).

4.3.2 Foraminiferal seasonality during the LGM

The signal recorded by *N. pachyderma* (sin.) and *G. bulloides* during the LGM is found to be biased towards summer conditions at high latitudes (polar/subpolar

waters for *N. pachyderma* (sin.), and between 40 – 60 °N/S for *G. bulloides*), and towards winter below 40 ° latitude (Fig. 4.7). In contrast, for *N. pachyderma* (dex.) and *G. ruber*, the seasonal imprint on T_r becomes only discernible at the edge of their distributions (poleward of 40 °N/S for *N. pachyderma* (dex.) and 35 °N/S for *G. ruber*), where the signal is biased towards summer conditions. At lower latitudes the recorded temperature signal is close to annual mean SST. Due to the fact that the seasonality of temperature in the tropics is not very pronounced, the temperature signal recorded by *G. sacculifer* in tropical waters reflects mostly annual mean conditions and is therefore not shown in the following figures.

Figs. 4.8–4.11 illustrate the maximum production month of each species predicted by the model for PD and LGM. It has to be noted that in regions where the annual distribution pattern has low variability (e.g. in the tropics or at regions where the annual foraminiferal cycle is typically bimodal), the maximum production month does not always have a significant imprint on the recorded temperature. In regions with a wide seasonal maximum or with a double peak only the absolute maximum is taken into account, resulting in a noisy pattern. In order to reduce this noise, the original data have been smoothed using a boxcar filter along both axes by three gridpoints. During the LGM the maximum production month coincides more often with summer months compared to modern the situation. For example, according to the model, *N. pachyderma* (sin.) presently occurs during summer months poleward of 60 ° latitude, and during spring between 40 – 60 ° latitude. During the LGM, the maximum production occurred during summer above 30 ° latitude, more evident in the southern hemisphere. The right panels of Figs. 4.8–4.11 show the shift of maximum production month from LGM to present conditions. Thus, positive values indicate that during the LGM maximum production occurred later in the year.

The model simulation suggests that the maximum production month could have shifted considerably between PD and LGM conditions, producing a large seasonal bias. The results show a very variable response for each species: Maximum seasonal bias for *N. pachyderma* (sin.) and *G. bulloides* occurs in the subantarctic front, around 60 °S and 40 °S respectively. In case of *N. pachyderma* (dex.) the largest change in seasonality takes place between 30 – 40 °N in the North Atlantic Ocean, where maximum production is shifted by up to 6 months. *G. ruber* (white) experiences a maximum shift of seasonality in tropical waters. Nevertheless, variations in foraminiferal seasonality in tropical waters do not affect the isotopic signal considerably, as temperature seasonality is small.

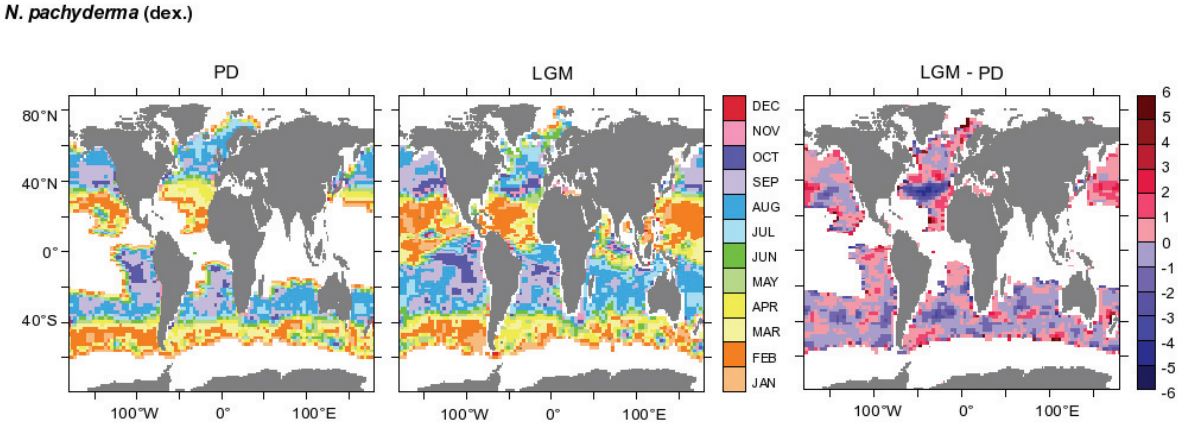

Figure 4.9: *Maximum production month of N. pachyderma (dex.) at present day (PD), Last Glacial Maximum (LGM) and the difference between both (in months). Positive values indicate that during the LGM, the maximum production was later in the year.*

4.4 Discussion

4.4.1 Comparison between model output and sediment samples

The distribution patterns of all species during the LGM are shifted to lower latitudes in response to the glacial cooling. According to our model prediction, during the LGM, *N. pachyderma* (sin.) extended its distribution to lower latitudes (Fig. 4.2), in response to favorable cold temperatures found between 40 – 50 ° latitude. During the LGM, the spatial distribution was wider compared to that for modern conditions, especially in the southern hemisphere. Core data and the model prediction compare favorably, although the lack of glacial sediment samples in the subantarctic region hampers the evaluation in this region.

Maximum cooling occurred around 40 – 50 °S and between 30 – 50 °N in the North Atlantic (more than 4°C cooling, Fig. 4.1). This cooling causes the distribution of foraminifera inhabiting these regions (mainly *G. bulloides* and *N. pachyderma* (dex.)) to be shifted towards warmer waters (Fig. 4.3–4.4). In tropical waters, the relative abundance of these species during the LGM is overestimated in comparison with sediment samples. Core data suggest that during the LGM the population of *N. pachyderma* (dex.) was diminished in response to unfavorable cold conditions. Instead, according to our predictions, the population was shifted to warmer regions rather than being reduced. In the case of *G. bulloides* the sedimentary record in the

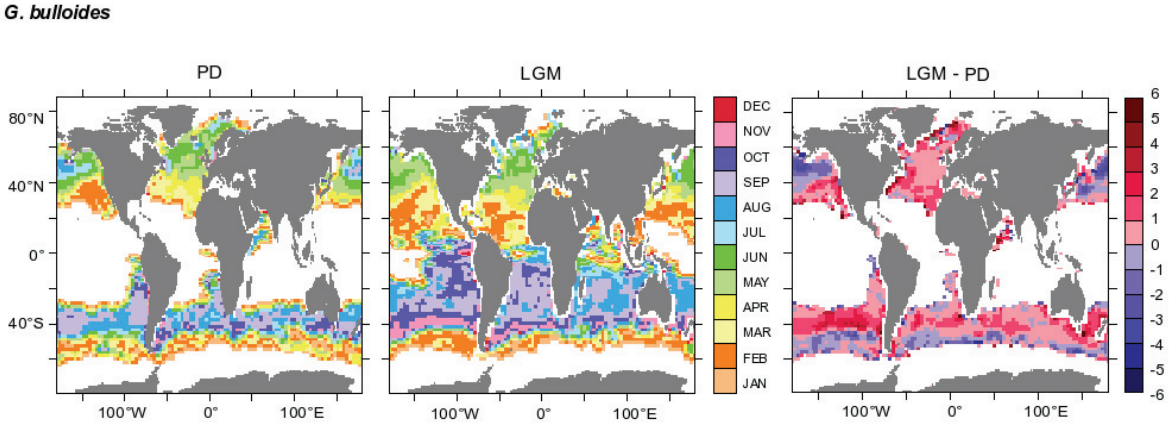

Figure 4.10: *Maximum production month of G. bulloides at present day (PD), Last Glacial Maximum (LGM) and the difference between both (in months). Positive values indicate that during the LGM, the maximum production was later in the year.*

North Atlantic Ocean shows a clear shift in its dominance area: at present day it occurs mainly between 40 – 50 °N, whereas during the LGM, north of 40 °N its relative abundance was very low (<10%). This shift in the dominance area from low to higher latitudes fits well with the model prediction. The overestimation of *G. bulloides* and *N. pachyderma* (dex.) in tropical waters brings as consequence the underestimation of the relative abundance of *G. ruber* (white) (Fig. 4.5).

In this ecosystem model, nutrient concentration below the mixed layer does not seem to play an important role in the biomass of phyto- and zooplankton. In the way the ecosystem model is parametrized, the phyto- and zooplankton reach an equilibrium state in which higher growth rate translates into higher mortality, keeping the concentration almost unaltered. Thus, foraminiferal abundance, which is related to food availability, is also unaffected.

4.4.2 Influence of seasonality on proxy records

Climate change can induce variations in the seasonality of foraminifera. Changes in the timing of maximum foraminiferal production may influence the proxy signal and lead to a bias in estimated paleotemperature. Fig. 4.12 illustrates some examples where, according to our model prediction, a shift in seasonality from LGM to present day conditions was noted. The maximum production peak is sometimes clearly shifted (Fig. 4.12 a,c and d), whereas in some other cases the double peak is

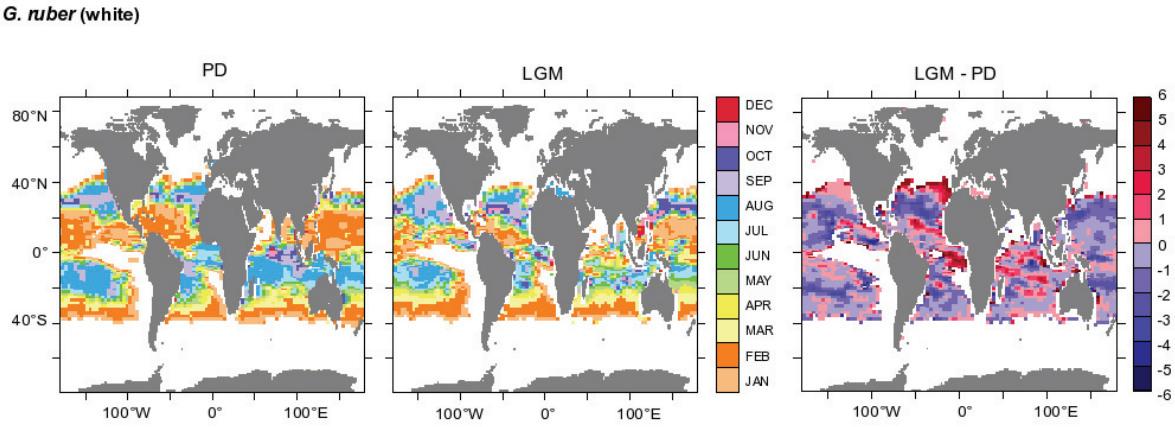

Figure 4.11: *Maximum production month of G. ruber (white) at present day (PD), Last Glacial Maximum (LGM) and the difference between both (in months). Positive values indicate that during the LGM, the maximum production was later in the year.*

transformed into a single maximum (Fig. 4.12 b).

The largest differences between present day and LGM conditions are found in the Southern Ocean and in the North Atlantic (Figs. 4.8–4.10). In particular, in the western North Atlantic glacial cooling is very pronounced, and as a consequence the maximum production month of *N. pachyderma* (sin.) and *G. bulloides* occurs later in the year, coinciding with the warmest season.

In some cases maximum production shifted by up to 6 months. This implies a considerable variation in recorded temperature. For example, our experiment with present day conditions suggests that, around 40°N in the North Atlantic, the isotopic signature in *G. bulloides* is biased towards winter temperatures, whereas during the LGM, it was biased towards summer conditions. As a consequence, using *G. bulloides* to reconstruct glacial SST in this region would underestimate the entire temperature variation by up to 2°C in the eastern North Atlantic and up to 6°C in the western region. Similarly, the change in seasonality of *N. pachyderma* (sin.) in the subantarctic front, between 40 – 60 °S, influences the interpretation of the temperature signal: During the LGM, the distribution of *N. pachyderma* (sin.) spreads equatorwards and maximum production occurred later in the year; thus, the mean population would record little change in the temperature signal.

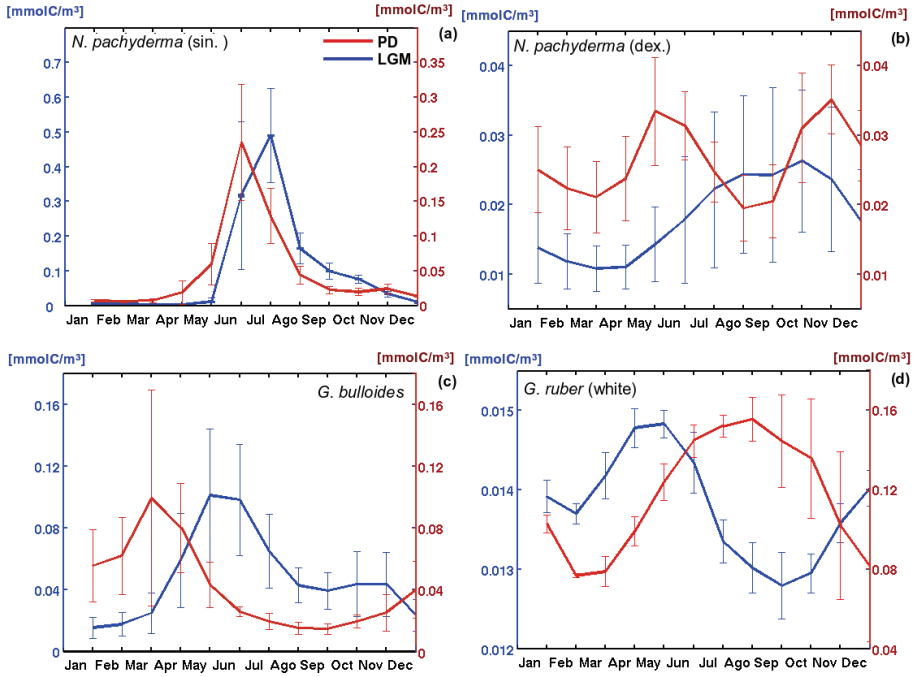

Figure 4.12: *Examples of modelled annual biomass [mmolC/m^3] variation of* ***(a)*** *N. pachyderma (sin.) in the North Atlantic (52–56°N, 36–43°W),* ***(b)*** *N. pachyderma (dex.) in the North Pacific (36–39°N, 151–158°E),* ***(c)*** *G. bulloides in the North Atlantic (39–43°N, 47–54°W) and* ***(d)*** *G. ruber (white) in the South Atlantic (22–25°S, 22–30°W) at PD (red) and LGM (blue). Lines represent mean values and error bars standard deviations over the region.*

Another interesting feature of the model output is the difference of the recorded signal by *N. pachyderma* (sin.) in the western and eastern North Atlantic. According to the LGM simulation, in the western and eastern regions of the North Atlantic, around 40 – 50 °N *N. pachyderma* (sin.) records a temperature signal above the annual mean, i.e. it lives mostly during summer, whereas in the central North Atlantic the recorded signal is biased towards winter (Fig. 4.7a). The GLAMAP reconstruction at North Atlantic subpolar waters based on planktonic foraminifera, one of the major departures from the CLIMAP (1981) pattern, was characterized by an anticyclonic gyre of warm water transported from the western Atlantic margin (summer SSTs of 5 – 7°C), and a cold current in the eastern North Atlantic, along the ice-covered British Isles penetrating into the center of the gyre (summer SSTs of 3- 4°C) (Pflaumann et al., 2003). This pattern with a cold gyre center and a warm surrounding current is difficult to explain physically, and the authors also discuss the possibil-

ity of an artifact resulting from lateral advection of polar fauna. According to our model prediction it could just be due to the fact that in the central North Atlantic the temperature signal corresponds to a winter signal, whereas in the western North Atlantic foraminifera record a summer signal.

In the same way, Duplessy et al. (1991) used the isotopic composition of *N. pachyderma* (sin.) and *G. bulloides* to reconstruct surface salinity during the LGM in the North Atlantic Ocean, assuming that the isotopic composition of foraminiferal shells is linearly related to summer SST. They reconstructed a tongue of highly saline surface water which penetrated to the central Atlantic up to 53 °N, south of Iceland. They also found a negative anomaly in δ^{18}O of sea water (interpreted as low salinity) in the Norwegian-Greenland seas, northeast of Iceland, and concluded that this was due to both the disappearance of the North Atlantic drift and the input of freshwater resulting from local precipitation and ice melting. Based on this paleosalinity distribution, Labeyrie et al. (1992) and Sarnthein et al. (1994) suggested that the major site of glacial North Atlantic deepwater formation was shifted to the central North Atlantic. However, our model prediction for *N. pachyderma* (sin.), which accounts for more than 98% of the total foraminifera assemblage (Pflaumann et al., 1996), suggests that the seasonality in the Norwegian Sea may have shifted from LGM to present day. At present day, maximum production occurs from April to June, whereas according to the model, it occurred during July-August at the LGM (Fig.4.8). The shift of one or two months in the seasonal production translates into a change of $\geqslant 1$°C in the recorded temperature signal, which corresponds to a reduction of the δ^{18}O anomaly of about 0.3. The negative anomalies in δ^{18}O found by Duplessy et al. (1991) in the Norwegian Sea (northeast of Iceland) could therefore be due to the fact that during the LGM *N. pachyderma* (sin.) calcified later in the year, and therefore recorded an isotopic signal corresponding to warmer conditions. Hence, the negative anomaly would be a consequence of temperature rather than of low salinity. Moreover, based on oxygen isotope records, Sarnthein et al. (1995) defined the LGM as a period of climatic stability and minimum meltwater flux. The surface water in the Norwegian Sea would, in this case, be dense enough for deepwater formation, as suggested by later studies (Weinelt et al., 1996; Schäfer-Neth and Paul, 2001).

For tropical species, shifts in seasonality do not seem to have major implications for paleoceanographic reconstructions. For example, the month of maximum production of *G. ruber* (white) and *G. sacculifer* shifted considerably between PD and LGM conditions between 20°S- 20°N. However,the flux-weighted temperature signal in tropical waters was found to be in agreement with the annual mean SST, suggesting the lack of a seasonal bias in foraminifera-based proxy records (Fig.4.7).

In subtropical waters, at the edge of its thermal distribution *G. ruber* (white) records summer conditions during the LGM, similar to those observed under modern conditions.

4.5 Conclusions

Our foraminifera model simulation suggests that the seasonality of foraminifera has changed from the LGM to the present day. This variation in the annual distribution pattern varies with the species and the oceanic region. In general, the changes in seasonality were greatest at the edge of the distribution of each species, where temperatures are at the lower limit of their tolerance range. During the LGM, the maximum production of subtropical and high-latitude foraminifera generally occurred at a warmer season of the year.

Changes in seasonality of the species recording a seasonal proxy signal, in particular species living at high latitudes associated with high temperature seasonality, have implications for paleoceanographic reconstructions. In contrast, for the species living in tropical waters the change in seasonality did not produce an important bias in estimated temperature, as the amplitude of the annual cycle of SST is relatively low, and therefore the recorded temperature is close to the annual mean SST.

Acknowledgments The CCSM3 climate model runs were performed on the IBM pSeries 690 Supercomputer of the Norddeutscher Verbund für Hoch- und Höchstleistungsrechnen (HLRN). This project was supported by the DFG (Deutsche Forschungsgemeinschaft) as part of the European Graduate College "Proxies in Earth History" (EUROPROX) and the DFG Research Center/Excellence Cluster "The Ocean in the Earth System".

Bibliography

Barrows, T and Juggins, S., Compilation of planktic foraminifera LGM assembages from the Indo-Pacific Ocean, doi:10.1594/PANGAEA.227319, 2002.

Bé, A. W. H., Ecology of Recent planktonic foraminifera: Part 2 – Bathymetric and seasonal distributions in the Sargasso Sea off Bermuda, Micropaleontology, 6, 373–392, 1960.

Bé, A. W. H. and Hamilton, W. H.: Ecology of Recent planktonic foraminifera, Micropaleontology, 13, 87–106, 1967.

Bé, A. W. H. and Tolderlund, D. S.: Distribution and ecology of living planktonic foraminifera in surface waters of the Atlantic and Indian Oceans, in The Micropalaeontology of Oceans, edited by: Funnell, B. M. and Riedel, W. R., 105–149, Cambridge University Press, 1967.

Bé, A. W. H., Biology of planktonic foraminifera, in: Foraminifera: Notes for a short course, edited by T. W. Broadhead, 51–92, The University of Tennessse, Knoxville, 1982.

Bishop, J. K. B. and Rossow, W. B.: Spatial and temporal variability of global surface solar irradiance, J. Geophys. Res., 96, 16 839–16 858, 1991.

Braconnot,P., Otto–Bliesner, B., Harrison, S., Joussaume, S., Peterchmitt, J. Y., Abe–Ouchi, A., Crucifix, M., E. Driesschaert, Th. Fichefet, C. D. Hewitt, M. Kageyama, A. Kitoh, A., Laíné, Loutre, M. F., Marti, O., Merkel, U., Ramstein, G., Valdes, P., Weber, S. L., Yu, Y. and Zhao, Y.: Results of PMIP2 coupled simulations of the Mid–Holocene and Last Glacial Maximum Part 1: experiments and large–scale features, Climate of the Past, 3, 261–277, 2007.

Cavalieri, D., Gloerson, P., and Zwally, J.: DMSP SSM/I daily polar gridded sea ice concentrations, October 1998 to September 1999, edited by: Maslanik, J. and Stroeve, J., National Snow and Ice Data Center, Boulder, CO, Digital media, 1990.

Collins, W. D., Bitz, C. M., Blackmon, M. L.: The Community Climate System Model Version 3 (CCSM3), J. Climate, 19, 2122–2143, 2006.

Conkright, M., Levitus, S., OBrien, T., Boyer T., Antonov, J. and Stephens: World Ocean Atlas 1998 CD–ROM Data Set Documentation, Tech. Rep. 15, NODC Internal Report, Silver Spring, MD, 16 pp., 1998.

Cox, P. M.: Description of the TRIFFID dynamic global vegetation model, Technical Note 24, Hadley Centre, 2001.

Cox, P. M., Betts, R. A., Bunton, C. B., Essery, R. L. H., Rowntree, P. R., and Smith, J.: The impact of new land surface physics on the GCM simulation of climate and climate sensitivity, Clim. Dynam., 15, 183-203, 1999.

Deuser, W. G., Ross, E. H., Hemleben, C., and Spindler, M., Seasonal changes in species composition, numbers, mass, size, and isotopic composition of planktonic foraminifera settling into the deep Sargasso Sea, Palaeogeogr. Palaeocl., 33, 103–127, 1981.

Duplessy, J. C., Labeyrie, L., Juillet–Leclerc, A., Maitre, F., Duprat, J. and Sarnthein, M.: Surface salinity reconstruction of the North Atlantic Ocean during the Last Glacial Maximum, Oceanologica Acta, 14, 311-324, 1991.

Eguchi, N. O., Ujiie, H., Kawahata, H. and Taira, A.: Seasonal variations in planktonic foraminifera at three sediment traps in the Subarctic, Transition and Subtropical zones of the central North Pacific Ocean, Mar. Micropaleontol., 48 , 149-163, 2003.

Fairbanks, R. G.: A 17,000–year glacio–eustatic sea level record: influence of glacial melting rates on the Younger Dryas event and deep–ocean circulation, Nature, 342, 637–642, 1989.

Fraile, I., Schulz, M., Mulitza, S. and Kucera, M.: Predicting the global distribution of planktonic foraminifera using a dynamic ecosystem model, Biogeosciences, 5, 891–911, 2008.

Gent, P. R., Bryan, F. O., Danabasoglu, G., Doney, S. C., Holland, W. R., Large, W. G., and McWilliams, J. C.: The NCAR climate system model global ocean component, J. Climate, 11, 1287–1306, 1998.

Hemleben, C., Spindler, M., and Anderson, O. R.: Modern Planktonic Foraminifera, Springer–Verlag, New York, 1989.

Honjo, S., Connell, J. F., and Sachs, P. L: Deep–ocean sediment trap: design and function of PARFLUX Mark II, Deep–Sea Res., 27, 745-753, 1980.

Honjo, S. and Doherty, K. W.: Large aperture time–series sediment traps: design objectives, construction and application, Deep–Sea Res., 35, 133-149, 1988.

Kalnay, E., Kanamitsu, M., Kistler, R., Collins, W., Deaven, D., Gandin, L., Iredell, M., Saha, S., White, G., Woolen, J., Zhu, Y., Chelliah, M., Ebisuzaki, W., Higgins, W., Janowiak, J., Mo, K. C., Ropelewski, C., Wang, J., Leetmaa, A., Reynolds, R., Jenne, R. and Joseph, D.: The NCEP/NCAR reanalysis project, Bulletin of the American Meteorological Society, 77, 437-471, 1996.

King, A. L. and Howard, W. R.: $\delta^{18}O$ seasonality of planktonic foraminifera from Southern Ocean sediment traps: Latitudinal gradients and implications for paleoclimate reconstructions, Mar. Micropal., 56, 1–24, 2005.

Kuroyanagi, A., Kawahata, H., Nishi, H., and Honda, M. C.: Seasonal changes in planktonic foraminifera in the northwestern North Pacific Ocean: sediment trap experiments from subarctic and subtropical gyres, Deep–Sea Res. II, 49, 5627–5645, 2002.

Kucera, M., Weinelt, M., Kiefer, T., Pflaumann, U., Hayes, A., Weinelt, M., Chen, M. T., Mix, A. C, Barrows, T., Cortijo, E., Duprat, J., Juggins, S., Waelbroeck, C.: Compilation of planktic Foraminifera census data, LGM and SSTs from the Pacific Ocean, doi:10.1594/PANGAEA.227329, 2004.

Kucera, M., Weinelt, M., Kiefer, T., Pflaumann, U., Hayes, A., Weinelt, M., Chen, M. T., Mix, A. C, Barrows, T., Cortijo, E., Duprat, J., Juggins, S., Waelbroeck, C.: Compilation of planktic Foraminifera census data, LGM and SSTs from the Pacific Ocean, doi:10.1594/PANGAEA.227325, 2004.

Kucera, M. , Rosell–Melé, A., Schneider, R., Waelbroeck, C. and Weinelt, M.: Multiproxy approach for the reconstruction of the glacial ocean surface (MARGO), Quaternary Sci. Rev., 24, 813-819, 2005.

Kucera, M.; Weinelt, M.; Kiefer, T.; Pflaumann, U. Hayes, A.; Weinelt, M.; Chen, M. T; Mix, A. C; Barrows, T.; Cortijo, E., Duprat, J., Juggins, S. and Waelbroeck, C.: Reconstruction of sea–surface temperatures from assemblages of planktonic foraminifera: multi–technique approach based on geographically constrained calibration datasets and its application to glacial Atlantic and Pacific Oceans, Quaternary Sci. Rev., 24, 951–998, doi:10.1016/j.quascirev.2004.07.014, 2005.

Labeyrie, L. D., Duplessy, J. C., Duprat, J., Juillet-Leclerc, A., Moyes, J., Michel, E., Kallel, N. and Shackleton, N. J.: Changes in vertical structure of the North Atlantic Ocean between glacial and modern times, Quaternary Sci. Rev., 11, 401-413, 1992.

Mahowald, N., Kohfeld, K., Hansson, M., Balanski, Y., Harrison, S. P., Prentice, I. C., Schulz, M., Rodhe, H.: Dust sources and deposition during the last glacial maximum and current climate: A comparison of model results with paleodata from ice cores and marine sediments, J. Geophys. Res., 104, 15895–15916, 1999.

Meissner, K. J., Weaver, A. J., Matthews, H. D., and Cox, P. M.: The role of land surface dynamics in glacial inception: a study with the UVic Earth System Model, Climate Dynamics, 21, 515527, DOI 10.1007/s00 38200303522, 2003.

Michaels, A. F., Caron, D. A., Swanberg, N. R., and Howse, F. A.: Planktonic sarcodines (Acantharia, Radiolaria, Foraminifera) in surface waters near Bermuda: abundance, biomass and vertical flux, J. Plankton Res., 17, 131–163, 1995.

Mix, A., 1987. The oxygen–isotope record of glaciation, in: North America and adjacent oceans during the last deglaciation. (The Geology of North America, Vol. K–3.), edited by Ruddiman, W. F., Wright, H. E., Geol. Sot. Am., Boulder CO, 111–135, 1987.

Mohiuddin, M. M., Nishimura, A., Tanaka, Y., and Shimamoto, A.: Regional and interannual productivity of biogenic components and planktonic foraminiferal fluxes in the northwestern Pacific Basin, Mar. Micropal., 45, 57–82, 2002.

Monterey, G. and Levitus, S.: Seasonal variability ofmixed layer depth for the world ocean, NOAA Atlas NESDIS 14, US Government Printing Office, Washington, D.C., 1997.

Moore, J. K., Doney, S. C., Kleypas, J. A., Glover, D. M., and Fung, I. Y., An intermediate complexity marine ecosystem model for the global domain, Deep–Sea Res. II, 49, 403–462, 2002.

Mulitza, S., Wolff, T., Pätzold, J., Hale, W., and Wefer, G., Temperature sensitivity of planktic foraminifera and its influence on the oxygen isotope record, Mar. Micropal., 33, 223–240, 1998.

Niebler, H. S.: Assemblage of planktonic foraminifera for the last glacial maximum (LGM) in sediment cores from the South Atlantic, Department of Geosciences, Bremen University, doi:10.1594/PANGAEA.55260, 2004.

Oda, M. and Yamasaki, M.: Sediment trap results from the Japan Trench in the Kuroshio domain: seasonal variations in the planktic foraminiferal flux, J. Foramin. Res., 35, 315–326, 2005.

Otto–Bliesner, B. L., Brady, E. C., Clauzet, G., Tomas, R., Levis, S., Kothavala, Z.: Last Glacial Maximum and Holocene climate in CCSM3, J. Climate, 19, 2526–2544, 2006a.

Otto–Bliesner, B. L., Tomas, R., Brady, E. C., Ammann, C., Kothavala, Z., Clauzet, G.: Climate sensitivity of moderate–and low–resolution versions of CCSM3 to preindustrial forcings, J. Climate, 19, 2567–2583, 2006b.

Peeters, F., Ivanova, E., Conan, S., Brummer, G. J., Ganssen, G., Troelstra, S., and van Hinte, J.: A size analysis of planktic foraminifera from the Arabian Sea, Mar. Micropal., 36, 31–63, 1999.

Peltier, W. R.: Global glacial isostasy and the surface of the ice–age Earth: The ICE–5G (VM2) model and GRACE, Annu. Rev. Earth Planet. Sci., 32, 111–149, 2004.

Pflaumann, U., Duprat, J., Pujol, C., and Labeyrie, L. D.: SIMMAX: A modern analog technique to deduce Atlantic sea surface temperatures from planktonic foraminifera is deep-sea sediments, Paleoceanography, 11, 15–35, 1996.

Pflaumann, U., Sarnthein, M., Chapman, M., de Abreu, L., Funnell, B. M.; Hüls, M., Kiefer, T., Maslin, M. A.; Schulz, H., Swallow, J.; van Kreveld, S. A, Vautravers, M., Vogelsang, E., Weinelt, M.: Glacial North Atlantic: Sea surface conditions reconstructed by GLAMAP 2000, doi:10.1594/PANGAEA.692144. Supplement to: Pflaumann, U., Sarnthein, M., Chapman, M., de Abreu, L., Funnell, B. M.; Hüls, M., Kiefer, T., Maslin, M. A.; Schulz, H., Swallow, J., van Kreveld, S. A, Vautravers, M., Vogelsang, E., Weinelt, M.: Glacial North Atlantic: Sea–surface conditions reconstructed by GLAMAP 2000, Paleoceanography, 18, 1065, doi:10.1029/2002PA000774, 2003

Prange, M., The low–resolution CCSM2 revisited: new adjustments and a present–day control run, Ocean Sci., 4, 151–181, 2008.

Reynolds, L. and Thunell, R. C.: Seasonal succession of planktonic foraminifera in the subpolar North Pacific, J. Foramin. Res., 15, 282–301, 1985.

Rossow, W. B. and Schiffer, R. A.: ISCCP cloud data products, B. Am. Meteorol. Soc., 72, 2–20, 1991.

Sarnthein, M., Winn, K., Jung, S. J. A., Duplessy, J. C., Labeyrie, L., Erlenkeuser, H. and Ganssen, G.: Changes in east Atlantic deepwater circulation over the last 30 000 years: eight time slice reconstructions, Paleoceanography 92, 209-267, 1994.

Sarnthein, M., Jansen, E., Weinelt, M., Arnold, M., Duplessy, J. C., Erlenkeuser, H., Flatϕy, A., Johannessen, G., Johannessen, T., Jung, S., Koc, N., Labeyrie, L., Maslin, M., Pflaumann, U. and Schulz, H.: Variations in Atlantic surface ocean paleoceanography, 50° 80°N: a time-slice record of the last 30,000 years, Paleoceanography, 10, 1063-1094, 1995.

Sautter, L. R. and Thunell, R. C., Seasonal succession of planktonic foraminifera: results from a four–year time–series sediment trap experiment in the northeast Pacific, J. Foramin. Res., 19, 253–267, 1989.

Sautter, L. R. and Thunell, R. C., Planktonic foraminiferal response to upwelling and seasonal hydrographic conditions: sediment trap results from San Pedro Basin, Southern California Bight, J. Foraminiferal Res., 21, 347-363, 1991.

Schäfer-Neth, C., and Paul, A.: Circulation of the glacial Atlantic: A synthesis of global and regional modeling, in *The northern North Atlantic: A changing environment*, edited by Schäfer, P., Ritzrau, W., Schlüter, M. and Thiede, J., Springer-Verlag, Berlin, Heidelberg, 441–462, 2001.

Schiebel, R. and Hemleben, D.: Modern planktic foraminifera, Paläontologische Zeitschrift, 79, 135–148, 2005.

Schmittner, A., Oschlies, A., Giraud, X., Eby, M., and Simmons, H. L.: A global model of the marine ecosystem for long–term simulations: Sensitivity to ocean mixing, buoyancy forcing, particle sinking, and dissolved organic matter cycling, Global Biogeochemical Cycles, 19, GB3004, doi:10.1029/2004GB002 283, 2005.

Tedesco, K., Thunell, R., Astor, Y. and Muller–Karger, F., The oxygen isotope composition of planktonic foraminifera from the Cariaco basin, Venezuela: Seasonal and interannual variations, Mar. Micropal., 62, 180–193, 2007.

Thunell, R. C., Honjo, S., Seasonal and interannual changes in the planktonic foraminiferal production in the North Pacific, Nature, 328, 335–337, 1987.

Weaver, A. J., Eby, M., Wiebe, E. C., Bitz, C. M., Duffy, P. B., Ewen, T. L., Fanning, A. F., Holland, M. M., MacFadyen, A., Matthews, H. D., Meissner, K. J., Saenko, O., Schmittner, A., Wang, H., and Yoshimori, M.: The UVic Earth System Climate Model: Model Description, Climatology, and Applications to Past, Present and Future Climates, Atmos. Ocean, 39, 361-428, 2001.

Weinelt, M. MARGO, SST : Compilation of global planktic foraminifera LGM SST data, doi:10.1594/PANGAEA.227620, 2004.

Xu, X., Yamasaki, M., Oda, M., and Honda, M. C.: Comparison of seasonal flux variations of planktonic foraminifera in sediment traps on both sides of the Ryukyu Islands, Japan, Mar. Micropal., 58, 45–55, 2005.

Yeager, S. G., Shields, C. A., Large, W. G., Hack, J. J.: The low–resolution CCSM3. J. Climate, 19, 2545–2566, 2006.

Weaver, A. J., Eby, M., Wiebe, E. C., Bitz, C. M., Duffy, P. B., Ewen, T. L., Fanning, A. F., Holland, M. M., MacFadyen, A., Matthews, H. D., Meissner, K. J., Saenko, O., Schmittner, A., Wang, H., and Yoshimori, M.: The UVic Earth System Climate Model: Model Description, Climatology, and Applications to Past, Present and Future Climates, *Atmos. Ocean*, 39, 361-428, 2001.

Weinelt, M. MARGO, SST: Compilation of global planktic foraminifera LGM SST data, doi:10.1594/PANGAEA.227620, 2004.

Weinelt, M., Sarnthein, M., Pflaumann, U., Schulz,,H., Jung, S. J. A. and Erlenkeuser, H.: Ice-free Nordic Seas during the Last Glacial Maximum?, Potential sites of deepwater formation, *Paleoclimates*, 1, 283–309, 1996.

Chapter 5

Vertical distribution of living planktonic foraminifera in the Azores Front

Abstract

Plankton tows from in the Atlantic Ocean allow analysis of vertical distribution of planktonic foraminifera in the water column. Two sites have been studied along a N- S transect in the region of the Azores Front (33- 36°N, 20°W) during April 2006. Multinet samples were collected between the surface and 300 m, in intervals of 20 m and 100 m, and foraminifera species were identified. Living and dead specimens were distinguished in order to recognize the living habitat of each species.

Maximum total foraminiferal abundance was found at the base of the mixed layer. Living specimens of G. falconensis, G. glutinata, G. humilis, G. ruber, G. rubescens *and* G. sacculifer *were limited to the upper 60 m.* G. bulloides *and* G. calida *showed preference for surface waters, but were not limited to it. In contrast,* G. scitula, G. truncatulinoides *and* G. hirsuta *occurred mainly in deeper waters, but occasionally were also found in shallow waters.*

The assemblage of the upper 100 m was compared to the output of a foraminiferal model. The foraminifera model predicted high relative abundance of G. bulloides *at this locations. Instead, in our samples we found very low concentrations; probably because the ecological niche of* G. bulloides *was occupied by other species not included in the model.*

5.1 Introduction

Inthe modern ocean, planktonic foraminiferal species prefer specific ecological habitats, and therefore the vertical distribution of the individual species in the water column depends on vertical variations in hydrographic parameters such as temperature, salinity, food availability, chlorophyll concentration, and light level (e.g., Bé et al., 1985; Deuser, 1987; Watkins et al., 1996; Guptha et al., 1997). Empty shell of foraminifera accumulated on the ocean floor are used to reconstruct past oceanic conditions. Thus, in order to offer better constrains in paleoceanographic interpretations, it is important to understand their modern vertical and horizontal distribution patterns, and the ecological parameters that control their life cycle. To

study the variations in the distribution of planktonic foraminifera, a mathematical model, which simulates the population dynamics of the different species, was developed (Fraile et al., 2008). This model predicts the monthly concentration of five of the most important modern planktonic foraminifera used in paleoceanography including *N. pachyderma* (sin.), *N. pachyderma* (dex.) (following the recommendation of Darling et al. (2006) here named *N. incompta*), *G. bulloides*, *G. ruber* (white) and *G. sacculifer*. The model has already been validated using sediment trap and core- top data situated all over the world for comparison. However, the model only predicts the living population in the mixed layer, whereas the sediment trap and core- top data represent the integrated population throughout the water column. The objective of this study is to compare the model output with living population collected with plankton nets in the water column and surface waters of the Azores Front, in the eastern North Atlantic.

5.2 Material and methods

5.2.1 Sampling and processing

The samples were taken by the research group of the Micropaleontology Department in the University of Tübingen in the Poseidon cruise 334, from 15 March to 3 April 2006 between Las Palmas and Messina (Fig. 5.1, lower panel). A multiple opening–closing net collected samples of plankton organism by vertical hauls (100-μm mesh size, 50x50 cm^2 opening) between the ocean surface water and 1000 m water depth across the hydrographic Azores Front in the eastern North Atlantic (Fig. 5.1, upper panel). At each station, the multinet was deployed twice between the sea–surface and 1000 m. The upper 100 m were sampled in 20 m depth intervals, and below 100 m, at 100–200–300–500–700–1000 m water depths. The results shown in this study correspond to the upper 300 m of the station POS334–67 (32°59′N 19°59′W) and upper 100 m of the station POS334–69 (36°59′N 19°59′W). The samples were preserved in solution of sea- water and 4% of formaline and hexamethyletramine until February 2007. In the laboratory, the samples were washed, and then foraminifera were picked, dried and sieved through a $63\,\mu m$ mesh before counting. Cytoplasm- bearing tests (living specimens when collected) were counted separately from empty tests (dead specimens). A detrended correspondence analysis (DCA, Hill and Gauch, 1980) was applied to planktonic foraminiferal census data. DCA assumes that species abundances are distributed unimodally along some underlying ecological gradient, and correlates the main gradients (axes) with given environmental variables.

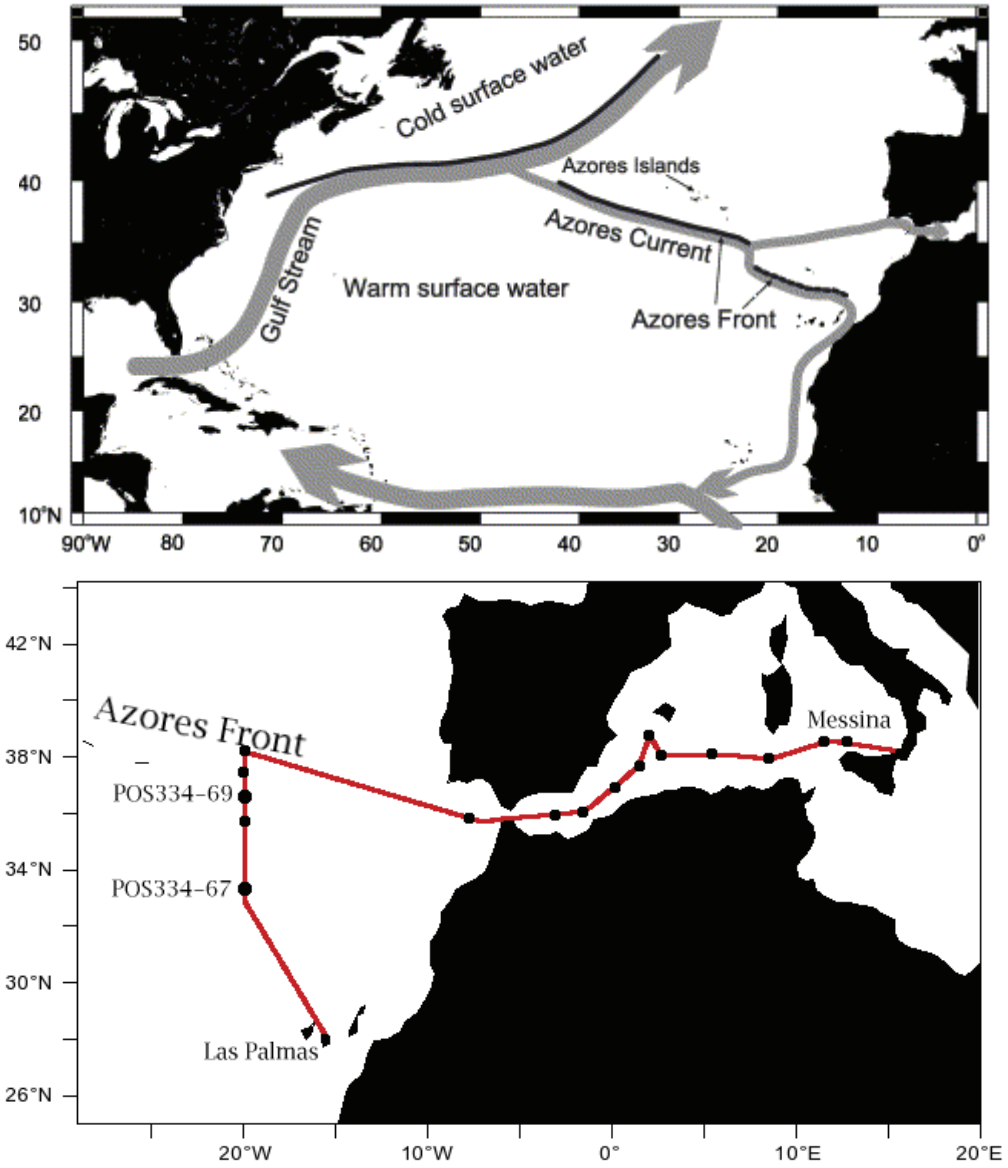

Figure 5.1: *General surface circulation in N. Atlantic (upper panel) (Modified from Rogerson et al., 2004) and map of the stations during the cruise POS334 (lower panel). POS334–67 and POS334–69 are the stations investigated in this study.*

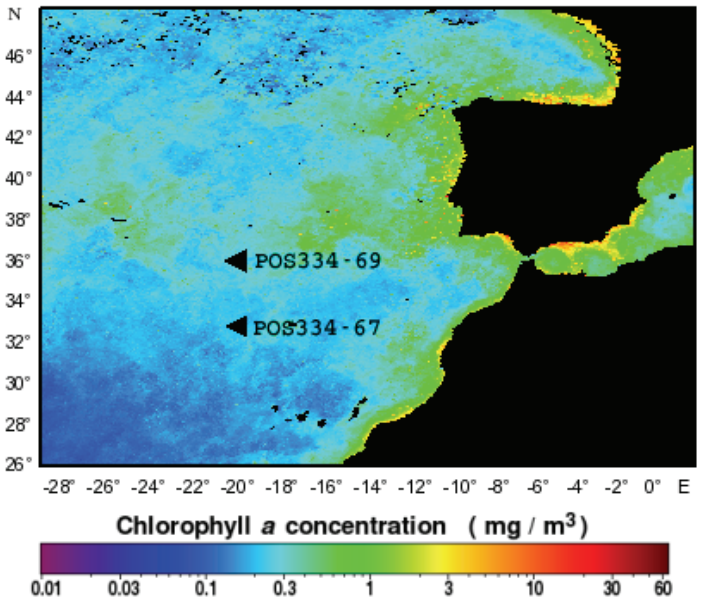

Figure 5.2: *Surface chlorophyll-α concentration in Azores region during March 2006. Both stations are located south of the high productivity area. Satellite image from SeaWIFS (available at http://seadas.gsfc.nasa.gov).*

5.2.2 Oceanographic setting

The area of study is characterized by a significant mesoscale activity, confirmed by the importance of eddies in the biological activity of the region (González et al., 2001; Huskin et al., 2001). The Azores Front is probably the main mesoscale structure influencing the dynamics of the area (Fernandez and Pingree, 1996). The Azores Front marks the boundary between the European surface water masses (cold and fresher) and African (warmer and saltier) surface water masses (Gould, 1985; Schiebel et al., 2002a), and extends across the Atlantic between 30–40°N. The Azores current, which coincides with the Azores Front, is the northern border of the subtropical North Atlantic gyre and acts as a continuous link to the south- eastern branch of Gulf Stream transporting subtropical waters towards the Iberian margin (Klein and Siedler, 1989; Alves et al., 2002). At water depths of 100–500 m, the North Atlantic Central Water (NACW) forms basically the permanent thermocline. The NACW st is relatively warm and salty but poorly ventilated.

The Azores Front is therefore an area of strong hydrographic transition, in terms of temperature and water column structure (Gould, 1985; Fasham et al, 1985). During the sampling period (end of March 2006) both stations were located south of the high productivity area (Fig. 5.2). Previous studies related changes in the plankton

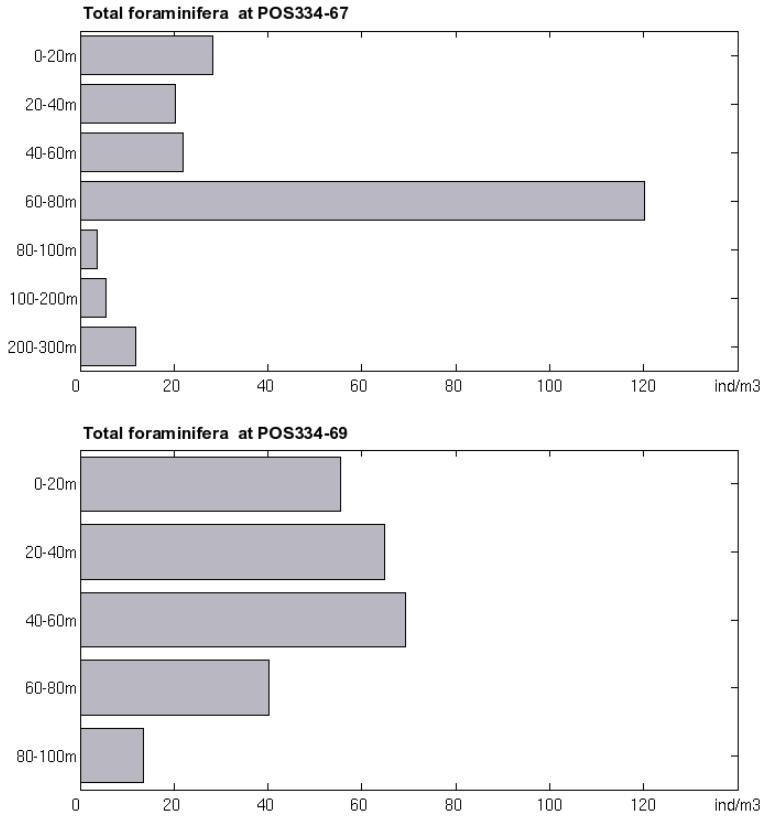

Figure 5.3: *Total foraminferal concentration (ind./m^3) at stations POS334–67 (32° 59′ N 19° 59′ W) and POS334–69 (36° 59′ N 19° 59′ W).*

assemblages across the Azores Front to the overall productivity and to the depth of the Deep Chlorophyll Maximum (DCM) (Fasham et al, 1985; Angel, 1989; Fernandez and Pingree, 1996; Schiebel et al., 2002a). The ecological signature of the Azores Current/Azores Front in the sedimentary record has already been used to investigate the history of the current system of the North Atlantic Ocean in the past (Schiebel et al., 2002b; Rogerson et al., 2004).

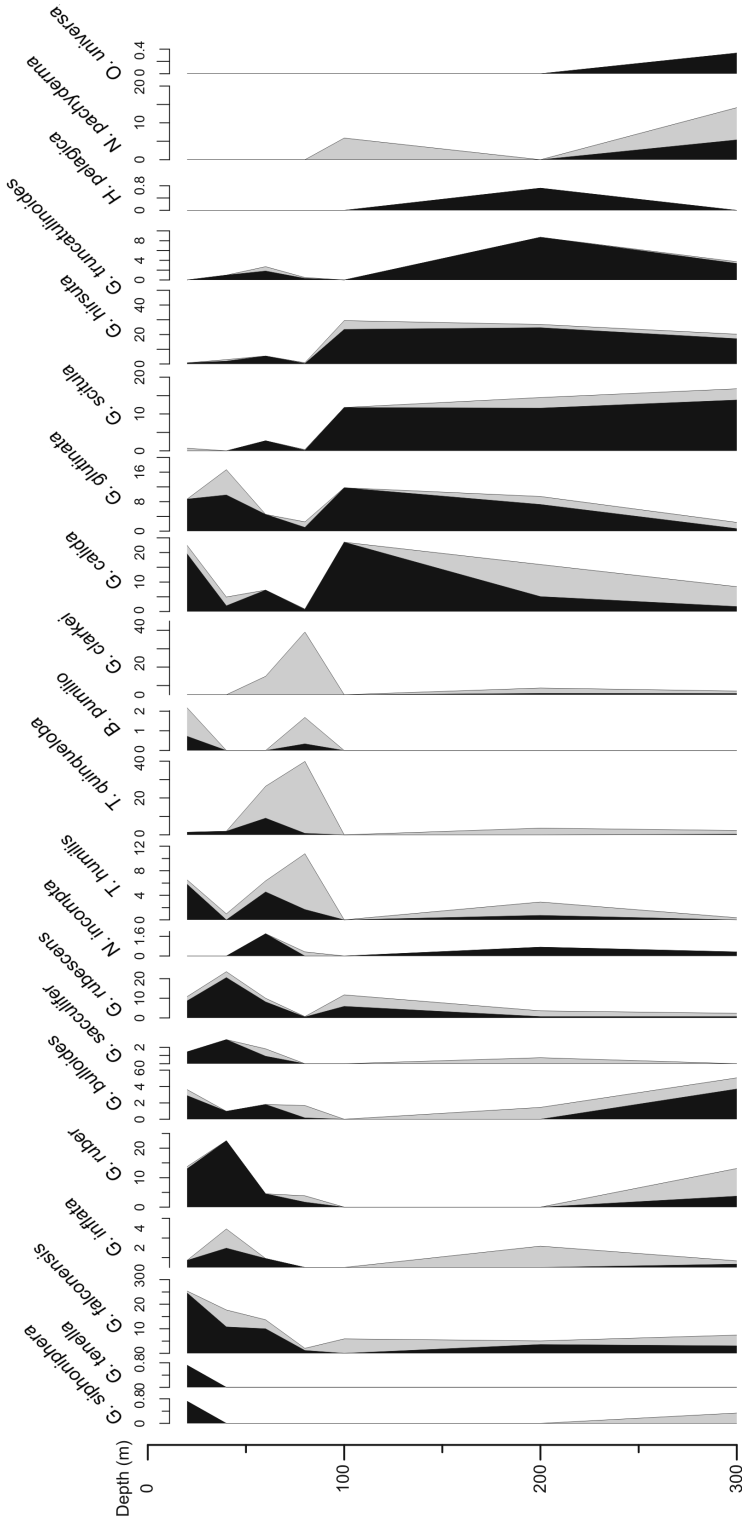

Figure 5.4: *Relative abundances of planktonic foraminifera species in the water column at site POS334–67, and relation between living (black) and dead (gray) specimens.*

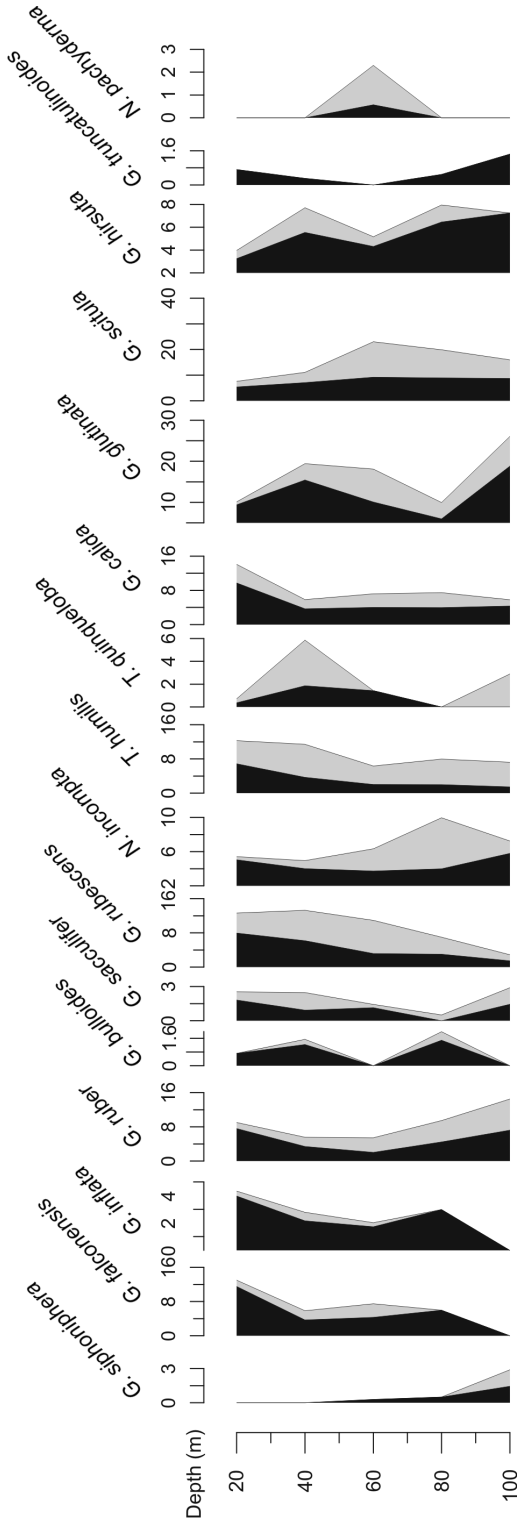

Figure 5.5: *Relative abundances of planktonic foraminifera species in the water column at site POS334–69, and relation between living (black) and dead (gray) specimens.*

5.3 Results

5.3.1 Total foraminiferal fauna

The vertical distribution of the overall planktonic foraminiferal abundances vary from site to site. In the southernmost site (POS334–67) the standing stocks of total foraminifera varied substantially with depth. An overview of the vertical distribution of total foraminifera at both stations is given in Fig. 5.3. Foraminiferal standing stock was comparatively low between 0–60 m (maximum of 28 ind/m^3), and in the sampling interval of 60– 80 m it increased up to 120 ind/m^3. Below 80 m the concentration decreased again rapidly. In contrast, at station POS334–69, most specimens were dwelling in the upper 80 m, where the total foraminiferal concentration remained relatively high and unchanged, but decreased below this depth.

5.3.2 Foraminiferal assemblage composition

The assemblage composition varied with depth (Fig. 5.4), most notable at the southern site (POS334–67). The southern fauna was dominated by *G. calida*, *G. falconensis*, *G. ruber*, *G. rubescens* in the upper 100 m. Among the deep- dwelling species, *G. hirsuta* and *G. scitula* were most frequent, and occurred in high numbers below 80 m. The extraordinary high standing stock of 120 ind/m^3, at 60–80 m depth at the station POS334–67 was due to high numbers juveniles of *G. quinqueloba*. In addition, *G. truncatulinoides* and *N. pachyderma* also increased their relative abundance below 80 m. Some species, e.g. *G. glutinata* did not show a clear pattern, maintaining the relative abundances relatively unchanged at different depths. Two maxima were found for *G. calida* and *G. bulloides*; one at surface and a second maxima between 80–200 m for *G. calida* and between 200–300 m for *G. bulloides*.
In the northernmost site (POS334–69, 36°N) we only analyzed the top 100 m. The foraminiferal assemblage was mainly composed of the same species as in POS334–67, but most of the species did not show a big variability within this depth (Fig. 5.5). At this station *N. pachyderma* occurred at shallower waters, and the concentration of *N. incompta* was higher compared to the southern site.

In order to recognize the depth habitat of each species, living and dead specimens were identified (Figs. 5.4–5.5). In this way, dead specimens that are sinking and may have a different depth habitat can be separated from the living population. At station POS334–67, living specimens of *G. bulloides* and *G. calida* were found at surface and also at deeper waters (below 100 m). In contrast, *G. falconensis*, *G. glutinata*, *G. humilis*, *G. ruber*, *G. rubescens*s and *G. sacculifer* were restricted to the photic zone, between surface and 100–130 m (Huskin et al., 2004). Living specimens of *G. scitula*, *G. truncatulinoides* and *G. hirsuta* were mainly found below 100 m in

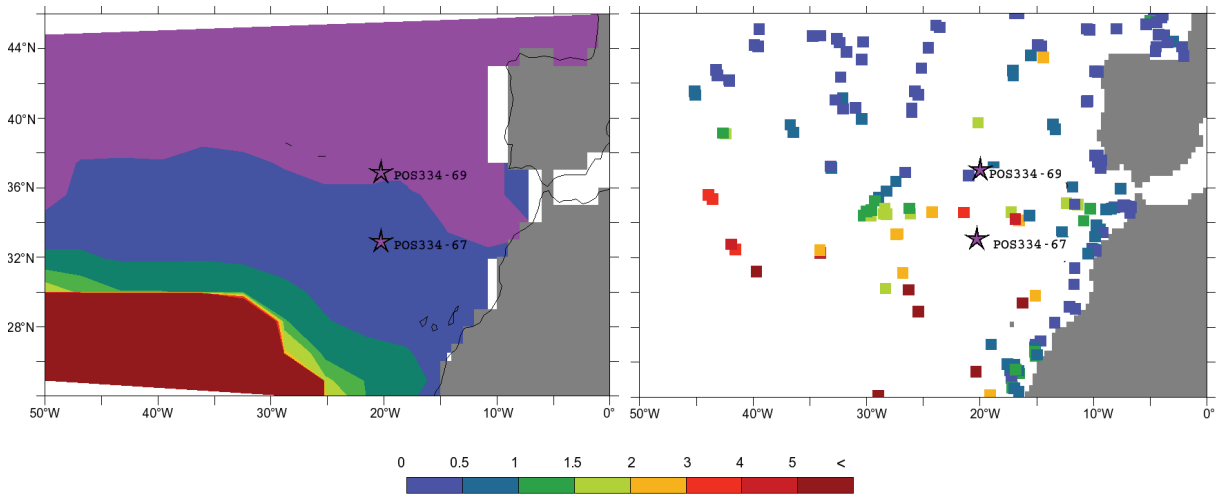

Figure 5.6: *Ratio between G. ruber and G. bulloides in the annual mean concentration predicted by the foraminifera model (left panel) (Fraile et al., 2008) and of surface sediments (right panel) (Pflaumann et al., 1996; Prell et al., 1999). The stars represent the two stations of this study.*

deeper waters, but some living specimens were also found between surface and 100 m depth.

In the northernmost station (POS334–69) living and dead specimens of all species were found at every depth (Fig. 5.5), although some species as *G. rubescens*, *G. humilis*, *G. calida* or *G. falconensis* decreased the number of living specimens with depth. In contrast, the number of living specimens of *G. scitula* and *G. hirsuta* increased with depth. In general, the northernmost station reflects less variability in the assemblage composition with depth.

5.3.3 Model prediction

We compared the model prediction with the living population assemblage in order to identify the physico–chemical conditions in which the foraminifera grew. Due to the fact that we used a non–linear dynamic model, inverse modeling was not possible. Instead, we analyzed the model output for modern conditions and we identified the sites where the model predicted a similar assemblage composition to that of the station POS334–67

Foraminiferal standing stocks of the upper 100 m of our samples were integrated (approximately corresponds to the mixed layer depth), and the ratio between two species was calculated. The species predicted by the foraminifera model are *N. pachyderma* (sin.), *N. incompta* (in the model named as *N. pachyderma* (dex.)), *G. bulloides*, *G. ruber* (white) and *G. sacculifer*. In the samples *N. incompta* and *N. pachyderma* were very scarce, and the model simulates total lack of *G. sacculifer*. Therefore, in order to compare plankton net and model data we focused on the the relative abundances between the remaining two species: *G. ruber* and *G. bulloides*. In POS334–67 (33°N 20°W) the ratio between *G. ruber*/*G. bulloides* found in our samples was ~ 4, whereas the model predicts *G. ruber*/*G. bulloides* ratio of 0.4 at the end of March (the time when the samples were collected) for the same location. Thus, in the model simulation the abundance of *G. bulloides* (and also of *N. incompta*, which was nearly absent in the samples) is higher than *G. ruber*, whereas in the plankton net data we found higher concentrations of *G. ruber*. The mismatch between *G. bulloides* and *G. ruber* is also visible when comparing the simulated annual mean concentration and core–top data (Fig. 5.6). In the model simulation, the border of the region where *G. bulloides* is dominant over *G. ruber* is shifted 4–6°southwards approximately.

Our center of interest is to analyze which are the physico–chemical conditions in which the model predicts the assemblage composition found in the plankton–net data. We selected the locations where the predicted rate between *G. ruber* and *G. bulloides* is most similar to that observed in the sample. Table 5.1 summarizes the locations where *G. ruber*/*G. bulloides* rates is within 10% of the observed value. It also shows the SST from World Ocean Atlas 2005 (Locarnini, 2006) and chlorophyll concentrations in the mixed layer from the ecosystem model (Moore et al., 2002) at this time of the year . The temperature at all locations was higher than at station POS334–67. In those locations where SST was within +2°C (marked with *) of the value at POS334–67, the chlorophyll concentrations was low. Therefore, in general, the model predicts a similar assemblage composition at warmer and/or lower productivity areas.

Table 5.1:

Locations where the model predicts a similar *G. ruber*/*G. bulloides* rate as the observed one at POS334–67 (33°N 20°W) at the end of march (marked with *: locations where the temperature deviation does not exceed +2°C).

Latitude [°N]	Longitude [°E]	$\frac{G.ruber}{G.bulloides}$	Temperature [°C]	Mixed–layer depth [m]	Chl [mg Chl/m^3]
Conditions at POS334–67 in April					
33	-20	3.893	17.54	84.73	0.2295
Model output					
January					
23.3	–21.6	3.54	21.11	89.85	0.27
–0.9	–135.8	3.64	25.95	57.56	0.22
–2.6	–90	4.00	24.30	25.00	0.16
–30	–14.4	3.93	24.11	25.00	0.10
February					
28.3	-28.8	3.65	20.19	139.5	0.26
0	–144	3.86	26.88	41.51	0.120
–0.9	–144	3.79	26.94	41.61	0.20
–3.5	7.2	3.88	28.14	25.00	0.21
–31.9	–147.6	3.60	22.72	25.00	0.12
March					
28.3	–169.2	3.79	18.96*	81.80	0.17
23.3	–122.4	3.71	19.07*	81.25	0.15
10.4	64.8	3.55	27.97	25.00	0.20
6.9	68.4	3.78	28.87	25.00	0.18
–3.5	7.2	3.76	28.74	25.00	0.21
–11.2	–86.4	3.99	26.30	25.00	0.17
–20.5	–90	3.77	23.56	39.10	0.15
–33.7	46.8	3.51	23.27	31.23	0.17
April					
28.3	–176.4	3.68	20.05	30.51	0.09
6.9	68.4	3.59	29.71	25.00	0.20
–3.5	7.2	3.81	28.37	25.00	0.23
–11.2	–86.4	3.54	25.78	26.84	0.16
–31.9	36	3.85	24.40	35.56	0.23
May					
26.5	–28.8	3.84	21.57	25.00	0.10
–4.3	–79.2	3.91	20.86	25.00	2.81

Continued on next page

Table 5.1 – continued from previous page

Latitude [°N]	Longitude [°E]	$\frac{G.ruber}{G.bulloides}$	Temperature [°C]	Mixed–layer depth [m]	Chl [mg Chl/m^3]
–6.9	–79.2	3.62	19.70	25.00	2.23
–21.8	–90	3.96	21.96	77.26	0.22
–31.9	–39.6	3.58	21.50	61.35	0.26
–35.6	25.2	3.57	19.70	25.00	0.86
June					
–28.3	82.8	3.62	20.48	36.47	0.15
July					
23.3	–25.2	3.50	23.47	40.36	0.17
–5.2	–86.4	3.91	22.05	31.92	0.23
–10.4	–86.4	3.85	21.97	43.89	0.23
–24.9	–93.6	3.70	20.59	34.17	0.16
–28.3	0	3.97	19.34*	25.00	0.14
August					
–0.9	–126	3.88	24.95	28.95	0.17
–6.9	86.4	3.93	21.28	37.79	0.22
–8.6	–86.4	3.91	21.21	43.02	0.21
–11.2	0	3.97	22.54	48.81	0.27
–20.5	–93.6	3.88	20.91	25.00	0.16
–28.3	100.8	3.71	18.76	64.07	0.13
September					
19.2	–18	3.56	24.90	25.00	1.03
0.9	–144	3.73	26.09	37.76	0.17
–13.9	–93.6	3.60	20.70	86.15	0.21
–19.2	7.2	3.71	17.71*	87.33	3.07
–28.3	104.4	3.60	18.81*	57.61	0.10
October					
30	140.4	3.60	25.70	36.30	0.24
20.5	–25.2	3.81	25.42	34.05	0.21
0	–129.6	3.55	24.07	25.00	0.16
–0.9	–97.2	3.62	22.08	25.00	0.17
–10.4	0	3.75	21.81	41.43	0.21
–28.3	165.6	3.77	20.91	32.72	0.12
–28.3	90	3.69	19.20*	34.20	0.08
–30	–126	3.56	20.23	60.37	0.14
November					
28.3	165.6	3.93	24.86	41.04	0.22
20.5	–25.2	3.73	24.74	48.15	0.24
–1.7	–144	3.82	26.36	55.25	0.21
–5.2	–90	3.63	21.92	25.00	0.17
–9.5	–90	3.51	21.77	50.96	0.17
–28.3	–100.8	3.96	20.98	42.27	0.12

Continued on next page

Table 5.1 – continued from previous page

Latitude [°N]	Longitude [°E]	$\frac{G.ruber}{G.bulloides}$	Temperature [°C]	Mixed–layer depth [m]	Chl [mg Chl/m^3]
December					
30	–133.2	3.66	19.09*	74.17	0.18
–8.6	–90	3.87	22.92	25.00	0.15
–9.5	3.6	3.97	23.63	26.86	0.19

5.4 Discussion

5.4.1 Depth habitat of the species

The total foraminiferal concentrations found in this study are similar to those reported by Schiebel et al. (2002b) in the same region. The mixed layer depths during April were 60 m and 85 m at the stations POS334–67 and POS334–69 respectively (Monterey and Levitus, 1997, climatological mixed–layer depth, based on the density difference criteria). Foraminiferal concentration seems to be strongly related to the mixed layer depth. At both stations, maximum foraminiferal concentrations were found at the base of mixed layer. However, the northern site POS334–69, showed higher foraminiferal standing stock through the water column. This was probably caused by the proximity of the high productivity zone associated to Azores Front, as reflected by the high chlorophyll concentration (Fig. 5.2).

DCA reveals that three major faunal assemblages can be identified at site POS334–67 (Fig. 5.7). The axis 1, which explains around 50% of the variance, can be interpreted as a gradient of depth (or a parmeter which varied with depth). Accordingly, the shallow–water assemblage is comprised by *G. tenella*, *G. sacculifer*, *G. siphoniphera*, *B. pumilio*, *G. inflata*, *T. quinqueloba*, *G. falconensis*, *G. ruber*, *G. rubescens* and *T. humilis*. The few living specimens we found in deeper waters probably represent sinking individuals. The deeper–dwelling assemblage includes *O. universa*, *N. pachyderma*, *G. scitula*, *G. clarkei*, *G. hirsuta* and *G. truncatulinoides*. These species live preferentially in deeper waters, but occasionally they can also live in shallow waters. The few living specimens we found in the upper part of the water column could be individuals migrating to shallow waters for reproduction. The third faunal assemblage encloses species with a intermediate depth habitat: *G. bulloides*, *G. calida*, *N. incompta* and *G. glutinata*. These species are not restricted to the surface waters although they have preference for it. The DCA from site POS334–69 reflects no clear differentiation in faunal groups, suggesting that the upper 100 m are well mixed and there are not clearly separated ecological niches (Fig. 5.8). However, the

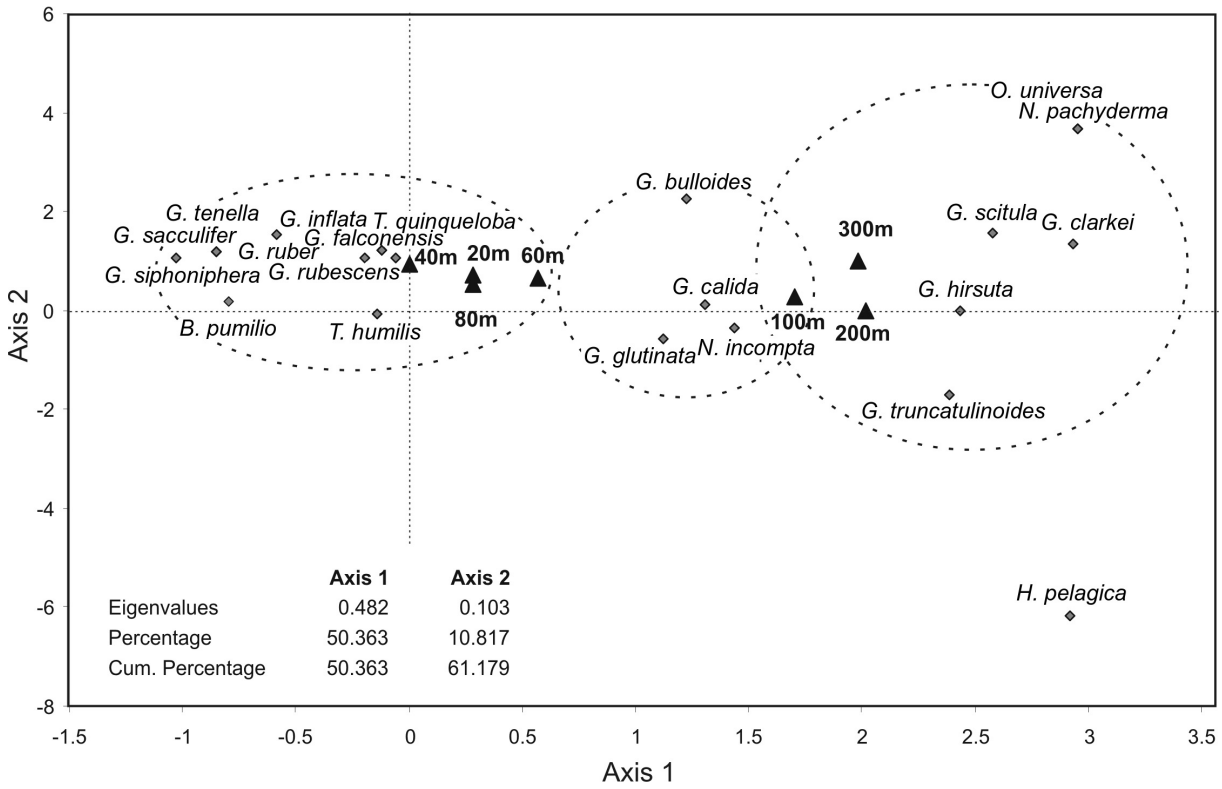

Figure 5.7: *Detrended Correspondence Analysis (DCA) at site POS334-67. Axis 1 (interpreted as depth explains 50% of the variance. Axis 2 coresponds to other factors which also play a role in explaining the various groups (11% of the variance).*

analysis from this site is limited to the upper 100 m and therefore the deep–dwelling species are absent.

5.4.2 Comparison between samples and model prediction

At the southernmost site, POS334–67 (32°59′N), the model does not predict the observed relative abundances between *G. ruber*, *N. incompta* and *G. bulloides* species. In the plankton–net samples the relative abundance of *G. ruber* was higher than *G. bulloides* and *N. incompta*, while the model simulation reflects the contrary. This could be due to a wrong parametrization of temperature tolerance of *G. ruber*. However, this situation occurs due to quite low concentrations of *G. bulloides* and *N. incompta*

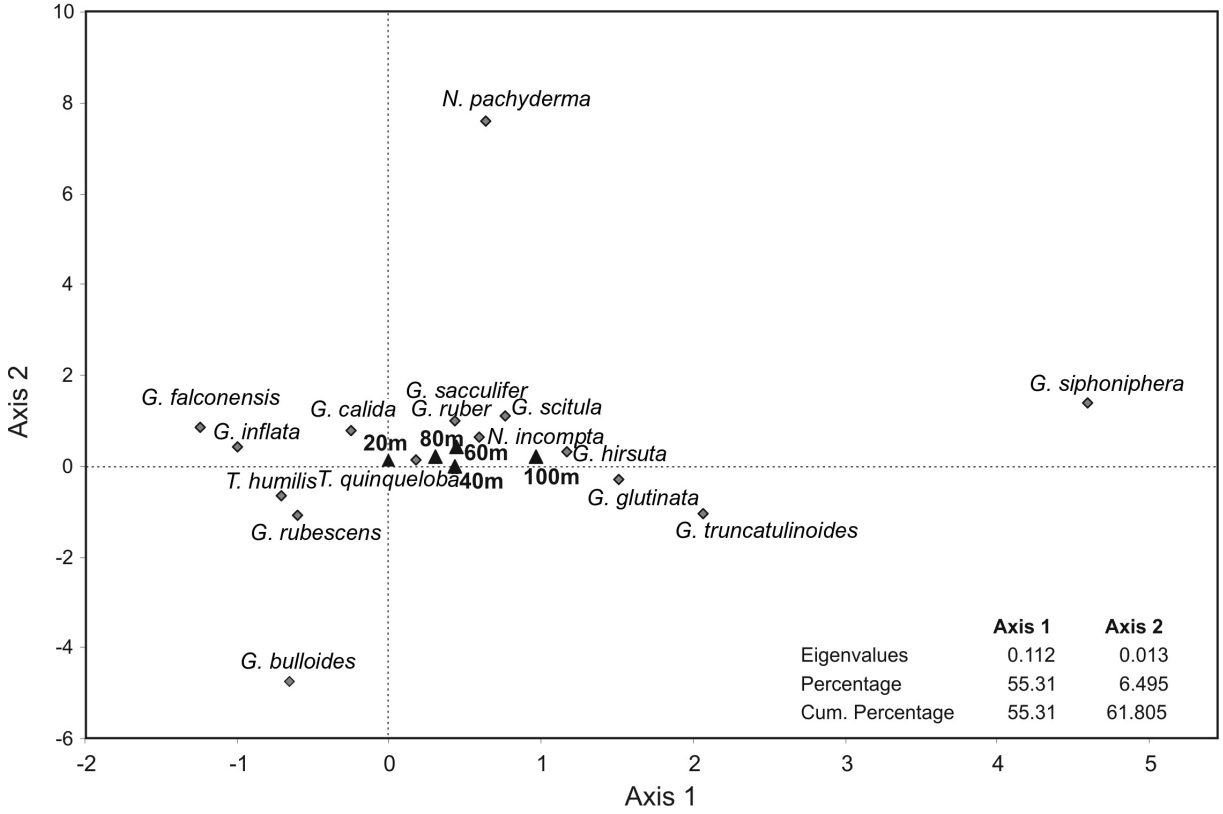

Figure 5.8: *Detrended Correspondence Analysis (DCA) at site POS334–69.*

rather than due to high concentrations of *G. ruber* (14 ind/m^3 in the upper 100 m). Therefore is more likely that the difference between the model output and observed data is due to the fact that the ecological niche of *G. bulloides* is occupied by other species not included in the model, like *G. glutinata* and *G. falconensis*. The samples were collected at the end of March, therefore it is probable that higher abundances of *G. bulloides* occurred later in the year, since it generally follows the spring algal bloom of the North Atlantic (Ganssen and Kroon, 2000).

5.5 Conclusions

Plankton–net studies along a N–S transect near the Azores Front in the region of eastern North Atlantic revealed that living planktonic foraminifera assemblage composition varies with depth. *G. falconensis*, *G. glutinata*, *G. humilis*, *G. ruber*, *G. rubescens* and *G. sacculifer* live mostly in the upper 60 m, while *G. scitula*, *G. truncatulinoides* and *G. hirsuta* prefer deep waters ($\geq$100 m depth). *G. bulloides* and *G. calida* have preference for surface waters, but can also live occasionally in deeper waters.

In general, the southernmost site (POS334–67) shows more stratified structure in species composition. DCA analysis showed that at this site the depth can explain 50% of the faunal variance. In contrast, in the northernmost site (POS334–69) we found a more homogeneous species composition with depth, suggesting that the frontal system causes strong mixing in the upper 100 m.

Most of species simulated with our foraminifera model were absent in the studied area, and the standing stocks of those species included in the model were very low. Therefore, a direct comparison between plankton–net data and model prediction was not possible. It is probable that species like *G. bulloides* occurred later in the year, as this species is link to phytoplankton dynamics. The dominant species collected in surface water samples were *G. falconensis*, *G. glutinata* and *G. calida*. An extension of the current model including more species in may improve the model results.

Acknowledgments I would like to thank the Micropaleontology group in the University of Tübingen for all the support and help received during my stay there. In particular, to Prof. Michal Kucera, who gave me excellent advices and motivation to follow with my work. Thanks also to the crew members of POSEIDON–334 for providing the plankton samples. Very special thank to Margret Bayer for all the time she expended patiently teaching me the identification of planktonic foraminifera species. I also would like to thank Catalina Gonzalez, from the University of Bremen, for all the helpful suggestions in multivariate analysis. This project was supported by the DFG (Deutsche Forschungsgemeinschaft) as part of the European Graduate Collegue “Proxies in Earth History” (EUROPROX).

Bibliography

Alves, M., Gaillard, F., Sparrow, M. Knoll, M. and Giraude, S.: Circulation patterns and transport of the Azores Front-Current system, Deep–Sea Res. II, 49, 3983–4002, 2002.

Angel, M. V.: Vertical profiles of pelagic communities in the vicinity of the Azores Front and their implications to deep ocean ecology, Prog. Oceanogr., 22, 1–46, 1989.

Bé, A. W. H., Bishop, J. K. B., Sverdlove, M. S., and Gardner, W. D.: Standing stock, vertical distribution and flux of planktonic Foraminifera in the Panama Basin, Mar. Micropal., 9, 307–333, 1985.

Darling, K. F., Kucera, M., Kroon, D., and Wade, C. M.: A resolution for the coiling direction paradox in *Neogloboquadrina pachyderma*, Paleoceanography, 21, 2011, doi:10.1029/2005PA001189, 2006.

Deuser, W. G.: Seasonal variations in Seasonal variations in isotopic composition and deep–water fluxes of the tests of perennially abundant planktonic foraminifera of the Sargasso Sea: results from sediment–trap collections and their paleoceanographic significance, J. Foram. Res., 17, 14–27, 1987.

Fasham, M. J. R., Platt, T., Irwin, B. and Jones, K.: Factors affecting the spatial pattern of the Deep Chrolophyll Maximum in the region of the Azores Front, in: Essays On Oceanography: A Tribute to John Swallow, edited by: Crease, J., Gould, W. J. and Saunders P. M., Prog. Oceanogr., vol. 14, Pergamon, Oxford, 129–166, 1985.

Fernandez, W. and Pingree, R. D.: Coupling between physical and biological fields in the North Atlantic subtropical front southeast of the Azores, Deep–Sea Res. I, 43, 1369–1393, 1996.

Fraile, I., Schulz, M., Mulitza, S. and Kucera, M.: Predicting the global distribution of planktonic foraminifera using a dynamic ecosystem model, Biogeosciences, 5, 891–911, 2008.

Ganssen, G. M. and Kroon, D.: The isotopic signature of planktonic foraminifera from NE Atlantic surface sediments: implications for the reconstruction of past oceanic conditions, J. Geol. Soc., 157, 693–699, 2000.

González, N., Anadón, R., Mouriño, B., Fernández, E., Sinha, B., Escánez, J. and de Armas, D.: The metabolic balance of the planktonic community in the N. Atlantic Subtropical Gyre, Limnol. Oceanogr., 46, 946–952, 2001.

Gould, W. J.: Physical oceanography of the Azores Front, in: Essays On Oceanography: A Tribute to John Swallow, edited by: Crease,J., Gould, W. J. and Saunders P. M., Prog. Oceanogr., vol. 14, Pergamon, Oxford, 167–190, 1985.

Guptha, M. V. S., Curry, W. B., Ittekkot, V., and Muralinath, A. S.: Seasonal variation in the flux of planktic foraminifera: Sediment trap results from the Bay of Bengal, northern Indian Ocean, J. Foramin. Res., 27, 5–19, 1997.

Hill, M. O. and Gauch, H. G.: Detrended correspondence analysis, an improved ordination technique, Vegetatio, 42, 47–58, 1980.

Huskin, I., Anadón, R., Medina, G., Head, R. N. and Harris, R. P.: Mesozooplankton distribution and copepod grazing in the Subtropical Atlantic near the Azores: influence of mesoscale structures, J. Plankton. Res., 23, 671–691, 2001.

Huskin, I., Viesca, L. and Anadón, R.:Particle flux in the Subtropical Atlantic near the Azores: influence of mesozooplankton, J.Plankton. Res., 26, 403–415, 2004.

Klein, B. and Siedler, G.: On the origin of the Azores Current, J. Geophys. Res., 94, 6159–6168, 1989.

Locarnini, R. A., Mishonov, A. V., Antonov, J. I., Boyer, T. P. and Garcia, H. E.: World Ocean Atlas 2005, Volume 1: Temperature. S. Levitus, Ed. NOAA Atlas NESDIS 61, U.S. Government Printing Office, Washington, D.C., pp. 182, 2006.

Monterey, G. and Levitus, S.: Seasonal variability ofmixed layer depth for the world ocean, NOAA Atlas NESDIS 14, US Government Printing Office, Washington, D.C., 1997.

Moore, J. K., Doney, S. C., Kleypas, J. A., Glover, D. M., and Fung, I. Y.: An intermediate complexity marine ecosystem model for the global domain, Deep–Sea Res. II, 49, 403–462, 2002.

Rogerson, M., Rohling, E.J, Weaver, P.P.E. and Murray, J.W.: The Azores Front since the Last Glacial Maximum, Earth Planet. Sc. Lett., 222, 779–789, 2004.

Schiebel, R., Waniek, J., Zeltner, A. and Alves, M.: Impact of the Azores Front on the distribution of planktic foraminifers, shelled gastropods and coccolithophorids, Deep–Sea Res. II, 49, 4035–4050, 2002a.

Schiebel, R., Schmuker, B, Alves, M and Hemleben, C: Tracking the Recent and late Pleistocene Azores front by the distribution of planktic foraminifers, J. Mar. Systems, 37, 213–227, 2002b.

Watkins, J. M., Mix, A. C., and Wilson, J.: Living planktic foraminifera: tracers of circulation and productivity regimes in the central equatorial Pacific, Deep–Sea Res. II, 43, 1257–1282, 1996.

Chapter 6

Summary

A numerical model for planktonic foraminifera has been designed in order to improve the accuracy of foraminifera-based paleotemperature reconstruction (chapter 2). This model is a non–linear dynamic model which considering ecological processes computes the growth rate of the most important planktonic foraminifera species used in paleoceanography: *N. pachyderma* (sin. and dex), *G. bulloides*, *G. ruber* (white) and *G. sacculifer*. The growth rate is integrated over a week, and ultimately, monthly concentration of each species is calculated for one hypothetical year. The model is constructed to examine foraminiferal variability on large spatial (global) and temporal (monthly) timescale, and its use at high temporal resolution is not recommended. The model domain is, at present, also restricted to the mixed layer, including only the first order parameters that control foraminiferal distribution (temperature and food). For the parametrization, we used the climatological temperatures from WOA98 (Conkright et al., 1998). To supply the foraminifera model with ecological information (food availability), we run the foraminifera module within an ecosystem model (Moore et al., 2002,b), which predicts the abundance of zooplankton and different groups of phytoplankton. For compatibility with the ecosystem model, the foraminifera model calculates foraminiferal abundance of each species via carbon biomass. However, our study is directed to paleotemperature reconstructions, and therefore our main interest is in species relative abundances and seasonality rather than in assessing the absolute biomass.

The model results have been compared to core–top, sediment–trap and plankton–net data. Overall, modeled relative abundance patterns are similar to the core–top faunal record. Although the comparison between simulated annual seasonal cycle and sediment–trap data bears some difficulties (short sampling periods, high interannual variability and lack of sediment–trap data in open ocean), for most of the locations the modeled seasonal variations agree with observational data. The comparison with plankton–net data in the North Atlantic (Azores Front) was not possible due to the fact that the species included in the model were absent at this time of the year (chapter 5). Instead, *G. calida*, *G. glutinata* and *G. falconensis* were dominant species at surface waters. An extension of the current model including these species

may improve the quality and the capability of prediction of the foraminifera model.

This model gives the opportunity to explore the response of planktic foraminifer to different boundary conditions. One of the problems that remains unsolved in paleoceanography is the seasonal bias associated to the seasonality of the organisms used for reconstructions. This differential foraminiferal production through the year has major implications for paleotemperature reconstructions. Proxy records for a species are weighted towards the values during the season of maximum production for that species. The record preserved in the sediment may reflect the integration of a flux patter, or may even represent only a short high–flux period of the year (e.g. seasonally ice–covered regions). Using this model, we determined the seasonal imprint of planktonic foraminifera on the sedimentary record. The results revealed that close to the upper geographical limit of occurrence of each species (high latitudes), the proxy signal is biased towards summer conditions; while at lower latitudes the signal often reflects annual mean conditions or is even biased towards winter.

Foraminifera are known by being sensitive to temperature. Thus, if the environmental conditions vary, foraminiferal production can shift in order to keep in the range of optimal temperature. Our sensitivity experiments suggest that under a global cooling of 2°C, the geochemical signal in most of the species will not entirely record the temperature variation, as the month of maximum production shifts to a warmer season. This phenomenon has implications when reconstructing glacial environments, as the basic assumption that the seasonality of foraminifera has remained unchanged through time may not be true. Forcing the model with boundary conditions different than modern, it is possible to derive ancient seasonalities, and is thus a powerful tool to improve proxy calibrations. Of special interest is the foraminiferal distribution during the Last Glacial Maximum, which we simulated using a global coupled climate model (chapter 4). Our findings show that foraminiferal seasonality during the LGM was different than that in modern days, and that the maximum production could have shifted by up to six months. It has major implications for the interpretation of foraminifera–based temperature reconstructions, as differences in temperature could just be an artifact resulting from differences in the calcification season. The seasonal imprint in the recorded temperature is maximum at mid and high latitudes. Instead, in tropical waters changes in foraminiferal cycle do not substantially affect the temperature signal, as the recorded temperature represents annual mean conditions.

Chapter 7

Conclusions

This study proved that modeling planktonic foraminiferal distribution at a global scale is possible. Using this foraminifera model we conclude that:

- The predicted relative abundances of the species for the present day conditions correspond well with core- top data. Seasonal variations overall agree with sediment- trap records for most of the locations, although the high interannual variability in the sediment- trap data hampers the comparison.
- The seasonal cycle of foraminifera has strong influence in the proxy signal recorded in their shells, in particular at middle and high latitudes. Using this model, the influence of seasonality in the recorded temperature, which corresponds to the flux- weighted annual mean temperature, can be quantified at each grid- point.
- The seasonal distribution of temperature- sensitive species can change under varying climatic conditions overprinting the true climatic signal. Changes in seasonal distribution in the tropics do not influence substantially the proxy record, as the temperature signal recorded by the shells reflects annual mean temperatures.
- The seasonality of foraminifera has changed from the LGM to the present day. During the LGM, the maximum production of subtropical and high-latitude foraminifera generally occurred at a warmer season of the year. As a consequence, assuming modern seasonality as a standard for glacial paleotemperature reconstructions could lead to a bias in foraminifera- based paleotemperature estimates.
- Using this foraminiferal model to predict maximum production month at glacial periods, we can explain discrepancies between reconstructions based on different proxies (e.g. alkenones vs. Mg/Ca, as suggested by Niebler et al., 2003), as well as discrepancies about the North Atlantic Deep water formation during the LGM based on foraminiferal $\delta^{18}O$ values (Duplessy et al., 1991 vs. Sarnthein et al., 1995).

7.1 Outlook

Future improvements may be achieved by including more foraminiferal species, as for example, *G. calida*, *G. glutinata* and *G. falconensis*, which constitute an important part of total foraminiferal fauna and where dominant in the upper water column of the Azores Front during March 2006. With the current version the model predicts some situations where the abundances of all five species included in the model are very low, resulting in dubious relative abundances. Increasing the number of species may solve this problem, and may also modify the results via interspecific competition.

Dividing the species in different genotypes could also improve the results, as different genotypes are often adapted to different environments. However, some genotypes occur globally whereas others are limited to specific area, and therefore, to differentiate genotypes is necessary to introduce regional parametrization. Moreover, there are neither clear indications so far which are the ecological preferences of each genotype, nor is it known which types dominate where. Future progressions in understanding the adaptations of genotypes associated with each morphospecies are crucial for paleoceanography and could lead to a more accurate model prediction.

Another important issue for paleoceanography is that foraminifera migrate vertically through the water column during their life cycle. Consequently the recorded temperature by shells is considered to reflect an integrated (and weighted) proxy signal over the upper water column depth interval in which specimens live and secret their calcite. The current version of the model is two–dimensional, and neglects all the vertical structure assuming that the mixed–layer is biologically homogeneous. Extending the current model in depth enables to account for the vertical structure of the water column including depth habitat of individual species. This opens the possibility to study the modification of the calcification pattern based on hydrographic conditions. Detailed information of depth habitat of the species is, thus, necessary in order to contribute to the extension of the current model.

Bibliography

Conkright, M., Levitus, S., O Brien, T., Boyer T., Antonov, J. and Stephens: World Ocean Atlas 1998 CD-ROM Data Set Documentation, Tech. Rep. 15, NODC Internal Report, Silver Spring, MD, 16 pp., 1998.

Duplessy, J. C., Labeyrie, L., Juillet-Leclerc, A., Maitre, F., Duprat, J. and Sarnthein, M.: Surface salinity reconstruction of the North Atlantic Ocean during the Last Glacial Maximum, Oceanologica Acta, 14, 311-324, 1991.

Moore, J. K., Doney, S. C., Kleypas, J. A., Glover, D. M., and Fung, I. Y.: An intermediate complexity marine ecosystem model for the global domain, Deep-Sea Res. II, 49, 403–462, 2002a.

Moore, J. K., Doney, S. C., Glover, D. M., and Fung, I. Y.: Iron cycling and nutrient-limitation patterns in surface waters ofthe World Ocean, Deep-Sea Res. II, 49, 463–507, 2002b.

Niebler, H. S., Arz, H. W., Donner, B., Mulitza, S., Pätzold, J., and Wefer, G.: Sea surface temperatures in the equatorial and South Atlantic Ocean during the last glacial maximum (23–19 ka), Paleoceanography, 18, 1069, doi:1010.1029/2003PA000902, 2003.

Sarnthein, M., Jansen, E., Weinelt, M., Arnold, M., Duplessy, J. C., Erlenkeuser, H., Flatϕy, A., Johannessen, G., Johannessen, T., Jung, S., Koc, N., Labeyrie, L., Maslin, M., Pflaumann, U. and Schulz, H.: Variations in Atlantic surface ocean paleoceanography, 50° 80°N: a time-slice record of the last 30,000 years, Paleoceanography, 10, 1063-1094, 1995.

Appendix A

Model notation and equations

A.1 Coupling between ecosystem and foraminifera models

The foraminifera model is included within an intermediate complexity marine ecosystem model for the global mixed layer (Moore et al., 2002,b). All code necessary to run the marine ecosystem model and the input files can be downloaded from $http://usjgofs.whoi.edu/mzweb/jkmoore/areadme.html$. The model is coded in Fortran 77, and it is structured in a way that includes the main module of global mixed layer grid code, which is the driving program ($bio\_2d_x3pV5.f$), the main module of marine ecosystem model code ($bio\_subs\_x3pV5.f$) and the numerical code for implementing the 4th order Runge–Kutta driver with adaptive stepsize control ($numerics\_subs.f$). The model is integrated for two years as spinup, and then, output data from a third year at 48 equally spaced weekly intervals is written to the output file. At the end, monthly mean is calculated and saved as final output file. High temporal resolution is not recommended, since the model is constructed to examine biological variability on large spatial (non-eddy resolving) and temporal (monthly) timescales.

The foraminifera model is included in the biological subroutine ($bio\_2d\_x3pV5.f$), which computes time derivatives resulting from biological and physical processes for a set of independent mixed layer cells on a global grid. For the parametrization we used the same input files, same common variables and same parameters as Moore et al. (2002) for the global mixed layer ecosystem model. For the bottom boundary conditions, effect of turbulent mixing at the base of mixed layer, entrainment–detrainment and upwelling–downwelling we follow the same procedure as the ecosystem model. Thus, when vertical velocity is ≤ 0 (downwelling occurs) mixed layer concentrations do not change, assuming that lateral transport of water with identical concentrations

replaces downwelled water. Upwelling reduces the total concentrations in the mixed layer as upwelled water concentration is lower than mixed layer concentration. The behaviour of biological variables under physical processes and the corresponding equations are described in $bio\_2d\_x3pV5.f$

A.2 Parameters for the foraminifera model

Internally, the model operates approximately at daily resolution (it adjusts stepsize at each time–step), rates are typically in [1/day].

A.2.1 Variables and initial values

psC	0.0125	*N. pachyderma* (sin.) carbon [mmolC/m^3]
pdC	0.0125	*N. pachyderma* (dex.) carbon [mmolC/m^3]
buC	0.0125	*G. bulloides* carbon [mmolC/m^3]
ruC	0.0125	*G. ruber* (white) carbon [mmolC/m^3]
saC	0.0625	*G. sacculifer* carbon [mmolC/m^3]
spC	0.0625	Small phytoplankton carbon [mmolC/m^3]
lpC	0.0625	Large ohytoplankton (diatom) carbon [mmolC/m^3]
zoC	0.0625	Zooplankton carbon [mmolC/m^3]
drC	0.0625	Detritus carbon [mmolC/m^3]
$max(NO3)$		Maximum nutrient concentration [mmolC/m^3]
$max(CHL)$		Maximum chlorophyll concentration [mmolC/m^3]
SST		Sea–surface temperature [°C]
$max(SST)$		Annual maximum SST [°C]
$min(SST)$		Annual maximum SST [°C]

A.2.2 Biological parameters common to all species

$G_{\max}(SP)$	1.08	Maximum foraminiferal growth rate when grazing on small phytoplankton
$G_{\max}(LP)$	1.08	Maximum foraminiferal growth rate when grazing on large phytoplankton
$G_{\max}(Z)$	2.16	Maximum foraminiferal growth rate when grazing on zooplankton
$G_{\max}(DR)$	1.08	Maximum foraminiferal growth rate when grazing on detritus
rl	0.06$^+$	foram linear mortality rate (%/day)
g	0.66$^+$	half saturation constant for grazing
GGE	0.3$^+$	portion of grazed matter added to zooplankton biomass

$^+$ denotes the same value as (Moore et al. (2002a))

A.2.3 Species specific biological parameters

N. pachyderma (sin.)		
T_{opt}	3.8	optimal temperature [°C]
σ	4.0	standard deviation of optimal temperature
$max(SST)$	24	maximum tolerated temperature tolerated [°C]
pl	1.0*	foram. quadratic mortality rate, to higher trophic levels
p_{spC}	0.3	preference for grazing on small phytoplankton [0–1]
p_{lpC}	0.7	preference for grazing on large phytoplankton [0–1]
p_{zoC}	0.0	preference for grazing on zooplankton [0–1]
p_{drC}	0.0	preference for grazing on detritus [0–1]
$p\prime_{spC}$	0.3	preference for grazing on small phytoplankton when main food source is missing [0–1]
$p\prime_{lpC}$	0.7	preference for grazing on large phytoplankton when main food source is missing [0–1]
$p\prime_{zoC}$	0.0	preference for grazing on zooplankton when main food source is missing [0–1]
$p\prime_{drC}$	0.0	preference for grazing on detritus when main food source is missing [0–1]
cl_{ps}	0.0	competition exerted by *N. pachyderma* (dex.) [0–1]
cl_{bu}	0.0	competition exerted by *G. bulloides* [0–1]
cl_{ru}	0.0	competition exerted by *G. ruber* (white) [0–1]
cl_{sa}	0.0	competition exerted by *G. sacculifer* [0–1]
d	0.0	*e*–folding constant, which controls the steepness of the Michaelis–Menton equation for competition

N. pachyderma (dex.)		
T_{opt}	15.0	optimal temperature [°C]
σ	6.0	standard deviation of optimal temperature
$max(SST)$	29	maximum tolerated temperature tolerated [°C]
$min(SST)$	-0.3	maximum tolerated temperature tolerated [°C]
pl	4.0*	foram. quadratic mortality rate, to higher trophic levels
p_{spC}	0.2	preference for grazing on small phytoplankton [0–1]
p_{lpC}	0.8	preference for grazing on large phytoplankton [0–1]
p_{zoC}	0.0	preference for grazing on zooplankton [0–1]
p_{drC}	0.0	preference for grazing on detritus [0–1]
$p\prime_{spC}$	0.4	preference for grazing on small phytoplankton when main food source is missing [0–1]
$p\prime_{lpC}$	0.6	preference for grazing on large phytoplankton when main food source is missing [0–1]
$p\prime_{zoC}$	0.0	preference for grazing on zooplankton when main food source is missing [0–1]
$p\prime_{drC}$	0.0	preference for grazing on detritus when main food source is missing [0–1]
cl_{ps}	0.2	competition exerted by *N. pachyderma* (sin.) [0–1]
cl_{bu}	0.5	competition exerted by *G. bulloides* [0–1]
cl_{ru}	0.8	competition exerted by *G. ruber* (white) [0–1]
cl_{sa}	0.0	competition exerted by *G. sacculifer* [0–1]
d	0.05	*e*–folding constant, which controls the steepness of the Michaelis–Menton equation for competition

G. bulloides		
T_{opt}	12.0	optimal temperature [°C]
σ	6.0	standard deviation of optimal temperature
$min(SST)$	-0.3	maximum tolerated temperature tolerated [°C]
pl	5.0*	foram. quadratic mortality rate, to higher trophic levels
p_{spC}	0.15	preference for grazing on small phytoplankton [0–1]
p_{lpC}	0.45	preference for grazing on large phytoplankton [0–1]
p_{zoC}	0.15	preference for grazing on zooplankton [0–1]
p_{drC}	0.25	preference for grazing on detritus [0–1]
$p\prime_{spC}$	0.2	preference for grazing on small phytoplankton when main food source is missing [0–1]
$p\prime_{lpC}$	0.8	preference for grazing on large phytoplankton when main food source is missing [0–1]
$p\prime_{zoC}$	0.0	preference for grazing on zooplankton when main food source is missing [0–1]
$p\prime_{drC}$	0.0	preference for grazing on detritus when main food source is missing [0–1]
cl_{ps}	0.0	competition exerted by *N. pachyderma* (sin.) [0–1]
cl_{pd}	0.1	competition exerted by *N. pachyderma* (dex.) [0–1]
cl_{ru}	0.5	competition exerted by *G. ruber* (white) [0–1]
cl_{sa}	0.5	competition exerted by *G. sacculifer* [0–1]
d	0.5	*e*–folding constant, which controls the steepness of the Michaelis–Menton equation for competition

G. ruber (white)		
T_{opt}	23.5	optimal temperature [°C]
σ	4.0	standard deviation of optimal temperature
$min(SST)$	5	maximum tolerated temperature tolerated [°C]
pl	5.0*	foram. quadratic mortality rate, to higher trophic levels
p_{spC}	0.0	preference for grazing on small phytoplankton [0–1]
p_{lpC}	0.2	preference for grazing on large phytoplankton [0–1]
p_{zoC}	0.6	preference for grazing on zooplankton [0–1]
p_{drC}	0.2	preference for grazing on detritus [0–1]
$p\prime_{spC}$	0.0	preference for grazing on small phytoplankton when main food source is missing [0–1]
$p\prime_{lpC}$	0.2	preference for grazing on large phytoplankton when main food source is missing [0–1]
$p\prime_{zoC}$	0.6	preference for grazing on zooplankton when main food source is missing [0–1]
$p\prime_{drC}$	0.2	preference for grazing on detritus when main food source is missing [0–1]
cl_{ps}	0.0	competition exerted by *N. pachyderma* (sin.) [0–1]
cl_{pd}	1.0	competition exerted by *N. pachyderma* (dex.) [0–1]
cl_{bu}	1.0	competition exerted by *G. bulloides* [0–1]
cl_{sa}	0.8	competition exerted by *G. sacculifer* [0–1]
d	1.0	*e*–folding constant, which controls the steepness of the Michaelis–Menton equation for competition

G. sacculifer		
T_{opt}	28.0	optimal temperature [°C]
σ	4.0	standard deviation of optimal temperature
$min(SST)$	15	maximum tolerated temperature tolerated [°C]
pl	4.0*	foram. quadratic mortality rate, to higher trophic levels
p_{spC}	0.0	preference for grazing on small phytoplankton [0–1]
p_{lpC}	0.1	preference for grazing on large phytoplankton [0–1]
p_{zoC}	0.7	preference for grazing on zooplankton [0–1]
p_{drC}	0.2	preference for grazing on detritus [0–1]
$p\prime_{spC}$	0.0	preference for grazing on small phytoplankton in exceptionally warm waters [0–1]
$p\prime_{lpC}$	0.3	preference for grazing on large phytoplankton in exceptionally warm waters [0–1]
$p\prime_{zoC}$	0.6	preference for grazing on zooplankton in exceptionally warm waters [0–1]
$p\prime_{drC}$	0.1	preference for grazing on detritus in exceptionally warm waters [0–1]
cl_{ps}	00.05	competition exerted by *N. pachyderma* (sin.) [0–1]
cl_{pd}	00.05	competition exerted by *N. pachyderma* (dex.) [0–1]
cl_{bu}	10.05	competition exerted by *G. bulloides* [0–1]
cl_{ru}	0.8	competition exerted by *G. ruber* (white) [0–1]
d	1.0	*e*–folding constant, which controls the steepness of the Michaelis–Menton equation for competition

* denotes maximum value which is reduced according to the temperature function T_func .

A.3 Model equations

$$T\_func = exp\left[-4000.0 \cdot \left(\frac{1.0}{SST + 273.15} - \frac{1.0}{303.15}\right)\right] \tag{A.1}$$

$$pl = pl \cdot T\_func \tag{A.2}$$

***N. pachyderma* (sin.)**

Growth rate:

$$\frac{\partial(psC)}{\partial t} = (p_{spC} \cdot TG_{spC} + p_{lpC} \cdot TG_{lpC}) \cdot GGE - f_{loss} \tag{A.3}$$

Mortality equations:

$$psC' = \max((psC - 0.01), 0) \tag{A.4}$$

$$f_{loss} = pl \cdot psC'^2 + rl \cdot psC' \tag{A.5}$$

Grazing equations:

$$\alpha = \frac{10}{\sigma \cdot \sqrt{2\pi}} \cdot \exp\left[-0.5 \cdot \left(\frac{SST - T_{\text{opt}}}{\sigma}\right)^2\right] \tag{A.6}$$

$$TG_{spC} = G_{\max}(SP) \cdot \alpha \cdot psC \cdot \frac{spC}{spC + g} \tag{A.7}$$

$$TG_{lpC} = G_{\max}(LP) \cdot \alpha \cdot psC \cdot \frac{lpC}{lpC + g \cdot 0.81} \tag{A.8}$$

$$TG_{zoC} = G_{\max}(Z) \cdot \alpha \cdot psC \cdot \frac{zoC}{zoC + g \cdot 0.81} \tag{A.9}$$

$$TG_{drC} = G_{\max}(DR) \cdot \alpha \cdot psC \cdot \frac{drC}{drC + g \cdot 0.81} \tag{A.10}$$

***N. pachyderma* (dex.)**

Growth rate:

$$\frac{\partial(pdC)}{\partial t} = (p_{spC} \cdot TG_{spC} + p_{lpC} \cdot TG_{lpC}) \cdot GGE - f_{loss} \tag{A.11}$$

if $lpC \leq 0.02$:

$$\frac{\partial(pdC)}{\partial(t)} = (p\prime_{spC} \cdot TG_{spC} + p\prime_{lpC} \cdot TG_{lpC}) \cdot GGE - f_{loss} \tag{A.12}$$

Mortality equations:

$$pdC' = \max((pdC - 0.01), 0) \tag{A.13}$$

$$f_{loss} = pl{\cdot}pdC'^2 + rl{\cdot}pdC' + \frac{pdC' \cdot d \cdot cl_{ps} \cdot psC}{psC \cdot d + 0.01} + \frac{pdC' \cdot d \cdot cl_{bu} \cdot buC}{buC \cdot d + 0.01} + \frac{pdC' \cdot d \cdot cl_{ru} \cdot ruC}{ruC \cdot d + 0.01} \tag{A.14}$$

Grazing equations:

$$\alpha = \left[\frac{15}{\sigma \cdot \sqrt{2\pi}} \cdot \exp\left[-0.5 \cdot \left(\frac{SST - T_{\text{opt}}}{\sigma} \right)^2 \right] \right]^{\frac{1}{1.2^{spC}}} \tag{A.15}$$

$$TG_{spC} = G_{\max}(SP) \cdot \alpha \cdot pdC \cdot \frac{spC}{spC + g} \tag{A.16}$$

$$TG_{lpC} = G_{\max}(LP) \cdot \alpha \cdot pdC \cdot \frac{lpC}{lpC + g \cdot 0.81} \tag{A.17}$$

G. bulloides

Growth rate:

$$\frac{\partial buC}{\partial t} = (p_{spC} \cdot TG_{spC} + p_{lpC} \cdot TG_{lpC} + p_{zoC} \cdot TG_{zoC} + p_{drC} \cdot TG_{drC}) \cdot GGE - f_{loss} \tag{A.18}$$

if $lpC \leq 0.02$:

$$\frac{\partial (psC)}{\partial (t)} = (p\prime_{spC} \cdot TG_{spC} + p\prime_{lpC} \cdot TG_{lpC}) \cdot GGE - f_{loss} \tag{A.19}$$

Mortality equations:

$$buC' = \max((buC - 0.01), 0) \tag{A.20}$$

$$f_{loss} = pl \cdot buC'^2 + rl \cdot buC' + \frac{buC' \cdot d \cdot cl_{pd} \cdot pdC}{pdC \cdot d + 0.1} + \frac{buC' \cdot d \cdot cl_{ru} \cdot ruC}{ruC \cdot d + 0.1} + \frac{buC' \cdot d \cdot cl_{sa} \cdot saC}{saC \cdot d + 0.1} \tag{A.21}$$

Grazing equations:

$$\alpha = \left[\frac{15}{\sigma \cdot \sqrt{2\pi}} \cdot \exp \left[-0.5 \cdot \left(\frac{SST - T_{\text{opt}}}{\sigma} \right)^2 \right] \right]^{\frac{1}{1.25^{lpC}}} \tag{A.22}$$

$$TG_{spC} = G_{\max}(SP) \cdot \alpha \cdot buC \cdot \frac{spC}{spC + g} \tag{A.23}$$

$$TG_{lpC} = G_{\max}(LP) \cdot \alpha \cdot buC \cdot \frac{lpC}{lpC + g \cdot 0.81} \tag{A.24}$$

$$TG_{zoC} = G_{\max}(Z) \cdot \alpha \cdot buC \cdot \frac{zoC}{zoC + g \cdot 0.81} \tag{A.25}$$

$$TG_{drC} = G_{\max}(DR) \cdot \alpha \cdot buC \cdot \frac{drC}{drC + g \cdot 0.81} \tag{A.26}$$

***G. ruber* (white)**

Growth rate:

$$\frac{\partial(ruC)}{\partial t} = (p_{lpC} \cdot TG_{lpC} + p_{zoC} \cdot TG_{zoC} + p_{drC} \cdot TG_{drC}) \cdot GGE \cdot nut_m \cdot chl_m - f_{loss} \tag{A.27}$$

Mortality equations:

$$ruC' = \max((ruC - 0.01), 0) \tag{A.28}$$

$$f_{loss} = pl \cdot ruC'^2 + rl \cdot ruC' + \frac{ruC' \cdot d \cdot cl_{pd} \cdot pdC}{pdC \cdot d + 0.01} + \frac{ruC' \cdot d \cdot cl_{bu} \cdot buC}{buC \cdot d + 0.01} + \frac{ruC' \cdot d \cdot cl_{sa} \cdot saC}{saC \cdot d + 0.01} \tag{A.29}$$

Grazing equations:

$$\alpha = \frac{10}{\sigma \cdot \sqrt{2\pi}} \cdot \exp\left[-0.5 \cdot \left(\frac{SST - T_{\text{opt}}}{\sigma}\right)^2\right] \tag{A.30}$$

$$TG_{spC} = G_{\max}(SP) \cdot \alpha \cdot ruC \cdot \frac{spC}{spC + g} \tag{A.31}$$

$$TG_{lpC} = G_{\max}(LP) \cdot \alpha \cdot ruC \cdot \frac{lpC}{lpC + g \cdot 0.81} \tag{A.32}$$

$$TG_{zoC} = G_{\max}(Z) \cdot \alpha \cdot ruC \cdot \frac{zoC}{zoC + g \cdot 0.81} \tag{A.33}$$

$$TG_{drC} = G_{\max}(DR) \cdot \alpha \cdot ruC \cdot \frac{drC}{drC + g \cdot 0.81} \tag{A.34}$$

$$nut_m = 3 \cdot \left[0.5 - 0.25 \cdot \left[\tanh\left(\frac{max(NO3)}{1.2} - 2\right) \cdot 2\right] + 0.006\right] \tag{A.35}$$

$$chl_m = 0.5 - 0.25 \cdot \left[\tanh\left(\frac{max(CHL)}{0.37} - 1.7\right) \cdot 2\right] + 0.006 \tag{A.36}$$

G. sacculifer

Growth rate:

$$\frac{\partial(saC)}{\partial t} = (p_{lpC} \cdot TG_{lpC} + p_{zoC} \cdot TG_{zoC} + p_{drC} \cdot TG_{drC}) \cdot GGE \cdot chl_m - f_{loss} \tag{A.37}$$

if $min(SST) \geq 26$:

$$\frac{\partial(psC)}{\partial(t)} = (p\prime_{lpC} \cdot TG_{lpC} + p\prime_{zoC} \cdot TG_{zoC} + p\prime_{drC} \cdot TG_{drC}) \cdot GGE - f_{loss} \tag{A.38}$$

Mortality equations:

$$saC' = \max((saC - 0.01), 0) \tag{A.39}$$

$$f_{loss} = pl \cdot saC'^2 + rl \cdot saC' + \frac{saC' \cdot d \cdot cl_{bu} \cdot buC}{buC \cdot d + 0.01} + \frac{saC' \cdot d \cdot cl_{ru} \cdot ruC}{ruC \cdot d + 0.01} \tag{A.40}$$

Grazing equations:

$$\alpha = \left[\frac{10}{\sigma \cdot \sqrt{2\pi}} \cdot \exp \left[-0.5 \cdot \left(\frac{SST - T_{\text{opt}}}{\sigma} \right)^2 \right] \right]^{0.15} \tag{A.41}$$

$$TG_{spC} = G_{\max}(SP) \cdot \alpha \cdot saC \cdot \frac{spC}{spC + g} \tag{A.42}$$

$$TG_{lpC} = G_{\max}(LP) \cdot \alpha \cdot saC \cdot \frac{lpC}{lpC + g \cdot 0.81} \tag{A.43}$$

$$TG_{zoC} = G_{\max}(Z) \cdot \alpha \cdot saC \cdot \frac{zoC}{zoC + g \cdot 0.81} \tag{A.44}$$

$$TG_{drC} = G_{\max}(DR) \cdot \alpha \cdot saC \cdot \frac{drC}{drC + g \cdot 0.81} \tag{A.45}$$

$$chl_m = 0.5 - 0.25 \cdot \left[\tanh \left(\frac{max(CHL)}{0.37} - 1.7 \right) \cdot 2 \right] + 0.006 \tag{A.46}$$

Bibliography

Moore, J. K., Doney, S. C., Kleypas, J. A., Glover, D. M., and Fung, I. Y.: An intermediate complexity marine ecosystem model for the global domain. Deep–Sea Res. II, 49, 403–462, 2002a.

Moore, J. K., Doney, S. C., Glover, D. M., and Fung, I. Y.: Iron cycling and nutrient-limitation patterns in surface waters ofthe World Ocean, Deep-Sea Res. II, 49, 463–507, 2002b.